The Hydrodynamic Theory of *p*-atic Liquid Crystals in the Complex Scalar Formulation

And the interplay of topological defects and hydrodynamic stresses

Miloš Joksimović

Thesis submitted for the degreee of
Master in Theoretical Physics
60 ECTS

Department of Physics
The Faculty of Mathematics
and Natural Sciences

UNIVERSITY OF OSLO
Autumn 2024

© 2024 Miloš Joksimović

The Hydrodynamic Theory of *p*-atic Liquid Crystals in the Complex Scalar Formulation
And the interplay of topological defects and hydrodynamic stresses

http://www.duo.uio.no

Printed: Reprosentralen, University of Oslo

The Hydrodynamic Theory of *p*-atic Liquid Crystals in the Complex Scalar Formulation

And the interplay of topological defects and hydrodynamic stresses

Miloš Joksimović

Under the supervision of professor
Luiza Angheluta-Bauer

Every problem is obsurdly simple when it is explained to you.

-*The Adventures of Sherlock Holmes*
The Dancing Men

Abstract

The hydrodynamic theory of p-atic liquid crystals is examined in the complex scalar formulation. We take the established formulations of the theory in the tensorial formulation as a starting point and us them to formulate dynamical equations in terms of the complex scalar order parameter in order to expose the universal aspects of p-atic liquid crystals and their dynamics. Significant emphasis will be placed on examining the structure of the tensorial p-atic order parameter. It will be shown that one feature of its structure is that it can always be reduced to only two free components for any p-atic, and that it therefore can be mapped to a complex scalar order parameter. This result will be used to expose the universal nature of the dynamics of dry p-atics, which are defined in the regime where dissipative forces are the dominant influence in the system. Finally, the complex scalar order parameter will be used to examine the interplay of p-atic topological defects and the hydrodynamic stresses that arise in p-atic liquid crystals from the coupling between the order parameter and the flow velocity.

Contents

1 Introduction **1**
1.1 Thesis roadmap . . . 3
1.2 Notation and conventions . . . 3

I Background **5**

2 Topological defects **6**
2.1 Something not so deeply hidden . . . 6
2.2 Homotopy theory . . . 12
2.2.1 Paths, loops and homotopies . . . 12
2.2.2 The fundamental group . . . 14
2.3 The unit director $\mathbf{n}$ . . . 15
2.4 The order parameter $\mathbf{\Psi}$ . . . 17

II Hydrodynamics of p-atics **19**

3 Dry p-atic liquid crystals **20**
3.1 The p-atic order parameter . . . 20
3.1.1 The independent components of a fully symmetric fully traceless tensor . . . 22
3.1.2 Rotation of a fully symmetric, fully traceless tensor . . . 25
3.1.3 The components of $q^{(p)}$ . . . 28
3.1.4 Complex scalar order parameter . . . 30
3.1.5 Coarse-graining of the microscopic order parameter . . . 32
3.1.6 Elementary defects in p-atics . . . 34
3.2 The universality of dry p-atics . . . 35

4 Coupling with the flow **40**
4.1 The dynamical equations . . . 40
4.1.1 Decomposition of the stress . . . 41
4.2 Defect induced flows . . . 42

III Summary and conclusions **49**

5 The p-atic order parameter and dry p-atic universality **50**

6 Defect induced flows in p-atics **52**

IV Appendices **54**

A Rescaling of dynamical variables **55**
A.1 Dry p-atic equations of motion . . . 55

B Calculations **57**
B.1 Calculations for Chapter 3 . . . 57
B.1.1 The rotation of a fully symmetric, fully traceless tensor . . . 57
B.1.2 Reformulation of the free energy . . . 59
B.1.3 Reformulation of the tensorial dynamical equation . . . 61
B.2 Calculations for Chapter 4 . . . 63

B.2.1 Reformulation of the stresses in terms of the complex scalar order parameter 63

C Supplementary figures **67**

List of Figures

1.1 Examples of ordered systems . . . 2

2.1 Generic $O(2)$ order parameter field $\mathbf{\Psi}$ . . . 6
2.2 Unit director field of the $O(2)$ order parameter $\mathbf{\Psi}$ . . . 7
2.3 $\mathbf{n}$ around P_1 . . . 8
2.4 Calculation of winding numbers . . . 9
2.5 Combined contour . . . 10
2.6 Phase of $\mathbf{\Psi}$ . . . 11
2.7 Path inequivalence . . . 13
2.8 Map of a contour $\mathcal{M}$ from real space to $\mathbf{n}$-space . . . 16

3.1 Microscopic nematic director . . . 21
3.2 Symmetry relations for a traceless symmetric rank-p tensor in two dimensions . . . 23
3.3 Trace relations for a traceless symmetric rank-p tensor in two dimensions . . . 24
3.4 Scalar vs. tensorial order parameter . . . 29
3.5 3-atic particle, $\boldsymbol{\nu}^{(3)}$ and ψ_3 . . . 31
3.6 Elementary p-atic defects . . . 35
3.7 Dry p-atic order parameter time evolution . . . 38
3.8 Isolated defect in a square domain with periodic boundary conditions . . . 39

4.1 Defect induced flows, no friction, $p = 2$ . . . 43
4.2 Defect induced flows, no friction, $p = 3$ . . . 44
4.3 Defect induced flows, no friction, $p = 4$ . . . 44
4.4 Defect induced flows, no viscosity, $p = 2$ . . . 44
4.5 Defect induced flows, no viscosity, $p = 3$ . . . 45
4.6 Defect induced flows, no viscosity, $p = 4$ . . . 45
4.7 Defect induced flows, friction and viscosity, $p = 2$ . . . 45
4.8 Defect induced flows, friction and viscosity, $p = 3$ . . . 46
4.9 Defect induced flows, friction and viscosity, $p = 4$ . . . 46
4.10 Defect induced flows, friction dominated, $p = 2$ . . . 46
4.11 Defect induced flows, friction dominated, $p = 3$ . . . 47
4.12 Defect induced flows, friction dominated, $p = 4$ . . . 47
4.13 Defect induced flows, viscosity dominated, $p = 2$ . . . 47
4.14 Defect induced flows, viscosity dominated, $p = 3$ . . . 48
4.15 Defect induced flows, viscosity dominated, $p = 4$ . . . 48

C.1 p-atic defect dissociation . . . 67
C.2 Dry p-atic magnitude relaxation to equilibrium . . . 67
C.3 Minimization of the dry p-atic free energy . . . 68
C.4 Time derivative of the p-atic free energy . . . 68
C.5 Dry p-atic time evolution for $p = 2, 3, 4$ . . . 69
C.6 4-atic particle, $\nu^{(4)}$ and ψ_4 . . . 70
C.7 5-atic particle, $\nu^{(5)}$ and ψ_5 . . . 71
C.8 6-atic particle, $\nu^{(6)}$ and ψ_6 . . . 72

List of Tables

1.1 Notational conventions 3
1.2 Variable names 4

Preface

One fine afternoon of August 2022, a professor at the Department of Theoretical Physics at the University of Oslo addressed a group of young, ambitious students freshly enrolled on the institute's master program, explaining how the purpose of a master's degree is for us to show that we can conduct a scientific or academic project, naturally, with the guidance of our advisors and supervisors, but mostly independently. That certainly sounded reasonable, and simple enough in principle, and so, being one of those young, ambitious students, you proceeded to plan and embark upon your journey through the fantastic realm of theoretical physics.

As time relentlessly marched on and brought you ever closer to the deadline for handing in your labour's fruits, the harsh reality of navigating through the world of academia made itself ever more evident, and other conversations with other professors soon revealed that the purpose of a master's degree is for you to show that you can make arguments "like a physicist", that you can cite references and contextualise your work in whatever field you're working in, and to satisfy whatever other requirements may be imposed by a very peculiar system whose ostensible function and design is to imbue us all with knowledge, understanding and the ideals of the Enlightenment.

Whatever the purpose of a master's degree is, I certainly hope - in the interest of securing the future prospects for me to continue on my journey - that this work satisfies all those formal requirements which may or may not have much to do with discovering and understanding the workings of the natural world.

However, for me this thesis has yet another purpose which is in some sense perhaps the closest to my heart.

When one first enters the world of institutionalised physics, it doesn't take long before one notices that there exists a seemingly ubiquitous notion in our field, which is that experiment and theory are somehow fundamentally different and distinct from each other; where experiment is the domain of the laboratory, of hard and tangible facts, observations and measurements, theory is the domain of abstract ideas and concepts, and all kinds of "constructions of the mind".

Although I am but a student, well aware of my ignorance about many things, no matter how much I try to leave room in my mind for the possibility that there is a legitimate reason for why this view persists, I cannot help but feel that it is a somewhat strange view. When one is working on the frontier of what is known, whether it be in the domain of theory or experiment, and there is no advisor, professor, textbook or paper one can consult to find the answer to one's questions, there is but one thing one can do in order to make progress - and that is to guess. Ideally, the guesses one makes would be guided by intuition and experience so that one isn't merely shooting in the dark, but nevertheless at the end of the day one is still guessing.

From this point of view, it is my firm belief not only that the realm of abstract ideas and "constructions of the mind" can be poked, probed and experimented on just as much as any physical system in our laboratories, but that this is the only thing we can do in order to gain any new knowledge and understanding. My hope is that I managed to convey these sentiments in this thesis, even if only as a vague hint hidden between the lines.

Producing a master thesis which holds up to any noteworthy standard of quality is by no means an easy challenge, as I'm sure anyone who has ever undertaken such a venture can testify. To have any chance of crossing the finish line with some sort of a complete product in one's hands, one is compelled to make all kinds of sacrifices along the way - one of the more costly ones being a significant reduction in the amount of time spent on and with people who one considers to be close in life. I think (and certainly hope) that most of those people in my life would say that I am generally available for them, and easy to reach and get in touch with. Yet, for the last couple of months leading up to the submission deadline, I have had to maintain a level of radio silence that is highly uncharacteristic of me, and render myself much more scarce than normal. In spite of this, I find that all the people who are close to me, all my friends, still remain as available and as close to me as ever, and for this I would like to express my immense gratitude, and acknowledgement of the fact that I have the best of friends in this world for being so patient and supportive in what has arguably been, in this regard, a rather selfish pursuit on my behalf.

Not any less challenging are the more technical aspects of producing a master thesis. When one is producing any written work, one often finds that the contents of one's mind become entangled with the contents of the page, at which point it becomes very difficult to determine what is and isn't communicated, and whether everything that should be communicated has made it to the page or if it is still stuck in the head. To this end, it is of invaluable help to have people who are willing to proofread one's work and lend a helping hand in correcting not only conceptual, narrative and communicational issues which inevitably find their way into any written work, but also formal, grammatical, punctuational and factual mistakes which may have evaded one's detection. On this note, I would especially like to thank Vedbjørn Øvereng, Kelly Weerman and Charlotte Castel for all their valuable feedback!

I would also like to express my heartfelt gratitude to my dear advisor Luiza for all the ways in which she helped me along my way through this adventure, whether it be all the interesting and stimulating discussions which motivated and inspired many intriguing ideas whose pursuit resulted in lots of intellectual pleasure and satisfaction, or all the times she went as far as to complete tasks which were solely my responsibility, all on her own initiative. It is my impression that not many professors and advisors would stretch themselves that far for their students, which she does despite the fact that as a full-time researcher and professor she has at least nine times as many things to do as I do as a mere student, and it is something that I greatly value and appreciate. A sincere note of thanks also to my co-advisor Vidar, especially for his help in incorporating the ComFiT numerical framework into my work, which saved me considerable time for not having to figure out a numerical implementation and solution of all the dynamical equations in order to be able to check my results and whether or not I am on the right track with my work.

Last, but certainly not least, I would like to thank my big brother Aleksandar for being one of the precious few people in my life who truly understand the meaning of ambition and the drive to work towards realising one's dreams and potentials, and for all the support he gives me towards these goals, as well as for being one of the biggest and most important course-correcting influences in my life, without which I would almost certainly be in a much less enviable place than I am presently.

Oslo
November 15th, 2024
Milos Joksimovic

Chapter 1

Introduction

One could say that the statement that we live in a universe which abounds with structure, order and patterns is a trivial one. After all, if there is one inescapable conclusion that follows from the millennia of human inquiry into the nature of the universe, then that conclusion must certainly be that our universe - for all its magnificent complexity - is a highly structured place, governed by discernible patterns and regularities, a sampling of which is given in Figure 1.1. As our instruments of observation advanced over time, it became clear that these structures and regularities exist from the smallest scales of waves and oscillations in the quantum fields that make up matter, up to the largest scales of galaxies, galaxy clusters and superclusters that make up the cosmic web and the large-scale structure of the universe.

One of the great goals of physics is to be able to describe and understand the properties and behaviour of these structures and the matter that we see in the world around us. Historically this venture has seen great success in the realm of liquids and gases, where our understanding has come so far that we may almost regard it as complete compared to many other fields of physics. This is perhaps best made evident by the fact that we have managed to employ the two fluids of most immediate concern to human life - water and air - to perform or contribute to all kinds of useful functions like transportation and energy production, or by the fact that in cases where water and air are too powerful to tame, we have still been able to use our understanding of their physics to better adapt the infrastructure on which we are ever more dependent for survival to their capricious nature.

However, although the notorious technical difficulties that are involved with solving the equations that describe the behaviour of isotropic fluids would indicate otherwise, the fact is that isotropic fluids such as air and water are some of the simplest forms of matter in our universe, and so the theories we have for describing and understanding them can only take us so far in our quest for a more general understanding of the physics of matter. Most of the matter we see in the world comes in varieties which have little or nothing to do with isotropic fluids, and for which different or altogether new conceptual and theoretical frameworks are therefore required if we are to have any chance of understanding their physical properties.

What sets these forms of matter apart from the isotropic fluids is the fact that their building blocks - be they molecules, or even larger microscopic particles - have some kind of structure to them which, when large numbers of them are put together and made to interact, leads to anisotropies which give these forms of matter properties that isotropic fluids don't have. Therefore, understanding how these anisotropies affect the behaviour and physical properties of such systems is crucial both in terms of practical applications of that understanding [1–3], as well as for the benefits that understanding will have for the development of theory.

One of the most familiar examples of anisotropic systems from everyday life are conventional liquid crystals which, since their discovery in the late 19^{th} century have seen all kinds of uses from soap and dish-washing detergent, to the technology behind the screen through which this text is likely being read. What gives liquid crystals their physical properties is the fact that they are made up of molecules that have a rod-like structure, which is to say that they are symmetric under rotations by π radians. As this became better and better understood, it didn't take long before we also understood that systems of particles with higher discrete rotational symmetries appear in nature - one of the more notable ones being the hexagonal cells which appear in plants and other biological tissues. Eventually, the theories for describing these systems got abstracted into a single theory of any system of particles which have a discrete $2\pi/p$ rotational symmetry. These systems, we call p-atic liquid crystals, or p-atics in short.

By definition, p-atics are systems whose particles are regular p-sided polygons,[1] and their study has become

[1] For the cases of $p = 1$ and $p = 2$ we obviously can't make regular polygons, so we think of the former as describing systems that are in some sense polar, while the latter describes systems of rod-like particles, such as conventional liquid crystals. Although we cannot

an increasingly popular pursuit in the recent decades. One of the major appeals of the theory of p-atic liquid crystals is its wide variety of applications to systems which are seemingly absolutely unrelated by simply varying a single parameter - the order p of the p-atic. One value of p might give us a theory which is useful for understanding conventional liquid crystals [4–6] and biological phenomena such as wound healing [7], and which can find applications in things such as treatment of cancer [8]. Other values of p might give us theories which an find all kinds of applications in the realm of technology and synthetic materials [1, 2, 9]. The same theory which can find applications in all these things turns out to even be applicable to fields of study as exotic as anyonic particles in quantum mechanics [10], showing that an understanding of p-atics has a seemingly limitless potential for enriching our understanding of other areas of physics and even other areas of natural science.

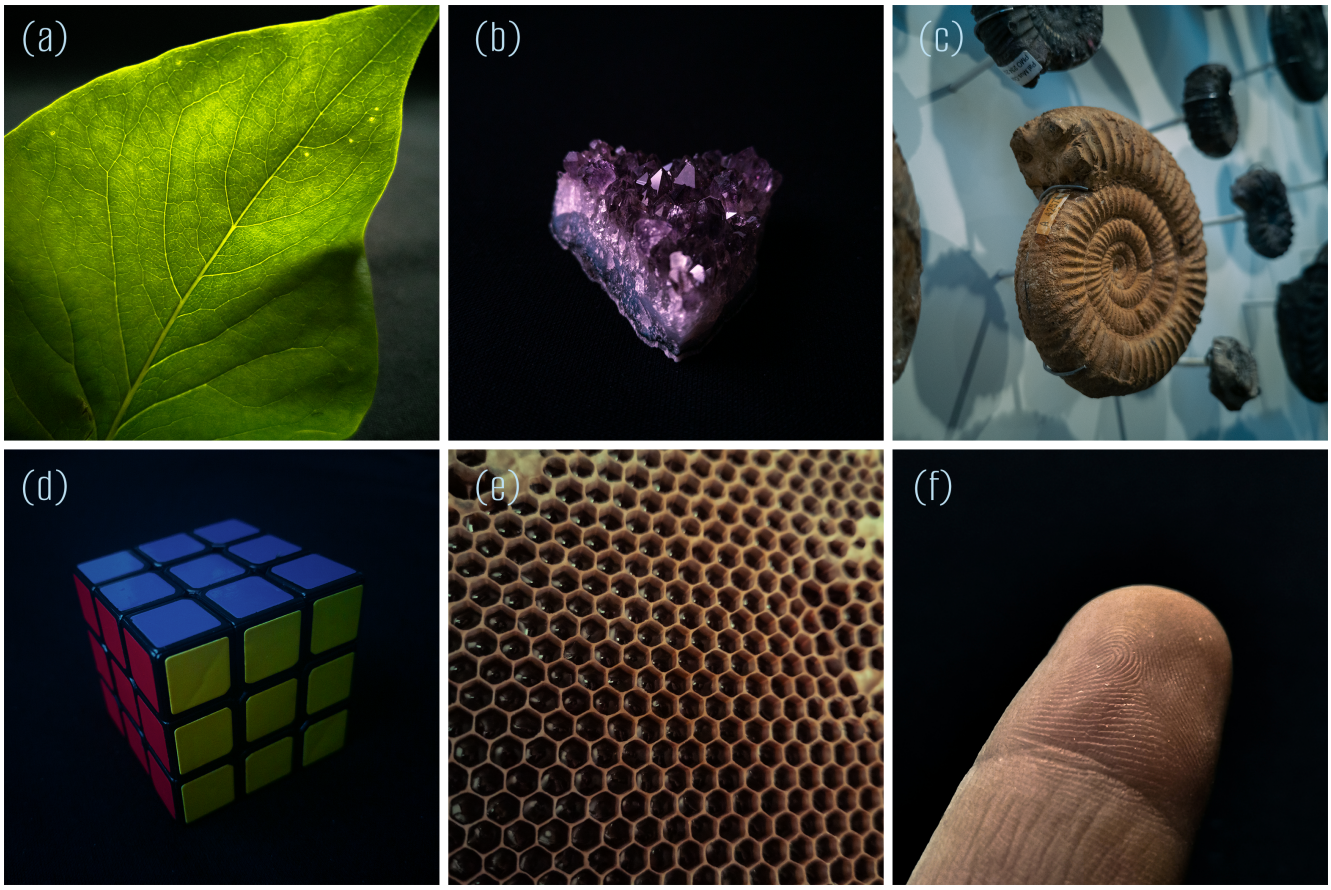

Figure 1.1: Some examples of ordered systems. (a) A lilac leaf - one example out of a virtual infinity of ways in which large collections of living cells collectively order and organize themselves in ways that give them capabilities that far exceed those of any individual cell, as exemplified in the leaf by its structure and rigidity, as well as the networks of channels that supply the cells with water and nutrients, as well as transporting the products of photosynthesis throughout the plant. (b) A sample of amethyst - arguably a more typical representative of an ordered collection of particles, where the arrangement of atoms is so regular that it persists to macroscopic scales, giving rise to the polyhedral structures that are characteristic of so many crystals. (c) Ammonite fossil - another example of the way life exploits the ordering properties of large numbers of particles for functional advantage - in this case in the form of the shell of this long extinct mollusk and its modern-day descendants. (d) A Rubik's cube - apart from being a well-studied object in group theory is also a symbol of humans' fascination with patterns and order not only in the realm of mathematical theory, but also in the more everyday form of toys and puzzles. (e) The honeycomb - perhaps one of the biggest poster children of symmetry and ordering, emerging as a consequence of the bees' need for a structure which can tile the plane, which can be build simultaneously by large numbers of bees, and which requires the least amount of wax to construct. (f) A fingertip with a fingerprint that contains a pair of topological defects, which may themselves be considered the fingerprints of ordered systems.

In this thesis, we will take one small piece of the immense fabric that is the theory of p-atic liquid crystals and try to throw some light on certain aspects of it. The central object of concern in the theory of p-atics is the p-atic order parameter. Mathematically, the two most common objects used as p-atic order parameters are rank-p tensors, and complex scalars. We want to examine the structure of those order parameters as well as the relationship between them, as this can help us to better understand the underlying properties of p-atics that govern their physics. The understanding of these relationships will also help us formulate the dynamics of a certain subclass of p-atics, known as dry p-atics, in a way which gives theoretical support to the observation that systems which seem to have nothing to do with each other physically can nevertheless be described by the same theory.

make regular polygons with $p = 1$ or $p = 2$ sides, what these systems nevertheless have in common with systems of regular polygons is that their "particles" are symmetric under rotations by $2\pi/p$. A vector, corresponding to $p = 1$, is symmetric under rotations by $2\pi/1 = 2\pi$, and rod-like particles ($p = 2$) are symmetric under rotations by $2\pi/2 = \pi$.

Another crucial aspect of systems which exhibit collective order like p-atic liquid crystals are their topological defects. The topological defects of any condensed matter system play an essential role in determining the physical and material properties of such systems. The peculiar aspect of p-atic particles being regular p-sided polygons gives their topological defects equally peculiar properties. Therefore, as a final step in our exploration of p-atic liquid crystals, we will also examine how p-atic defects induce flows of matter in the system through the various forms of hydrodynamic stress which emerge as a consequence of the structure of the p-atic paricles.

1.1 Thesis roadmap

As one of the defining features of ordered media is the presence of topological defects, we will spend some time developing the theory for topological defects for systems which break $O(2)$ symmetry. This will be the subject of Chapter 2 in the first part of the thesis.

In the next part, we will turn our attention to p-atic liquid crystals specifically, where we will spend some time in Chapter 3 constructing the appropriate order parameter for p-atics. Along this way, we will also investigate the structure of the tensorial p-atic order parameter and its relationship to the complex scalar order parameter - these two being the most commonly used forms of order parameter in the field of p-atics.

Once the order parameter is constructed, we will formulate the dynamics of dry p-atic liquid crystals and use the complex scalar order parameter to demonstrate that these dynamics are universal, which is to say that they do not depend on the value of p.

Finally, in Chapter 4 we will examine the relationship between the p-atic topological defects and the hydrodynamic stresses that emerge from the coupling of the order parameter and the flow velocity.

1.2 Notation and conventions

In the world of abstract mathematical concepts it shouldn't take a lot of effort to make a strong argument for the importance of maintaining good notational hygiene when communicating ideas that are far outside the domain of everyday human intuition. In this thesis we will mostly be using fairly standard mathematics and equally standard notation to express it, with the most important general notational conventions for our purposes summarized in Table 1.1. In the few places where we don't use standard established notation, this will be explained in the main text.

Vectors	$\mathbf{u}$, $\mathbf{v}$, ...
Tensors	A, B, ...
Tensor components	$A_{i_1,\ldots,i_p}$, $B_{i_1,\ldots,i_p}$, ...
Permutation of p elements of $\{1,2\}$, where k elements are 2	π^k
i'th element from the permutation π^k	π^k_i

Table 1.1: Notational conventions that will be used throughout this thesis.

The last two entries of Table 1.1 warrant some further elaboration. In most calculations involving the p-atic order parameter tensor we will be interested in summing over its components labeled by permutations of their indices rather than the specific configurations of the indices. Being a rank-p tensor, the components of the order parameter tensor will naturally be labeled by p indices, which can take only two values - 1 and 2, say - in two dimensions. Then, the set of all possible combinations of indices for that tensor can be broken up into a family of sets $\mathcal{P}$ based on the number k of indices in any given combination that are equal to one of the possible index values, for example 2. In other words

$$\mathcal{P} = \{\, P_k \mid \; P_k \text{ is the set of all permutations of } k \text{ 2's and } p-k \text{ 1's}\} \; .$$

Then, π^k stands for any element of the set P_k in $\mathcal{P}$, while π^k_i is the i'th element in π^k.

For example, for a rank-4 tensor, the family of sets $\mathcal{P}$ will be

$$\begin{aligned}\mathcal{P} \;=\; &\{\{1111\}\,,\,\{1112,\,1121,\,1211,\,2111\}\,,\\ &\{1122,\,1221,\,2211,\,1212,\,2112,\,2121\}\,,\\ &\{1222,\,2122,\,2212,\,2221\}\,,\,\{2222\}\}\;.\end{aligned}$$

If we are now interested in index combinations for which $k = 1$, then we will be considering the set

$$P_1 = \{1112,\,1121,\,1211,\,2111\}\;,$$

and π^1 might be any one of these permutations, for example

$$\pi^1 = 1121\,.$$

The individual indices π^1_i are then

$$\pi^1_1 = 1,\,\pi^1_2 = 1,\,\pi^1_3 = 2,\;\text{ and }\;\pi^1_4 = 1\,.$$

Microscopic p-atic unit director	$\boldsymbol{\nu}^{(p)}$
Macroscopic p-atic unit director	$\mathbf{n}^{(p)}$
Microscopic scalar p-atic order parameter	ψ_p
Real and imaginary components of ψ_p	ψ_R, ψ_I
Macroscopic scalar p-atic order parameter	Ψ_p
Real and imaginary parts of Ψ_p	Ψ_R, Ψ_I
Microscopic p-atic order parameter tensor	$q^{(p)}$
Macroscopic p-atic order parameter tensor	$Q^{(p)}$
(Microscopic or macroscopic) director phase	ϑ_p
(Microscopic or macroscopic) order parameter phase	θ_p

Table 1.2: Variable names that will be used throughout the thesis and their meanings.

Part I

Background

Chapter 2

Topological defects

One of the big insights of statistical mechanics is that phase transitions generally lead to symmetry breaking and the emergence of order parameters as a distinct class of thermodynamic variables which, along with the more familiar ones like temperature and pressure give us a more complete description of the physics of condensed matter systems. Depending on the system under consideration, these order parameters can be any kinds of mathematical objects, with all sorts of algebraic and geometric properties. However, one of the most common types of symmetry breaking in condensed matter physics is the breaking of rotational symmetry, and because the systems we will consider in this thesis exhibit just such symmetry breaking, it will be pertinent for us to examine the structure of the corresponding class of order parameters more closely before embarking on a more specific treatment of p-atic liquid crystals. Concretely, we want to investigate the properties of order parameters which can be used to characterize the breaking of rotational symmetry in two dimensions, i.e. the breaking of $O(2)$ symmetry.

The most typically used objects for describing systems with broken $O(2)$ symmetry are vectors and vector fields, and the purpose of this chapter is to examine the general topological properties of two-dimensional vector fields, and to see how those properties will be relevant for our treatments of p-atic liquid crystals.

2.1 Something not so deeply hidden

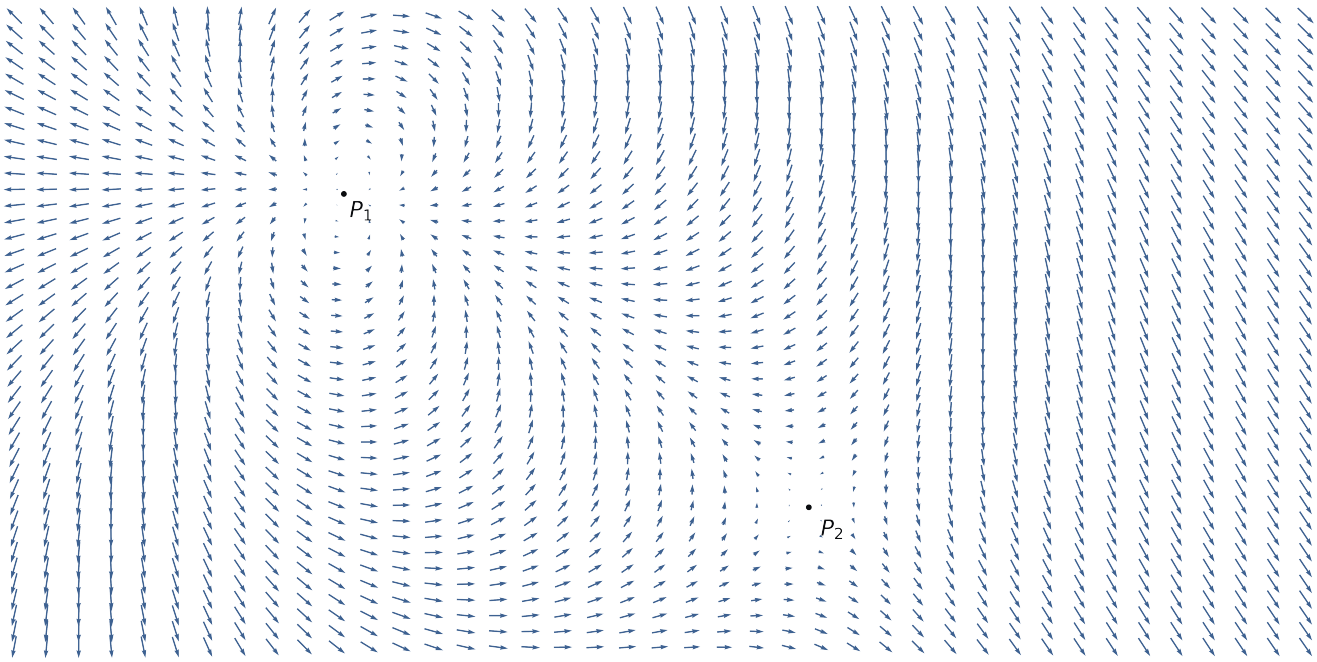

Figure 2.1: Two dimensional vector field $\mathbf{\Psi}$ defined on all of space. The two points P_1 and P_2 with positions $\mathbf{r}_1$ and $\mathbf{r}_2$ are points where the value of the field is zero, i.e. $\mathbf{\Psi}(\mathbf{r}_1) = \mathbf{\Psi}(\mathbf{r}_2) = \mathbf{0}$.

Let us imagine that we are given an order parameter in the form of a two-dimensional vector field $\mathbf{\Psi}$, such as the one in Figure 2.1, which is associated with a two dimensional physical system with broken $O(2)$ symmetry. For the time being, we will not concern ourselves with what exactly the vector field $\mathbf{\Psi}$ represents or how we interpret it in

a physical context. For our present purposes, it suffices to simply think of it as a two-dimensional vector field.

Certainly $\mathbf{\Psi}$ in Figure 2.1 seems to be continuous everywhere - both its phase and its magnitude look like they are varying smoothly, so we might conclude that $\mathbf{\Psi}$ is a well-behaved vector field. Furthermore, for this particular $\mathbf{\Psi}$ we can see that there are two points - P_1 and P_2 - where the value of $\mathbf{\Psi}$ is zero. Now, if we spend some time looking carefully at a vector field such as this, it might not be long before a question occurs to us: what does the direction of $\mathbf{\Psi}$ approach as we approach the points P_1 and P_2? Obviously, the answer is hard to determine by considering $\mathbf{\Psi}$ as it is given to us, because the closer we get to either point, the shorter the vector gets, making it ever harder for us to see its orientation. Of course, we can easily avoid this issue by getting rid of any variations in the magnitude of $\mathbf{\Psi}$, such that only variations in its phase remain. We do this in the standard way, by defining the unit director

$$\mathbf{n} \equiv \frac{\Psi}{|\Psi|}\,, \tag{2.1}$$

which we can write as

$$\mathbf{n} = \left(\cos\theta\left(r,\phi\right), \sin\theta\left(r,\phi\right)\right)\,, \tag{2.2}$$

where r and ϕ are the radial and polar coordinates in the plane, while the phase $\theta\left(r,\phi\right)$ of $\mathbf{\Psi}$ indicates the direction of $\mathbf{\Psi}$ relative to the x-axis at the point (r,ϕ).

The unit director field we get for $\mathbf{\Psi}$ in Figure 2.1 is shown in Figure 2.2. We can see that at any generic point, any two vectors in the immediate vicinity of that point are generally oriented in a similar direction. However, this is clearly not the case for the points P_1 and P_2. For these points we can see that any pair of vectors in their vicinity can generally have drastically different orientations. This would be true no matter how close we get to P_1 and P_2, so it would seem that the director $\mathbf{n}$ isn't of much use to us either in answering our question about the directionality of $\mathbf{\Psi}$ around these points.

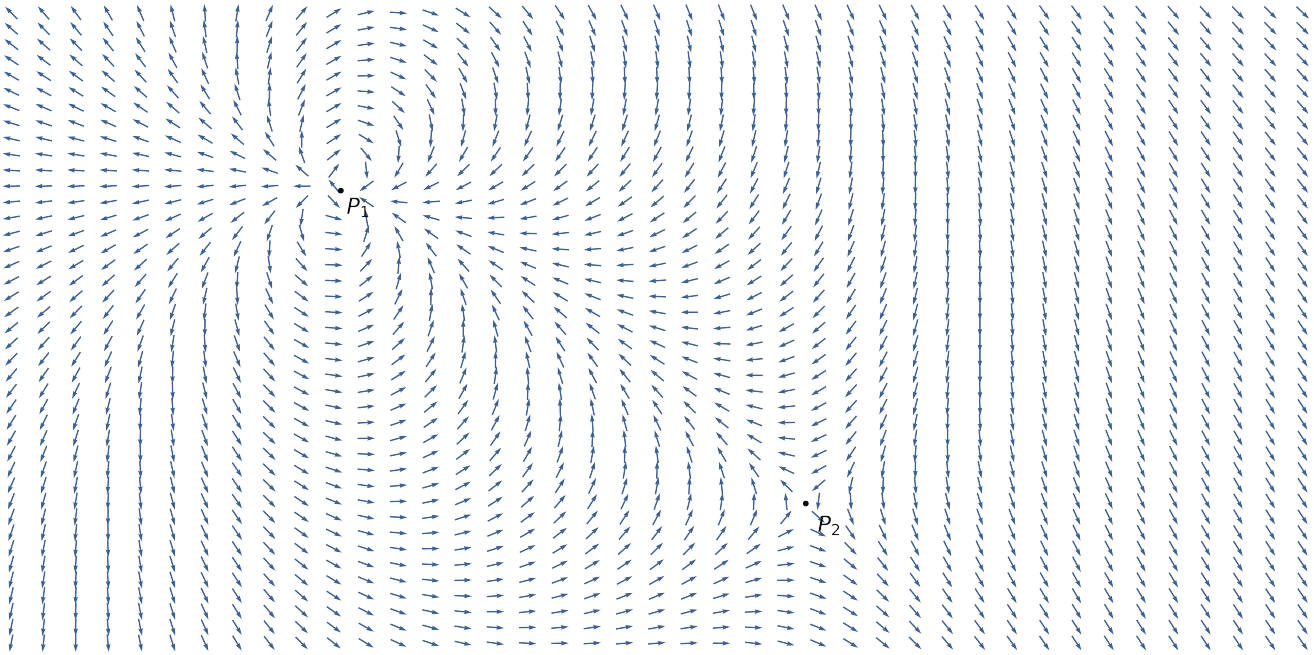

Figure 2.2: The unit director field $\mathbf{n} \equiv \mathbf{\Psi}/\left|\mathbf{\Psi}\right|$ for $\mathbf{\Psi}$ given in Figure 2.1.

Of course, the problem here lies in the definition of $\mathbf{n}$ in eq. (2.1), or rather, the field $\mathbf{\Psi}$ that we are inserting into that definition. If we let $\mathbf{r}_1$ and $\mathbf{r}_2$ be the positions of the points P_1 and P_2 respectively, such that

$$\mathbf{\Psi}\left(\mathbf{r}_1\right) = \mathbf{\Psi}\left(\mathbf{r}_2\right) = \mathbf{0}\,,$$

then we will clearly have

$$\lim_{\mathbf{r}\to\mathbf{r}_i} \mathbf{n} \equiv \lim_{\mathbf{r}\to\mathbf{r}_i} \frac{\mathbf{\Psi}}{|\mathbf{\Psi}|} \to \frac{\mathbf{0}}{0}\,,\ i = 1,2\,,$$

which is, of course, undefined. Specifically, using the expression for $\mathbf{n}$ in eq. (2.2), we can see that as $\mathbf{r}$ approaches $\mathbf{r}_1$ or $\mathbf{r}_2$, the *phase* of $\mathbf{\Psi}$ becomes undefined. This means that even when we have a vector field $\mathbf{\Psi}$ which is perfectly well-defined and continuous over some region of space, if there are any points in that region where $\mathbf{\Psi}$ is zero, then $\mathbf{\Psi}$ must necessarily have singularities in its phase at these points. These phase singularities will be masked by

virtue of the magnitude of $\mathbf{\Psi}$ going to zero at their positions in such a way as to make $\mathbf{\Psi}$ as a whole continuous and well-defined at all points.[1] A simple example of such a field would be

$$\mathbf{\Psi} = y\hat{\imath} + x\hat{\jmath}\,,$$

which is manifestly continuous and well-defined everywhere, and yet its phase is undefined at $x = y = 0$.

We can therefore see that the question we asked about the direction of $\mathbf{\Psi}$ around its zero points is an ill-posed question. We cannot sensibly talk about the directionality of a vector field as we approach points where its direction is undefined. What we might ask ourselves instead, then, is whether or not this is all we can say about $\mathbf{\Psi}$. In cases where the phase of $\mathbf{\Psi}$ is singular at one or more points, can we only say that the phase is singular at these points, or is there any way in which we can characterize these phase singularities that makes them in any sense distinct from each other?

To see how we can begin answering these questions, let us first look at the field $\mathbf{n}$ in Figure 2.2 more closely around the point P_1, as shown in Figure 2.3.

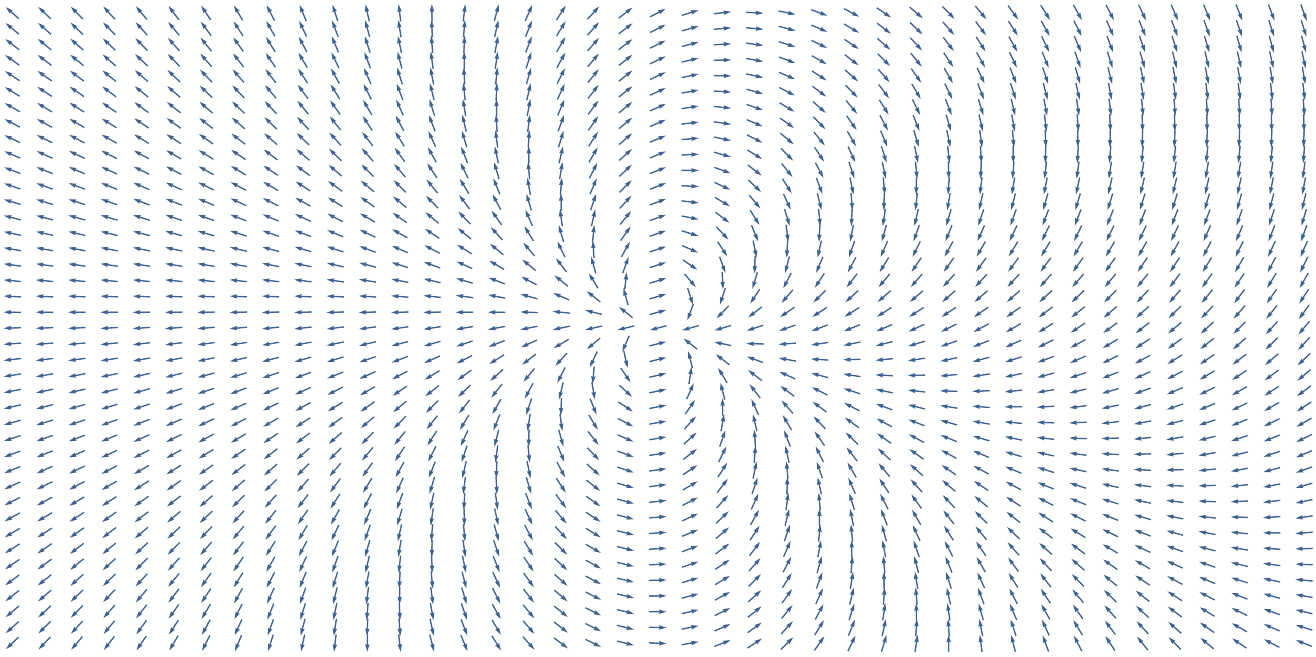

Figure 2.3: The unit director field $\mathbf{n}$ in the vicinity of the point P_1.

As earlier, if we spend some time looking at this vector field, we may at some point notice that there is one major difference in the way in which it varies over any region that contains the point P_1 as opposed to any region that does not contain that point. Namely, if we consider the field over some region which contains P_1, we may get a vague sense that the field is somehow twisting in on itself at that point. For example, if we take some arbitrary point on the horizontal line that passes through P_1, where $\mathbf{n}$ is generally pointing in the negative x direction, and we start circumnavigating P_1 from that point, then $\mathbf{n}$ will start to rotate in the clockwise or counter-clockwise sense[2], only to end up pointing in the negative x direction again by the time we get back to the line we started from. This will, of course, continue if we keep going around all the way back to our starting point. However, for any region which does not contain P_1 (ignoring the phase singularity at P_2 for now), we will never observe this kind of behaviour.[3]

Let us see, then, whether we can formalize this intuitive notion of the twisting of $\mathbf{n}$ around a point of singular phase, and make it more quantitative. Clearly, what we want is some measure of the amount by which $\mathbf{n}$ rotates when we circumnavigate a phase singularity once. The most natural quantity to employ for this purpose is, of course, the phase of $\mathbf{n}$ itself. Specifically, we want to compute the total increment in the phase of $\mathbf{n}$ over a single circulation around the phase singularity. To this end, we begin by defining a contour $\mathcal{M}$ which loops around the

[1] In a similar way to how the function $f(x) = \left(x^2 - a^2\right) / (x - a)$ is continuous at the point $x = a$, even though it's not defined there.

[2] Depending on whether we circumnavigate the singular point in the clockwise or counter-clockwise sense.

[3] Alternatively, we can also arrive at this insight by considering the streamlines of the field. For any region containing P_1 all streamlines in that region will pass through P_1, and there will always be streamlines that originate and terminate at P_1. In fact, for this particular $\mathbf{n}$, all but one streamline will originate and terminate at P_1. For any region that does not contain P_1, however, this will not be the case. Any streamline that enters such a region will also leave it, and every point in that region will have one and only one streamline passing through it.

singular point once, but is otherwise arbitrary.[4] Since $\mathbf{n}$ is well-defined everywhere except at the phase singularity, we can evaluate it over all of $\mathcal{M}$ and calculate the total increment in its phase θ along $\mathcal{M}$. This, of course, will be given simply as the integral of $d\theta$ over $\mathcal{M}$. Now, from the definition of $\mathbf{n}$ in eq. (2.1) it is clear that if $\mathbf{\Psi}$ is continuous everywhere, then $\mathbf{n}$ will also be continuous everywhere - except at points where $\mathbf{\Psi} = \mathbf{0}$ - which means that $\mathbf{n}$ must certainly be continuous on $\mathcal{M}$. Furthermore, because we are integrating $d\theta$ along a closed path, the initial and final orientations of $\mathbf{n}$ over this integration must be the same, and therefore it follows that if $\mathbf{n}$ rotates around itself as we traverse $\mathcal{M}$, the total increment in θ must be an integer multiple of 2π. We will call this integer *the winding number* of the phase singularity, and we define it as

$$m \equiv \frac{1}{2\pi} \oint_{\mathcal{M}} d\theta \,. \tag{2.3}$$

By construction, the magnitude of m tells us the number of times $\mathbf{n}$ rotates around itself around any given phase singularity, while the sign of m tells us the sense of rotation: for $m < 0$, the rotation of $\mathbf{n}$ is clockwise, and for $m > 0$ the rotation is counter-clockwise.[5]

With this definition of the winding number, we can turn our attention back to the field $\mathbf{n}$ in Figure 2.2 and, at least in principle, compute the winding numbers for the phase singularities at P_1 and P_2. In this case, however, we will forego getting into the details of evaluating the integral in m explicitly, and instead satisfy ourselves with obtaining the values of m by visual inspection of the field. We will justify this by the assumption that $\mathbf{n}$ is continuous everywhere except at P_1 and P_2, and by the fact that m is an integer, and as such is not prone to being read off inaccurately. We can therefore infer the winding numbers for the singularities at P_1 and P_2 from Figures 2.4a and 2.4b respectively, which also illustrate the general idea behind the procedure by which we define m. For the singularity at P_1, we see that we have

$$m_1 = \frac{1}{2\pi} \oint_{\mathcal{M}_1} d\theta = 2 \,,$$

while for the one at P_2 we have

$$m_2 = \frac{1}{2\pi} \oint_{\mathcal{M}_2} d\theta = -1 \,.$$

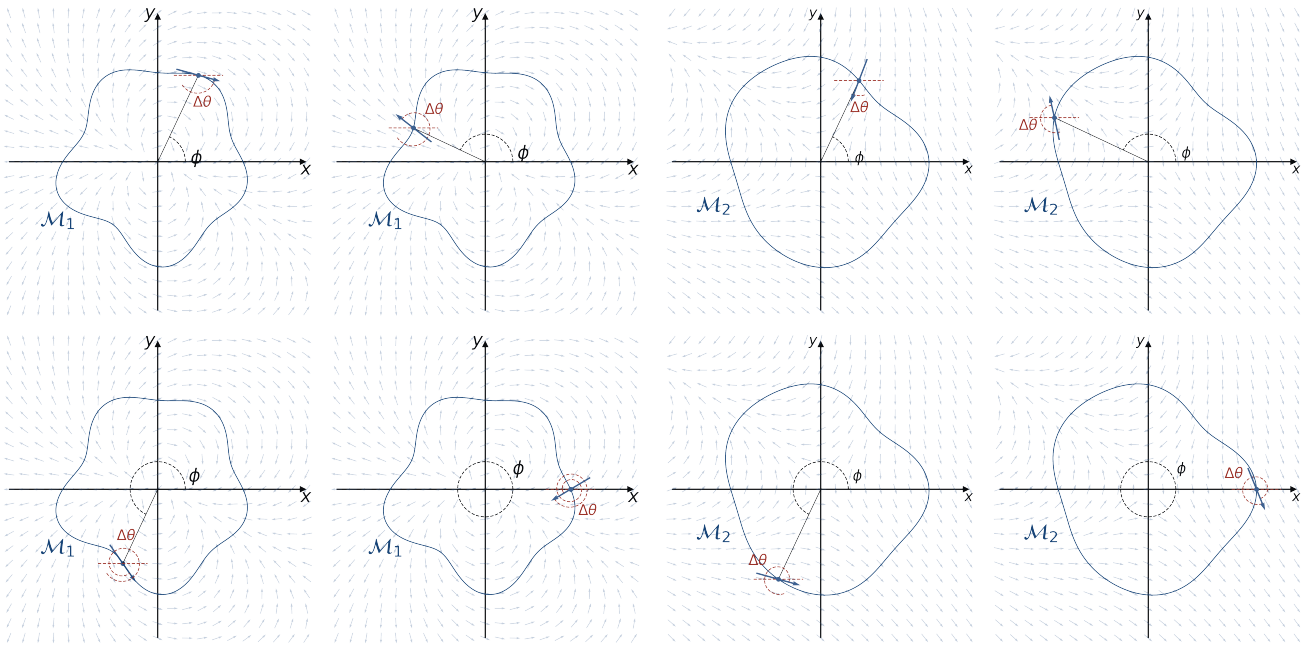

Figure 2.4: Illustration of the calculation of the winding number or the phase singularities of $\mathbf{n}$ from Fig. 2.2. The red dashed lines indicate the total increment in the phase of $\mathbf{n}$ from its starting value at $\phi = 0$ at any given step during the integration. The blue arrow on the integration contour represents the value of $\mathbf{n}$ at that point, and is enlarged to improve readability. For convenience, the coordinate system is shifted so that either P_1 or P_2 is at the origin when calculating their respective winding numbers. (a) Calculation of the winding number for the phase singularity at P_1. (b) Calculation of the winding number for the phase singularity at P_2.

[4] This is motivated by the fact that in our intuitive argument above we made no assumptions as to the exact way in which we went around the singular point. We will see later why this assumption is justified.

[5] Technically, the sign of m tells us the sense of rotation of $\mathbf{n}$ relative to the sense in which we traverse $\mathcal{M}$. $m < 0$ means that $\mathbf{n}$ rotates in sense opposite to the sense in which we traverse $\mathcal{M}$, while $m > 0$ means that $\mathbf{n}$ rotates in the same sense as the sense in which we traverse $\mathcal{M}$.

This result seems to indicate that even though we would have no way of distinguishing between the phase singularities of a vector field $\mathbf{n}$ by evaluating the phase at or in the vicinity of those points, we do nevertheless have a way of distinguishing between them by computing their winding numbers. If two phase singularities differ from each other by their winding numbers, we may tentatively conclude that they are not equivalent to each other.

Now, although our initial inquiry concerned the characterization of *individual* phase singularities, the resulting definition of the winding number in eq. (2.3) naturally brings with it a new question: what value would we get for m if we were to evaluate it for a contour which encloses multiple phase singularities?

To address this question, we will return briefly to an observation we made in the line of reasoning that led us to the definition of the winding number in the first place. For the sake of this argument, we will assume that we have a unit vector field $\mathbf{n}$ which has only one phase singularity and is otherwise continuous. As we already argued, the winding number of the phase singularity must always be an integer for such a field, which means, naturally, that the winding number can only change its value discretely. We have already seen one way in which this can come about - simply change the configuration of $\mathbf{n}$ within the contour along which we are evaluating the integral in eq. (2.3), and the value of m will in general change. However, if we fix the configuration of $\mathbf{n}$ over the region within the contour, then the only way the value of m could change would be for the phase of $\mathbf{n}$ to change discontinuously along the contour. But, by assumption, the only point where $\mathbf{n}$[6] is discontinuous is the point of singular phase within the contour, which means that there can be no discontinuous jump in the phase of $\mathbf{n}$ on the contour or anywhere outside it. Therefore, it follows that the value we compute for m must be the same for any contour that loops once around the phase singularity, or, equivalently, that the value of m must be invariant under any continuous deformation of the original integration contour.[7,8]

This means that if we have some contour $\mathcal{M}$ which encloses multiple phase singularities, we can evaluate m by deforming that contour continuously into a contour $\mathcal{M}'$ with parts that loop only around one phase singularity each, and which are all joined to each other by straight and parallel segments with arbitrarily small separation between them. This is illustrated in Figure 2.5 for the unit director $\mathbf{n}$ in Figure 2.2.

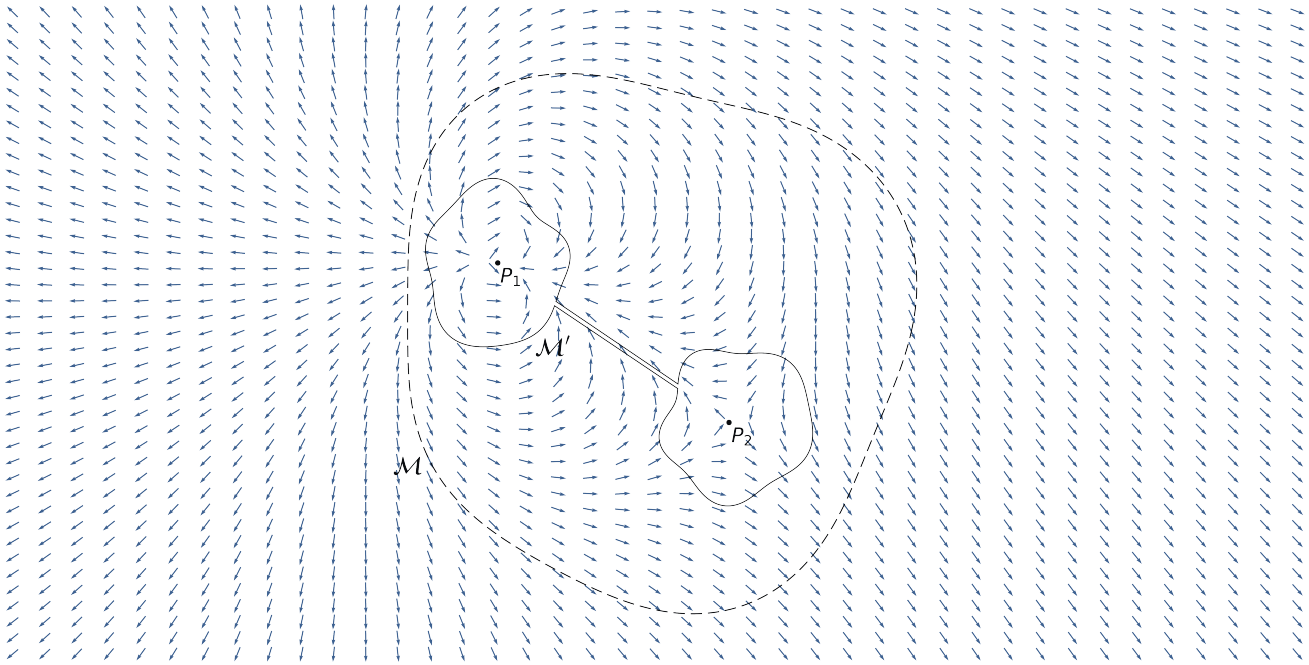

Figure 2.5: The contour $\mathcal{M}'$ (solid) which we use to compute the value of the winding number around two phase singularities. This contour is obtained from a continuous deformation of some generic contour $\mathcal{M}$ (dashed), and consists of two parts that loop around each their own singular point, and two straight parallel sections that are arbitrarily close to each other and which join the two other parts to each other to make a single contour.

By construction, the contour $\mathcal{M}'$ will have the property that whatever the integral of $d\theta$ along one of the straight segments contributes to the total value of m, its adjacent straight segment makes an equal and opposite contribution

[6] Or, to be more precise, the phase of $\mathbf{n}$.

[7] Hence we see why we didn't need to make any assumptions on the form of the integration contour when we first defined the winding number.

[8] Of course, there is nothing particular about the field having only one phase singularity that makes this observation true. It would hold just as well for a field with multiple phase singularities, provided that the contour is deformed in such a way as to never cross any one of them.

which will cancel out the first. Therefore, the only remaining contributions to m must be the integrals around the parts of $\mathcal{M}'$ which loop around each of the phase singularities. For our example $\mathbf{n}$, we have already determined the winding numbers of the individual phase singularities at P_1 and P_2, which means that for both of them we must have

$$m_{12} = \frac{1}{2\pi} \oint_{\mathcal{M}'} d\theta = m_1 + m_2 = 2 - 1 = 1 \,.$$

Interestingly, it seems that calculating the winding number for multiple phase singularities does not give us the ability to determine whether we really have multiple phase singularities within our integration contour or whether we have only one, whose winding number is simply the sum of the winding numbers of more than one. We will see that this is not a coincidence, but a fundamental feature of any two-dimensional (unit) vector field which contains phase singularities.

Now, despite the fact that we have managed to derive a method for distinguishing between individual phase singularities, which also happens to give us a way to characterize multiple phase singularities in a vector field, most of the arguments we've made so far have been motivated by observing the specific example fields in Figures 2.1 and 2.2, and although none of the arguments made any concrete assumptions about the exact details of the fields[9], there are still important questions which we cannot yet answer with the results we've derived. For instance, we said that the winding number of the phase singularity at P_1 for $\mathbf{n}$ in Figure 2.2 is $m_1 = 2$, but we have no way of knowing on the basis of our results whether that is the only possible configuration of $\mathbf{n}$ which would give us that value of m, or if there are other possibilities, and if there are, we have no way of determining whether or not they are distinguishable from each other on some basis other than their associated winding numbers. This also ties into our observation that two phase singularities with different winding numbers are not equivalent to each other. It is not clear from anything we've done so far what this equivalence entails, and in what sense two phase singularities may or may not be considered to be equivalent.

Therefore, it would clearly be advantageous for us to further formalize the somewhat heuristic observations we've made thus far, and to formulate a more robust classification scheme for phase singularities which will allow us to answer the questions just raised, and also give us a more solid foundation upon which we can base the observations we've made in this section.

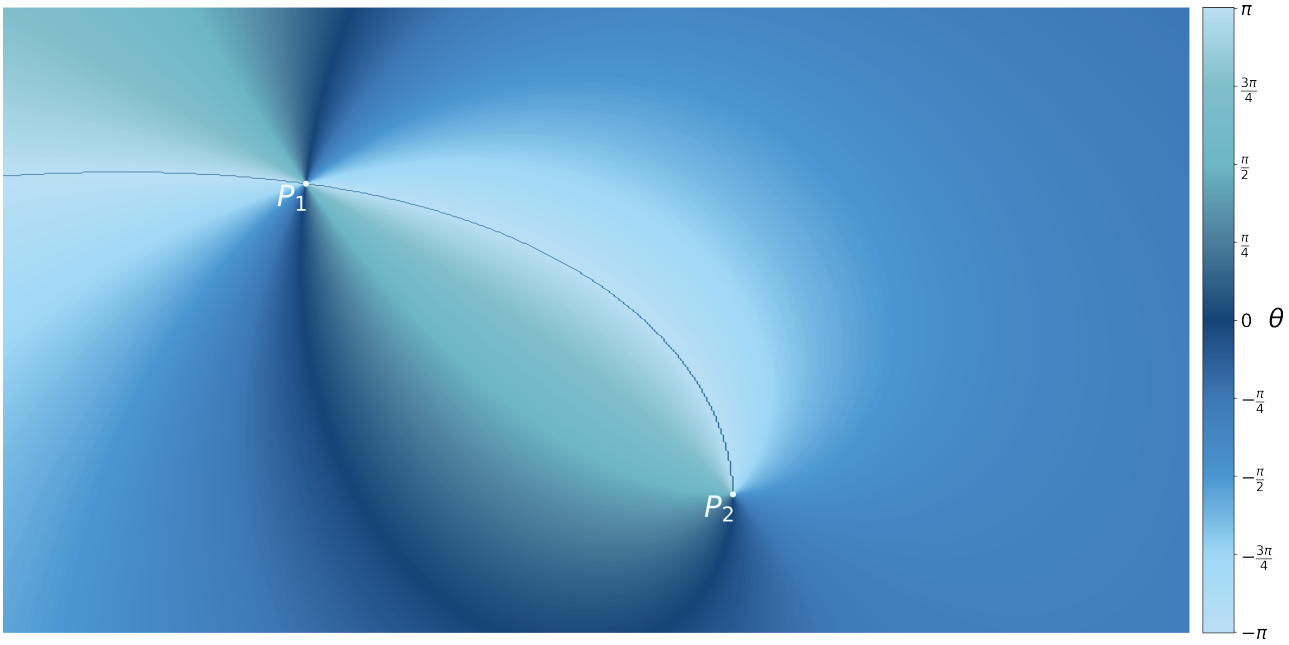

Figure 2.6: Visualization of the phase of $\mathbf{\Psi}$ ($\mathbf{n}$) from Figure 2.1 (Figure 2.2). The dark curve passing through P_1 and P_2 represents the region where θ undergoes a discontinuous jump from $-\pi$ to π or vice versa. This figure makes more evident the reason why we get the values for m_1, m_2 and m_{12} that we do. Any contour that loops around P_1 once will intersect the singular region twice, and so give a $2\pi m_1 = 2 \cdot 2\pi$ contribution to the increment in theta along that contour. Likewise, any contour that loops around P_2 once will only intersect the singular curve once, giving a $2\pi m_2 = -1 \cdot 2\pi$ contribution to the total increment in θ along the contour (the negative sign being due to θ going from larger to smaller values when circumnavigating P_2 in the clockwise sense). Finally, this figure also gives us one way in which we can also make sense of the value of the winding number over a contour which encloses both P_1 and P_2. Since these two points are the only two phase singularities in the field, and we see that the singular curve leaves the point P_1, and there is no returning curve to either P_1 or P_2, it follows that the curve must extend out indefinitely. Therefore, any contour that encircles both P_1 and P_2 must necessarily intersect this curve once, giving an $m_{12} \cdot 2\pi = 1 \cdot 2\pi$ contribution to the total increment in θ around it.

[9] Apart from the fairly reasonable assumption of continuity, except at a finite number of isolated points.

Before we proceed to do so, it is worth emphasizing one subtle point which will be important for us to bear in mind in our coming analyses. Most of the arguments we have made in this section are formulated in terms of the unit director $\mathbf{n}$. However, in the beginning of the section we said that $\mathbf{\Psi}$ is the vector field that represents our hypothetical order parameter, and since $\mathbf{\Psi}$ is the vector field that we eventually want to relate to physics, one might worry that the arguments we have made using $\mathbf{n}$ and the conclusions we drew from them don't hold for $\mathbf{\Psi}$, and that they therefore won't be useful to us later. However, what we have really been talking about in this whole section is the *phase* of $\mathbf{\Psi}$ (see also Figure 2.6), since it is the phase that contains the singular aspects of $\mathbf{\Psi}$. For our present purposes, the unit director $\mathbf{n}$ simply serves as an auxiliary quantity which we use to visualize the phase of $\mathbf{\Psi}$ in a way which helps us expose the phase singularities and analyze their structure. Our main result - the winding number m - is defined in terms of the phase of $\mathbf{\Psi}$, and since $\mathbf{n}$ and $\mathbf{\Psi}$ share the same phase, everything we have said so far is as applicable to $\mathbf{\Psi}$ as it is to $\mathbf{n}$.

2.2 Homotopy theory

Now that we have established that not all phase singularities in (two-dimensional) vector fields are the same, we want to look a little more closely into what exactly this means, and in what way this statement depends on the structure and geometry of the vector field.[10] In the previous section our approach has largely been to make observations about one specific, but arbitrary vector field and in a somewhat bottom-up manner reason our way to the notion of a winding number as a characteristic of phase singularities in vector fields and as a means by which we can distinguish between them. In this section we will take more of a top-down approach, starting from more abstract and seemingly unmotivated concepts and working our way back to two-dimensional vector fields. We will then see how the two approaches meet in the middle to give us a classification scheme for phase singularities in vector fields, as well as to give us deeper understanding of their geometry and why the observations we made in the previous section are true.

2.2.1 Paths, loops and homotopies

For this entire section, we will be working in a topological space $(R, \mathcal{T})$, which we will assume is connected. Specifically, we will assume that R is *path* connected. A path between two points $x, y \in R$ is a map

$$\gamma(s) : [0,1] \to R\,,\ \gamma(0) = x,\ \gamma(1) = y\,, \tag{2.4}$$

that is continuous in s. Then, for our purposes, the condition that R is path connected can be taken to mean that for any two points $x, y \in R$ there exists a map of the form of eq. (2.4).

In the special case where the points x and y are the same point, the definition in eq. (2.4) becomes the definition of a *loop* in R *based* at x. In other words, a loop in R based at x is defined as

$$\gamma(s) : [0,1] \to R\,,\ \gamma(0) = \gamma(1) = x\,, \tag{2.5}$$

with γ continuous in s. For certain applications, it will prove to be useful to also define an *inverse* of a loop γ, which is simply defined as the loop obtained by traversing γ in the opposite direction. In other words

$$\gamma^{-1}(s) : [0,1] \to R\,,\ \gamma^{-1}(s) \equiv \gamma(1-s)\,. \tag{2.6}$$

If we have more than one loop based at the same point, we may combine them to form a new loop as follows. Given two loops $\alpha(s)$ and $\beta(s)$ based at x, we define their composition $(\alpha \circ \beta)(s)$ by

$$(\alpha \circ \beta)(s) \equiv \begin{cases} \alpha(2s)\,, & s \in \left[0, \frac{1}{2}\right] \\ \beta(2s-1)\,, & s \in \left[\frac{1}{2}, 1\right] \end{cases}\,. \tag{2.7}$$

Sometimes we may come across two maps γ and $\tilde{\gamma}$ whose images consist of exactly the same points, which is to say that they will give exactly the same paths (or loops) in R. However, it would be wrong to conclude that γ and $\tilde{\gamma}$ are the same map, because although the two paths might be the same, their parametrizations may be different, as exemplified in eq.'s (2.8) and (2.9) (see also Figure 2.7).

An example of this can be seen in the fact that the composition of two loops in eq. (2.7) is not associative, i.e.

$$(\alpha \circ (\beta \circ \gamma))(s) \neq ((\alpha \circ \beta) \circ \gamma)(s)\,.$$

[10] The following treatise draws a lot of inspiration from that of Ref. [11], to whose author I owe many thanks for elucidating this topic for me.

The reason for this is that although both $(\alpha \circ (\beta \circ \gamma))(s)$ and $((\alpha \circ \beta) \circ \gamma)(s)$ produce the same loops in R, they are parameterized differently. For the former, we have

$$(\alpha \circ (\beta \circ \gamma))(s) \equiv \begin{cases} \alpha(2s), & s \in \left[0, \frac{1}{2}\right] \\ \beta(4s-2), & s \in \left[\frac{1}{2}, \frac{3}{4}\right] \\ \gamma(4s-3), & s \in \left[\frac{3}{4}, 1\right] \end{cases}, \tag{2.8}$$

whereas the latter is given as

$$((\alpha \circ \beta) \circ \gamma)(s) \equiv \begin{cases} \alpha(4s), & s \in \left[0, \frac{1}{4}\right] \\ \beta(4s-1), & s \in \left[\frac{1}{4}, \frac{1}{2}\right] \\ \gamma(4s-1), & s \in \left[\frac{1}{2}, 1\right] \end{cases}. \tag{2.9}$$

In certain situations, however, we will only be interested in the paths or loops themselves, and not the exact way in which they are parameterized. It would therefore be useful if we had some way of defining an equivalence relation which would allow us to consider two (or more) maps which result in the same paths or loops as being the same. That equivalence relation can be found in the form of a homotopy. Given two continuous functions f and g from some topological space X to R, a homotopy between f and g is a map H given as

$$H(x,t) : X \times [0,1] \to R, \; H(x,0) = f(x), \; H(x,1) = g(x), \tag{2.10}$$

and which is continuous in both x and t. If such a map as in eq. (2.10) exists between f and g, we say that f and g are *homotopic*. Because we are focusing our attention on paths and loops in R, we will in the following take the space X to be the unit interval $[0,1]$.

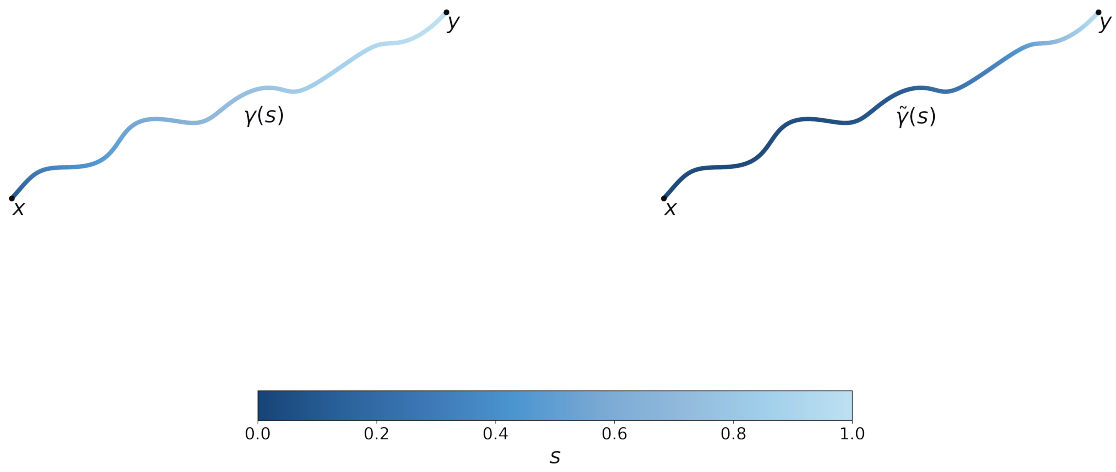

Figure 2.7: The inequivalence of two paths γ and $\tilde{\gamma}$ between x and y in R. The two paths consist of exactly the same points and will therefore look the same geometrically, but their parametrizations will be different, as indicated by the value of the parameter s along each of the paths. In other words, the maps γ and $\tilde{\gamma}$ are not the same maps, and we therefore do not consider the paths as being the same either.

The definition of a homotopy in eq. (2.10) imposes an equivalence relation on all paths and loops in R which are homotopic to each other. The resulting equivalence classes of paths and loops in R will prove to be very useful for characterizing the topology of R, as will become evident shortly.

Another feature of a homotopy as defined in eq. (2.10) is that it allows for the possibility of mapping one path or loop into another one which has no points in common with the first one. For this reason, this form of a homotopy is sometimes referred to as a *free* homotopy. However, for the purposes of characterizing the topology of R, a more restrictive notion of a homotopy is needed. Specifically, we need what is known as a *based* homotopy between loops which has the property that it maintains a single point - known as the base point of the homotopy - in common between the loops.

The definition of a based homotopy is essentially the same as that of a general homotopy in eq. (2.10) with the additional requirement that the base point x is maintained throughout the homotopy. Formally, a based homotopy between two loops α and β can be defined as

$$H(s,t):\,[0,1]\times[0,1]\to R\,,\;H(s,0)=\alpha(s)\,,\;H(s,1)=\beta(s)\,,\;H(0,t)=H(1,t)=x\;\forall\;t\,, \tag{2.11}$$

with the same requirement of continuity in s and t as before, and with x being the base point of the homotopy. The benefit of this form of a homotopy is that it allows us to exploit the composition law for loops in eq. (2.7) to impose a group structure on the equivalence classes of loops in R, which is something that cannot be done on the set of individual loops.

If we denote the set of all loops in R which are homotopic to a loop α by $[\alpha]$, and likewise so for the set of all loops in R that are homotopic to a loop β, then we can define the composition of the two equivalence classes as

$$[\alpha]\circ[\beta]=[\alpha\circ\beta]\;. \tag{2.12}$$

This composition law can be shown to satisfy the group axioms of associativity, the existence of an identity element and the existence of an inverse element.

The associativity axiom

$$[\alpha]\circ([\beta]\circ[\gamma])=([\alpha]\circ[\beta])\circ[\gamma]$$

follows directly from the definition of of the composition law in eq. (2.12), since, as we have seen in eq.'s (2.8) and (2.9) the composition of more than two loops differs only in parametrizations, which ceases to be relevant when we consider equivalence classes of loops rather than specific loops.

The existence of the identity element follows simply from considering the equivalence class $[\epsilon]$ of all loops which are homotopic to the special loop ϵ that is given as

$$\epsilon(s):\,[0,1]\to R\,,\;\epsilon(s)\equiv x\;\forall\;s\,. \tag{2.13}$$

Then it can be shown that

$$[\alpha]\circ[\epsilon]=[\epsilon]\circ[\alpha]=[\alpha]\;\;\forall\;\;[\alpha]\;.$$

Finally, the existence of the inverse element $[\alpha]^{-1}$ follows from considering the equivalence class $\left[\alpha^{-1}\right]$ of all loops which are homotopic to the inverse loop α^{-1} of α, as defined in eq. (2.6). Then it follows that

$$[\alpha]^{-1}\circ[\alpha]=[\alpha]\circ[\alpha]^{-1}=[\epsilon]\;.$$

Thus the set of equivalence classes of loops in R based at x, together with the composition law in eq. (2.12) constitute a group, which we call the *fundamental group of R at x*, and which is most commonly denoted as $\pi_1(R,x)$.

2.2.2 The fundamental group

The fundamental group $\pi_1(R,x)$ of a topological space R at a point $x\in R$ will in general be different for different points x. However, if R is path connected, then it can be shown that it is possible to construct a path isomorphism between the fundamental group $\pi_1(R,x)$ and $\pi_1(R,y)$. This means that in a path connected space, the fundamental groups $\pi_1(R,x)$ are all isomorphic to a single group $\pi_1(R)$, which is known as *the* fundamental group of R.

The usefulness of the fundamental group is that it carries information about the basic geometry of a space, in particular - the information about the holes in that space.

For example, in the Euclidean plane (indeed, in any Euclidean space $\mathbb{R}^n$) every loop can be shrunk down to a point, or, more formally, every loop α is homotopic to the constant map ϵ in eq. (2.13). Therefore, we conclude that the Euclidean plane has no holes in it, and the fundamental group of the plane is simply the trivial group consisting only of the identity element. This is usually expressed as

$$\pi_1\left(\mathbb{R}^2\right)=0\,.$$

The same goes for the 2-sphere $\mathcal{S}^2$; any loop on the surface of the sphere is homotopic to the constant map, and therefore

$$\pi_1\left(\mathcal{S}^2\right)=0\,.$$

On the other hand, if the topological space is a punctured plane - which we will call P - then there will be loops in that space which are *not* homotopic to the constant map. If a given loop winds around the puncture, then there is no way for that loop to be shrunk to a point without breaking the loop. What distinguishes different equivalence classes of homotopic loops in P, then, is the number of times the loops in a given equivalence class wind around the puncture, in other words - their winding numbers. Two loops that wind around the puncture n times can be continuously deformed into each other,[11] but a loop that winds around the puncture m times cannot be continuously deformed into one that does so n times. The sense in which a loop winds around the puncture cannot be affected by continuous deformations either, meaning that the winding number of a loop must be an integer, with its sign indicating the sense in which the loop winds around the puncture. A class of homotopic loops that wind around the puncture n times can be combined under the combination law in eq. (2.12) with a class of loops that wind around the puncture m times into a single class of loops that wind around the puncture $n+m$ times. Therefore, it follows that the fundamental group of the punctured Euclidean plane must be the group of integers under addition, i.e.

$$\pi_1(P) = \mathbb{Z}\,.$$

The exact same reasoning holds if the topological space under consideration is the circle $\mathcal{S}^1$, which means that we must also have

$$\pi_1\left(\mathcal{S}^1\right) = \mathbb{Z}\,.$$

The fundamental group can also be more complicated depending on the topological space. For example, the fundamental group of the torus $\mathcal{T}$ is

$$\pi_1(\mathcal{T}) = \mathbb{Z}^2 = \mathbb{Z}\times\mathbb{Z}\,,$$

where $\times$ indicates the group theoretic direct product of the group $\mathbb{Z}$ with itself. The elements of the fundamental group of the torus are tuples of integers (m,n) where one of the integers indicates the number of times a given loop winds around the "hole" of the torus and the other indicates the number of times the loop winds around the "body" of the torus.

The importance of the fundamental group of a topological space in the context of condensed matter physics and the study of ordered media is that it can be used to extract information about the order parameter of a system that is essential for understanding its physics. In our case the order parameters of concern are those that can be used to describe systems with broken $O(2)$ symmetry, and in the following we want to examine the aspects of the fundamental group associated with such order parameters that are relevant for our study of p-atic liquid crystals.

2.3 The unit director n

As we have seen in Section 2.1 the points where a two-dimensional vectorial order parameter goes to zero correspond to points where the phase of the vector is singular. These phase singularities manifest themselves physically in systems of ordered particles as distortions or kinks in the ordering, and we call these distortions *defects*. As was also shown in Section 2.1, these defects can be characterized by their associated winding numbers, and now that we have the notion of a fundamental group, we are also in a position to answer the questions raised at the end of Section 2.1 about the equivalence (or lack thereof) between defects. The fundamental group will also enable us to understand how defects combine with each other in systems with broken $O(2)$ symmetry.

In light of the closing remarks of Section 2.1 we will, for the time being, restrict our attention to the unit director field $\mathbf{n}$, keeping in mind the relationship it has (eq. (2.1)) to the vector $\mathbf{\Psi}$. To avoid having to say things as cumbersome as "the unit vector associated with the order parameter", we will, also for the time being, refer to $\mathbf{n}$ as "the order parameter", even though strictly speaking that term is reserved for $\mathbf{\Psi}$.

Formally, the unit vector field $\mathbf{n}(\mathbf{r})$ is a map

$$\mathbf{n}:\ \Omega\to R\,,\ \Omega\subseteq\mathbb{R}^2\,,$$

where the domain Ω could be all of (two-dimensional) space or some subspace which represents, for example, some system we are studying. The codomain R of the map is what we will call the *order parameter space* associated with $\mathbf{n}$, whose structure generally depends on the nature of the map. Since $\mathbf{n}$ is a unit vector field, all possible values it can take can be represented by points on the unit circle. Therefore, the order parameter space associated with $\mathbf{n}$ must be a circle, which is to say[12]

$$R = \mathcal{S}^1\,.$$

[11] And therefore belong to the same equivalence class.

[12] Because we are presently restricting our attention only to the vector $\mathbf{n}$, it will be understood that "order parameter space" is taken to mean specifically $\mathcal{S}^1$ unless otherwise stated.

This means that the integration contours $\mathcal{M}$ which we used in Section 2.1 to define the winding number of defects get mapped under $\mathbf{n}$ to loops around a circle (Fig. 2.8), which will in general wind around the circle some number of times. The number of times those loops wind around the order parameter space is precisely the winding number of the defect, and we can understand the reason for why this is with the help of the fundamental group.

As we have seen in the previous section, the fundamental group of the circle is the group of integers under addition. This means that the only essential difference between different loops in the order parameter space is the number of times they wind around the circle. Now, the winding number of a given defect in $\mathbf{n}$ is by construction a measure of the number of times $\mathbf{n}$ winds around the circle as we traverse the integration contour in eq. (2.3). Therefore, when $\mathcal{M}$ is mapped to a loop in order parameter space under $\mathbf{n}$, the number of times that loop winds around the circle must be given by the winding number of the defect. This means that although different defects will generally map a given integration contour $\mathcal{M}$ to different loops in order parameter space, if different defects map $\mathbf{M}$ to loops with the same winding number, then those defects must be topologically equivalent to each other! We therefore conclude that the winding number of a given defect is the only meaningful way in which we can distinguish between it and other defects.

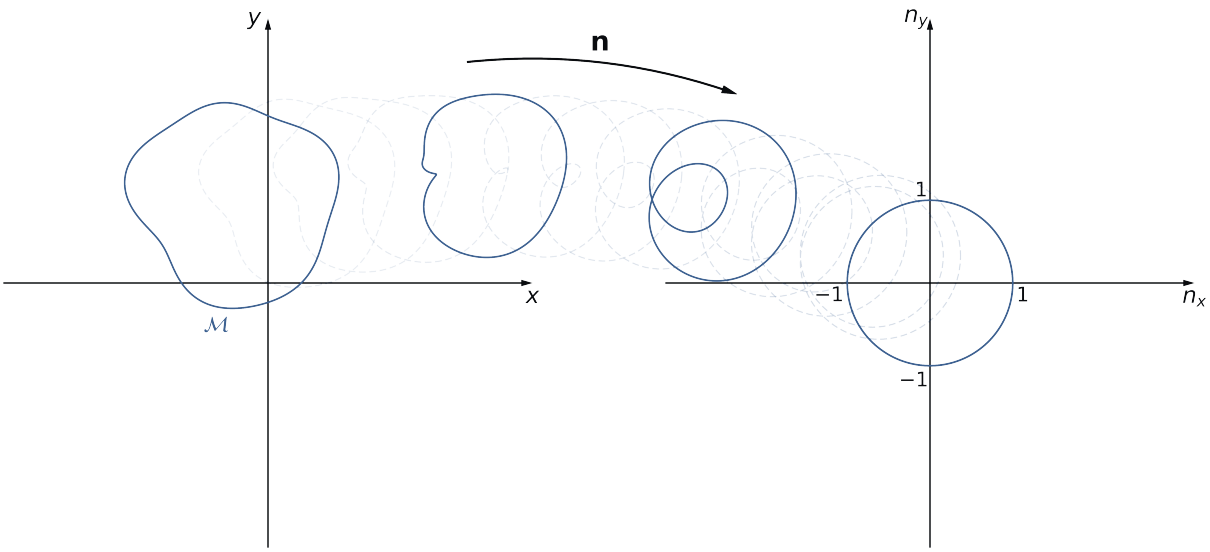

Figure 2.8: Illustration of the map of an arbitrary contour $\mathcal{M}$ from real space into the order parameter space associated with $\mathbf{n}$.

Another observation from Section 2.1 that we can understand in light of the topological considerations from the previous section is the invariance of the winding number under continuous deformations of the integration contour $\mathcal{M}$. Suppose we have a configuration of $\mathbf{n}$ such that $\mathbf{n}$ is continuous everywhere except for a single defect at the origin. Then, at a fixed radius r_0 from the origin the function $\mathbf{n}(r_0, \phi)$ simply gives a mapping of a circle of radius r_0 into the order parameter space. If we take this circle to be an integration contour $\mathcal{M}_0$, then the continuity of $\mathbf{n}$ means that it can be used to construct a homotopy $\mathbf{n}_\mathcal{M}$ between $\mathcal{M}_0$ and any other circle $\mathcal{M}_1$ with radius $r_1 \neq r_0$. However, as we have just seen, the resulting loops in order parameter space will all be homotopic for each other for every circle under the homotopy $\mathbf{n}_\mathcal{M}$, meaning that the winding number must be invariant under any continuous deformation of a circular contour that encloses the defect. From this it readily follows that the same must be true for any continuous deformation of the integration contour, and thus we see on a more abstract level why the same conclusions that we made in Section 2.1 must be true.

The final relevant insight that we gain from homotopy theory pertains to the way defects in a system with broken $O(2)$ symmetry combine with each other. As we have just argued, the defects that correspond to loops in order parameter space with the same winding number must all be topologically equivalent. Furthermore, because the fundamental group of the order parameter space is the group of integers under addition, it follows that the set of loops with winding number m_1 and the set of loops with winding number m_2 can be combined to make the set of loops with winding number $m_{12} = m_1 + m_2$. From the equivalence between loops in order parameter space and defects in $\mathbf{n}$, it therefore follows that defects with winding number m_1 and defects with winding number m_2 can be combined to make defects with winding number $m_{12} = m_1 + m_2$. This is precisely what we have seen from the calculation of the winding number of $\mathbf{n}$ in Figure 2.2 along a contour which encloses both defects! The configura-

tion of $\mathbf{n}$ within that contour[13] can be continuously deformed to a configuration with a single defect with winding number $m_{12} = 1$. Of particular importance in this regard is the special case when the two original defects have winding numbers of equal magnitude and opposite sign. In this case, the two defects combine into a configuration which has no defects in it, which is a process that we call *defect annihilation*.

At this point, it becomes important to address the distinction between $\mathbf{n}$ and $\mathbf{\Psi}$ as order parameters, since that introduces some non-trivial differences in the analyses we have done so far which we cannot neglect. Therefore, as a final note before we move on to the physics of p-atics, we want to address those distinctions.

2.4 The order parameter $\mathbf{\Psi}$

Unlike the unit director $\mathbf{n}$ which we have been considering until now, the kind of order parameter that will be relevant for our treatment of p-atics is a vector $\mathbf{\Psi}$[14] which can vary in both phase *and* magnitude. As we will see in Section 3.1.5, although the magnitude of $\mathbf{\Psi}$ can vary, on physical grounds there will exist some maximum value which it cannot exceed. This means that whereas the order parameter space associated with the unit director $\mathbf{n}$ is a circle, the order parameter associated with a vector such as $\mathbf{\Psi}$ is the disk $\mathcal{D}^2$.

This is a slight complication, because the fundamental group of the disk - like that of the Euclidean plane - is just the trivial group, i.e.

$$\pi_1\left(\mathcal{D}^2\right) = 0\,.$$

Generally, it will still be the case that the integration contour $\mathcal{M}$ in the definition of the winding number of a defect will be mapped under $\mathbf{\Psi}$ to a loop in the order parameter space[15] such that the winding number of the loop corresponds to that of the defect. However, because the fundamental group of the order parameter space is now the trivial group it follows that every loop in that space can be continuously shrunk to a point, which might lead one to naïvely conclude that every defect in $\mathbf{\Psi}$ is equivalent to a defect with zero winding number. This is not entirely correct, however, as defects with non-zero winding number in systems with order parameters such as $\mathbf{\Psi}$ do appear and persist without spontaneously rearranging themselves into configurations with zero winding number.

Therefore, a more careful analysis is needed to properly understand the structure of defects in an order parameter like Ψ. One way in which this analysis can be done, which is due to Skogvoll et. al. [12], is to consider the the *area* of the loop in order parameter space that is the image of the integration contour $\mathcal{M}$ under $\mathbf{\Psi}$ rather than the winding number of the loop. One can then define a quantity analogous to the winding number as the fraction of the area of the disk[16] that is taken up by the area of the loop. From this, one can then construct a defect density field, which can further be used in deriving the dynamics of the defects in a given system, and more.

However, for the purposes of this thesis this approach will not be necessary since all the relevant results are already obtained in the preceding analyses. The only caveat lies in the fact that they can be applied only in regions where the magnitude of $\mathbf{\Psi}$ is close enough to its maximum value that the integration contour is mapped to a loop that is close to the edge of the disk such that the order parameter space may for all practical purposes be considered to be a circle rather than a disk. We often call this region the *far-field*, whereas the region in the vicinity of a defect, where the magnitude of $\mathbf{\Psi}$ is significantly smaller than its maximum value is called the *core* of the defect.

In this chapter, we have seen how systems which break $O(2)$ symmetry can exhibit distortions, or defects, in their ordering. For vectorial order parameters, the defects appear as singularities in the order parameter phase, and we have also seen how the defects can be characterized by their associated winding numbers. Crucially, the winding numbers of the defects are not dependent on the exact configuration of the order parameter - they are a topological property of the order parameter space. As we have seen, the way in which the defects combine with each other is equally dependent on the topology of the order parameter space. Because of this intricate dependence of the nature of the defects on the topology of the order parameter space, we call them *topological defects*. For the same reason, the associated winding numbers of the defects are often called their topological *charge*.

Despite the fundamental dependence of the structure of the defects on the topology of the order parameter space, the topological considerations in this chapter are only a part of the picture when it comes to understanding the physical properties of ordered systems. For a more complete understanding of their physics, one must consider

[13] And indeed any other contour which encloses both defects.

[14] Strictly speaking a vector is just one kind of order parameter we can use to describe p-atics, and we use it in this chapter since the topological analyses we have been doing are arguably most intuitively understood in terms of vectors. As we will see in the next chapter, the order parameter that we want to use for p-atics, namely a complex scalar, has an order parameter space associated with it which is isomorphic to that of a vector $\mathbf{\Psi}$ like the one we are considering in this chapter.

[15] That is, $\mathcal{D}^2$.

[16] Which is determined by the maximum magnitude of $\mathbf{\Psi}$.

energetic arguments to determine how topological defects propagate through the systems under study and how they affect the overall physics of the systems in which they appear.

Part II

Hydrodynamics of p-atics

Chapter 3

Dry p-atic liquid crystals

Now that we have laid down all the necessary groundwork in Part I, we are in position to start looking into the physics of p-atic liquid crystals. Our overarching goal is to examine how the hydrodynamic stresses in p-atics govern the dynamics of topological defects and how we can formulate these dynamics in terms of a complex scalar order parameter using a tensorial formulation as a starting point.

As a first step toward this goal, we will begin by formulating a dynamical equation for p-atic liquid crystals in a regime where dissipative forces such as friction and viscosity are the dominant influences in the system. Intuitively, we often think of the resulting dynamical equations as describing systems of particles where the dissipative forces are strong enough to prevent the particles from changing their position[1], which results in there being no flow of matter anywhere in the system. For this reason we call these systems "dry" p-atics.

We use these *overdamped dynamics* as a starting point because they allow us to take a natural first step in our departure from thermodynamic equilibrium by formulating an evolution equation using the principle of minimization of a free energy functional. This will be the subject of the whole of the present chapter, and in the next chapter we will take the next step and couple the order parameter to a flow, which will allow us to investigate the interplay between the resulting hydrodynamic stresses and topological defects.

Before we can do any of these things, however, we first need to construct an appropriate p-atic order parameter for which we can subsequently formulate our dynamical equations.

3.1 The p-atic order parameter

To describe the physics of systems of particles with dihedral symmetry, we need an order parameter that embodies this symmetry in some way. We will therefore begin our construction of an order parameter on the microscopic scale, by considering the symmetry properties of a single p-atic particle centered at the origin of some coordinate system. Once we have a microscopic order parameter, we can use the standard methods of coarse-graining to obtain a macroscopic order parameter which we can use to formulate the dynamical equations of p-atics.

Historically, the systems whose particles are symmetric under the dihedral group that were some of the first to be studied systematically are conventional liquid crystals, which we often call *nematics*, and which in the context of p-atics correspond to the case $p = 2$. Their order parameters are traditionally defined by using the microscopic unit director $\boldsymbol{\nu}^{(2)}$ (Fig. 3.1) to construct a tensor $q^{(2)}$ which is symmetric under the transformation $\boldsymbol{\nu}^{(2)} \to -\boldsymbol{\nu}^{(2)}$, just as rod-like particles are. Additionally, this order parameter tensor would need to contain only information about the anisotropies in the system, since an ordered system of structured particles is by its very nature anisotropic. One way in which we can define such an order parameter tensor in d dimensions is

$$q^{(2)} \equiv \boldsymbol{\nu}^{(2)} \otimes \boldsymbol{\nu}^{(2)} - \frac{\mathrm{Tr}\left(\boldsymbol{\nu}^{(2)} \otimes \boldsymbol{\nu}^{(2)}\right)}{d}\mathbb{I},$$

where the first term originates from the requirement that $q^{(2)}$ be invariant under $\boldsymbol{\nu}^{(2)} \to -\boldsymbol{\nu}^{(2)}$, while the second term ensures the removal of the isotropic part of $\boldsymbol{\nu}^{(2)} \otimes \boldsymbol{\nu}^{(2)}$, with $\mathbb{I}$ being the (isotropic) identity tensor. Since $\boldsymbol{\nu}^{(2)}$ is a unit vector, we will have $\mathrm{Tr}\left(\boldsymbol{\nu}^{(2)} \otimes \boldsymbol{\nu}^{(2)}\right) = 1$, and since we are restricting ourselves to two dimensional space, it follows that we can write $q^{(2)}$ as

$$q^{(2)} = \boldsymbol{\nu}^{(2)} \otimes \boldsymbol{\nu}^{(2)} - \frac{1}{2}\mathbb{I}. \tag{3.1}$$

[1] But not so strong as to prevent them from changing their orientation, as otherwise there would be no dynamics for us to describe.

The resulting order parameter tensor has some interesting algebraic properties which are worth noting. First of all, being defined as the difference of two manifestly symmetric tensors, it readily follows that $q^{(2)}$ must itself be symmetric. Secondly, we can also see that $q^{(2)}$ is a traceless tensor:

$$\mathrm{Tr}\, q^{(2)} = \nu_i^{(2)}\nu_i^{(2)} - \frac{1}{2}\delta_{ii} = \left(\nu_1^{(2)}\right)^2 + \left(\nu_2^{(2)}\right)^2 - 1 = 0\,.$$

These two properties - symmetry and a vanishing trace - will prove to be essential for the structure and geometric properties of the order parameter tensor for a general p-atic.

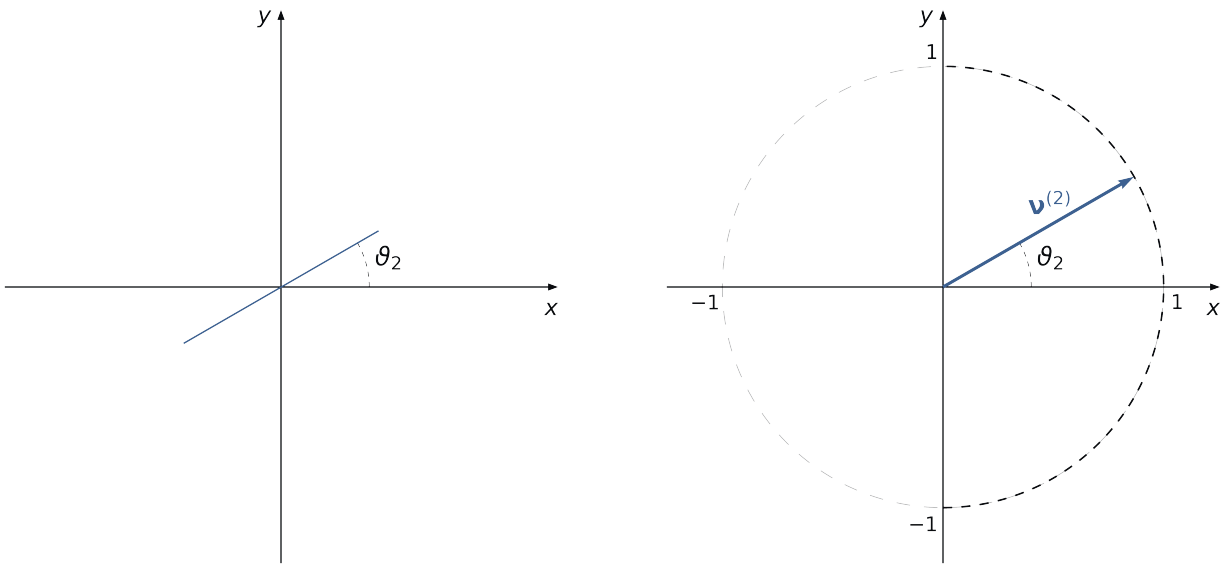

Figure 3.1: Left: a nematic particle centered at the origin, rotated with respect to the x-axis by an angle ϑ_2. Right: the unit director $\boldsymbol{\nu}^{(2)}$ that describes the orientation of the nematic particle. Highlighted around the circumference of the unit circle is the arc that corresponds to the range of values of ϑ_2 that gives all the unique orientations of the nematic particle. In this case, $\vartheta_2 \in [-\pi/2, \pi/2]$.

We can get a glimpse as to why these properties are important if we write the components of $\boldsymbol{\nu}^{(2)}$ and $q^{(2)}$ in terms of the microscopic particle direction ϑ_2, as shown in Figure 3.1. In terms of ϑ_2, $\boldsymbol{\nu}^{(2)}$ will simply be given as

$$\boldsymbol{\nu}^{(2)} = (\cos\vartheta_2, \sin\vartheta_2)\ ,$$

which gives us for $q^{(2)}$:

$$q^{(2)} = \begin{pmatrix} \nu_1^2 - \frac{1}{2} & \nu_1\nu_2 \\ \nu_1\nu_2 & \nu_2^2 - \frac{1}{2} \end{pmatrix} = \begin{pmatrix} \cos^2\vartheta_2 - \frac{1}{2} & \cos\vartheta_2 \sin\vartheta_2 \\ \cos\vartheta_2 \sin\vartheta_2 & \sin^2\vartheta_2 - \frac{1}{2} \end{pmatrix} = \frac{1}{2}\begin{pmatrix} \cos 2\vartheta_2 & \sin 2\vartheta_2 \\ \sin 2\vartheta_2 & -\cos 2\vartheta_2 \end{pmatrix}$$

(note that the symmetry and tracelessness are even more manifest in these expressions for $q^{(2)}$). We can now clearly see that the components of the nematic order parameter tensor "rotate" twice as fast as the director $\boldsymbol{\nu}^{(2)}$ does, which is simply another manifestation of the symmetry under the transformation $\boldsymbol{\nu}^{(2)} \to -\boldsymbol{\nu}^{(2)}$, now expressed in terms of the direction of $\boldsymbol{\nu}^{(2)}$. The transformation $\boldsymbol{\nu}^{(2)} \to -\boldsymbol{\nu}^{(2)}$ is equivalent to rotating $\boldsymbol{\nu}^{(2)}$ by $2\pi/2 = \pi$, i.e. increasing ϑ_2 by π. Doing that explicitly, we get

$$q^{(2)}_{\mathrm{rot.}} = \frac{1}{2}\begin{pmatrix} \cos\left(2\left[\vartheta_2 + \pi\right]\right) & \sin\left(2\left[\vartheta_2 + \pi\right]\right) \\ \sin\left(2\left[\vartheta_2 + \pi\right]\right) & -\cos\left(2\left[\vartheta_2 + \pi\right]\right) \end{pmatrix} = \frac{1}{2}\begin{pmatrix} \cos\left(2\vartheta_2 + 2\pi\right) & \sin\left(2\vartheta_2 + 2\pi\right) \\ \sin\left(2\vartheta_2 + 2\pi\right) & -\cos\left(2\vartheta_2 + 2\pi\right) \end{pmatrix}$$

$$= \frac{1}{2}\begin{pmatrix} \cos 2\vartheta_2 & \sin 2\vartheta_2 \\ \sin 2\vartheta_2 & -\cos 2\vartheta_2 \end{pmatrix} = q^{(2)}\,.$$

In other words, $q^{(2)}$ remains unchanged when rotating a nematic particle by π, which is a direct consequence of $q^{(2)}$ being symmetric and traceless. If either of the two constraints were absent, then the nematic order parameter tensor would not have the structure needed to embody the symmetry of nematic particles, which we see directly from the explicit calculation of its components in terms of $\boldsymbol{\nu}^{(2)}$.

Now, because we would like the order parameter tensor $q^{(p)}$ for an arbitrary p-atic to be invariant under rotations by $2\pi/p$, we might surmise that we can define it in an analogous way, as the fully symmetric, fully traceless p-th

tensorial power of the unit director $\boldsymbol{\nu}^{(p)}$. Indeed, this is one of the two most common ways of constructing the order parameter in the field of p-atics. We will also use this as our starting point here, and define a microscopic p-atic order parameter tensor $q^{(p)}$ as [13]

$$q^{(p)} \equiv \sqrt{2^{p-2}} \left[\!\!\left[\left(\boldsymbol{\nu}^{(p)}\right)^{\otimes p} \right]\!\!\right], \tag{3.2}$$

where the prefactor $\sqrt{2^{p-2}}$ is included for convention, while the brackets $[\![\cdots]\!]$ indicate taking the fully symmetric and fully traceless part of whatever tensor is inside them. In other words, the operation represented by $[\![\cdots]\!]$ ensures that $q^{(p)}$ will satisfy

$$q^{(p)}_{i_1 \ldots i_m \ldots i_n \ldots i_p} = q^{(p)}_{i_1 \ldots i_n \ldots i_m \ldots i_p} \; \forall \; m \neq n \,, \tag{3.3}$$

and

$$\sum_{i_m = i_n} q^{(p)}_{i_1 \ldots i_m \ldots i_n \ldots i_p} = q^{(p)}_{i_1 \ldots 1 \ldots 1 \ldots i_p} + q^{(p)}_{i_1 \ldots 2 \ldots 2 \ldots i_p} = 0 \; \forall \; m \neq n \,. \tag{3.4}$$

In the case of the nematic order parameter tensor $q^{(2)}$, it was straightforward enough to verify its invariance under rotations by $2\pi/2 = \pi$ by explicit evaluation of its components in terms of the microscopic director $\boldsymbol{\nu}^{(2)}$. However, for a general p-atic the order parameter tensor will have 2^p components in two dimensions, which very quickly renders the analogous calculation of its components in terms of $\boldsymbol{\nu}^{(p)}$ and ϑ_p much more prohibitive with increasing values of p.

However, the definition of $q^{(p)}$ as a fully symmetric and fully traceless tensor brings with it an enormous simplification which we can use to obtain the components of $q^{(p)}$ in terms of ϑ_p in an indirect way. As it turns out, we can show that any rank-p tensor which satisfies the constraints in eq.'s (3.3)-(3.4) is always going to have only two independent components in two dimensions regardless of the value of p. This means that if these two components are known, then the entire structure of order parameter tensor can be obtained from those two components using eq.'s (3.3) and (3.4). Therefore, as a first step in this procedure, we will want to verify that such a tensor as $q^{(p)}$ does indeed have only two independent components before we proceed to find the explicit form of all of its components.

3.1.1 The independent components of a fully symmetric fully traceless tensor

A general rank-p tensor $q^{(p)}$ has 2^p independent components in two dimensions. However, as we have just discussed, the p-atic order parameter tensor is defined as a fully symmetric and fully traceless tensor, and as such its components cannot be completely unconstrained. Indeed, the constraints its components must obey are encapsulated in equations (3.3) and (3.4). These constraints will, naturally, reduce the number of independent components of the p-atic order parameter tensor to a number less than 2^p, and we want to show that every fully symmetric, fully traceless rank-p tensor will always have exactly two independent components in two dimensions.

The proof is in principle a simple matter of counting up the total number of unique constraint equations that the conditions of symmetry and tracelessness give us. This, in turn, will immediately give us the number of independent tensor components, since we know how many components we have in the general, unconstrained case.

We will begin by considering the symmetry condition first. By definition, what this condition does is to equate all pairs of tensor components whose index configurations differ from each other by a single interchange of some pair of indices. This means that if we consider an arbitrary component, then the symmetry condition will set that component equal to all other components whose index configurations can be obtained by an interchange of any pair of its indices.

Now, we know from elementary combinatorics that given any finite discrete set, any permutation of the elements of that set can be made into any other permutation through a finite number of pairwise interchanges of elements. In particular, this will be true for the indices of any given tensor component, which means that given some arbitrary tensor component, the symmetry condition will always allow us to construct a chain of equalities which will set that component equal to any other component with the same number of indices of each allowed value, even if the two components are not directly equated to each other by symmetry (see Figure 3.2b).

In other words, as far as the symmetry condition is concerned, all components that have the same number of indices of each possible value will be equal to each other. More formally, we can see that the symmetry condition imposes an equivalence relation on the set of components of $q^{(p)}$, breaking the set up into a family of equivalence classes. What distinguishes these equivalence classes from each other is the total number of indices of each possible value in their elements rather than the actual configurations of those indices. In two dimensions each index can only take two values - 1 or 2 - which is convenient for us because it allows us to characterize the equivalence classes

with a single number k of indices of their elements that are equal to 2.[2] This means that we can write the family of equivalence classes as

$$\mathcal{S} = \{S_k \,|\, k \in \{0, ..., p\}\} \ ,$$

where the equivalence classes S_k themselves can be expressed as

$$S_k = \left\{ q^{(p)}_{\pi^k} \middle| \, \pi^k \text{ is a permutation of } k \text{ 2's and } p-k \text{ 1's} \right\} \ , \tag{3.5}$$

or, more compactly

$$S_k = \left[q^{(p)}_{\pi^k} \right] \ .$$

Our goal now is to find the number of unique constraint equations that we get from the symmetry condition, and to do that we can begin by considering one particular, but arbitrary equivalence class S_k.

Within a single equivalence class, we are going to have some number N_k of tensor components which will be related to each other by some number $n_{S,k}$ of symmetry equations. We can easily deduce that N_k will simply be the number of permutations that we can make of k 2's and $p-k$ 1's, since this is by definition what determines which components are members of the equivalence class, and thus also the cardinality of that equivalence class. This number will of course be given by the binomial coefficient, which is to say

$$N_k = \binom{p}{k} \ .$$

The relationship between the components within a single equivalence class and all the symmetries between them is illustrated in Figure 3.2 for the components of a rank-4 tensor with $k = 2$. We can immediately see in Figures 3.2a and 3.2b that the number of equations is much too big for the number of components - in this particular case, we have $N_k = 6$ while $n_{S,k} = 12$. Indeed, we can show that this will be true in general.[3]

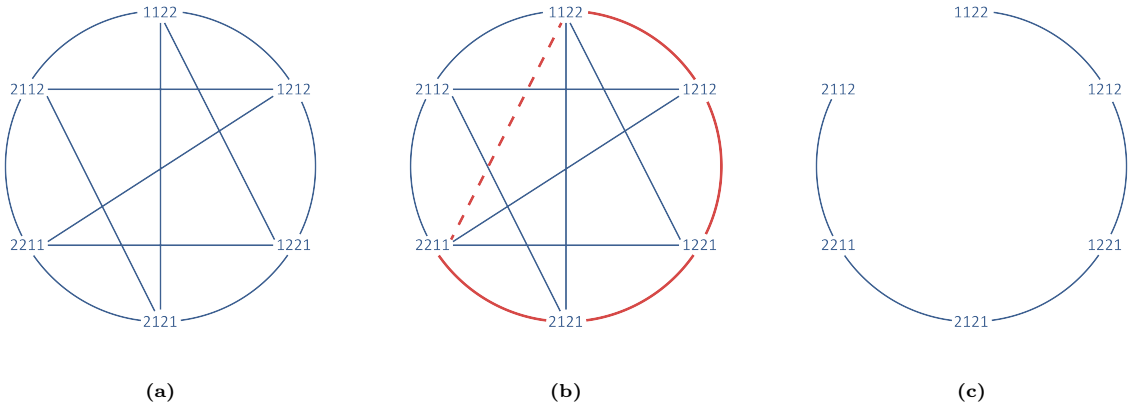

Figure 3.2: Schematic representation of the equations that can be made from the symmetry condition between the components of a rank-4 tensor with $k = 2$. Every line represents an equality sign between the components it connects. Only the index configurations are shown in order to reduce clutter. (a) All possible equations due to symmetry between the components of a rank-4 tensor with $k = 2$. (b) Two components that are not directly related via symmetry are nevertheless indirectly equated to each other. (c) The smallest number of unique equations to determine all the components within an equivalence class. In this particular case, that number is ${}_4C_2 - 1 = 5$.

To find the smallest number of equations (i.e. the smallest value of $n_{S,k}$) that we would need to determine all the components within a single equivalence class, we can imagine writing out all the components within that equivalence class in a sequence such that the index configuration of any component in the sequence differs from the ones adjacent to it by a single interchange of a pair of indices. The number of equations $n_{S,k}$ would then be the number of connections we can make between N_k points when we only connect points that are adjacent to each other (Fig. 3.2c). In other words, the smallest number $n_{S,k}$ of symmetry equations that we need to determine

[2] Because there are only two possible values for each index, we could just as well keep track of the number of 1's instead of 2's - the argument is completely symmetric in that regard.

[3] The total number of symmetry equations within a single equivalence class will simply be the number of pairwise interchanges of indices that we can make - which will be the number of indices that are equal to 2 times the number of indices which are equal to 1, i.e. $k\,(p-k)$ - times the number of components in the equivalence class - ${}_pC_k$, all divided by two to account for overcounting. In other words, the number of symmetry equations within a single equivalence class will be $(k\,(p-k)\,/2)\ {}_pC_k$, which will in general be greater than ${}_pC_k$.

all the components within the equivalence class will simply be the number of adjacent connections we can make between N_k points. This number will of course just be one less than the number of points, which means that

$$n_{S,k} = N_k - 1 = \binom{p}{k} - 1 \,.$$

This is the smallest number of constraint equations due to symmetry that we need to determine all the tensor components within a single equivalence class. The smallest number of symmetry equations that we would need across all the equivalence classes will then be given as the sum of $n_{S,k}$ from 1 to $p-1$. We don't include $k = 0$ and $k = p$ in the sum, since those values of k correspond to the components whose indices are all either 1 or 2, and to which the symmetry condition therefore doesn't apply.[4] Performing this summation gives us

$$N_S = \sum_{k=1}^{p-1} n_{S,k} = \sum_{k=1}^{p-1} \left[\binom{p}{k} - 1 \right] = \sum_{k=0}^{p} \binom{p}{k} - \binom{p}{0} - \binom{p}{p} - \sum_{k=1}^{p-1} 1 = 2^p - 1 - 1 - (p-1) = 2^p - p - 1 \,.$$

Our next order of business is to find the corresponding number of constraint equations that we get from the condition of tracelessness. We may begin by recalling that the tracelessness condition states that we must have

$$q^{(p)}_{i_1 \ldots i \ldots i \ldots i_p} = q^{(p)}_{i_1 \ldots 1 \ldots 1 \ldots i_p} + q^{(p)}_{i_1 \ldots 2 \ldots 2 \ldots i_p} = 0$$

for any pair of indices. In other words, we must have

$$q^{(p)}_{i_1 \ldots 2 \ldots 2 \ldots i_p} = -q^{(p)}_{i_1 \ldots 1 \ldots 1 \ldots i_p}$$

for any pair of indices. Now, because of the equivalence between the tensor components that is imposed by the symmetry condition, it readily follows that we can replace the component on the left side of the equality with any other component that has the same number of indices of each value, and likewise so on the right-hand side. This means that the trace doesn't only relate specific components to each other, but entire equivalence classes. Specifically, we must have

$$\left[q^{(p)}_{\pi^{k+2}} \right] = \left[-q^{(p)}_{\pi^k} \right] \,. \tag{3.6}$$

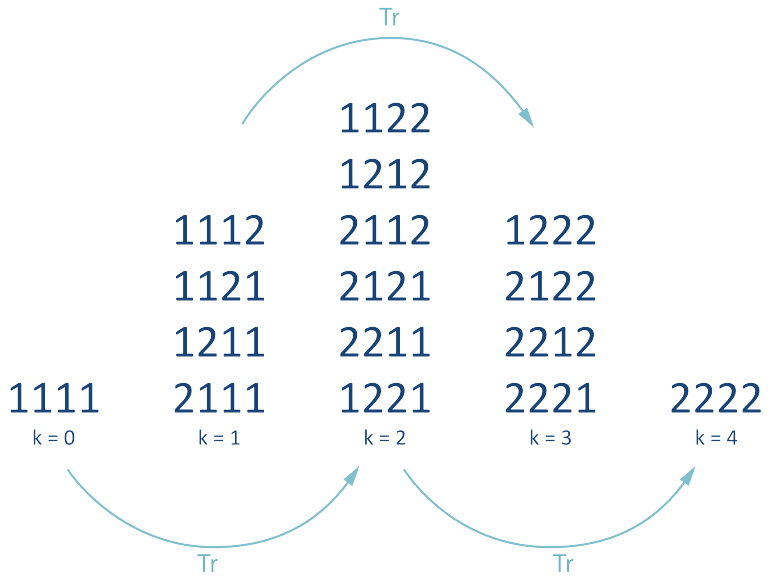

Figure 3.3: Illustration of the equivalence of components of a rank-4 tensor imposed by both the symmetry and tracelessness conditions. Each column represents one equivalence class S_k as defined in eq. (3.5), and the equivalence classes are in turn related to each other by the condition of tracelessness, as indicated by the arrows. With the symmetry condition alone, a general rank-p tensor would have $p + 1$ independent components - in this case 5 - one independent component for each equivalence class S_k. The condition of tracelessness further reduces this number to only two by relating all equivalence classes S_k with k even and all equivalence classes S_k with k odd.

This means that the smallest number of equations due to the tracelessness condition that we need to determine all the components in the tensor will simply be the number of equalities of the form of eq. (3.6) that we can make between the equivalence classes. From the recursive relation in eq. (3.6) it is clear that the tracelessness condition

[4] Or to which it applies trivially in the sense that $q^{(p)}_{11\ldots1} = q^{(p)}_{11\ldots1}$ and $q^{(p)}_{22\ldots2} = q^{(p)}_{22\ldots2}$ under the interchange of any pair of indices. Either way, the symmetry condition adds no non-trivial constraint equations for $k = 0$ and $k = p$.

relates all equivalence classes of tensor components with an even number of 2's in their index configurations and all equivalence classes of components with an odd number of 2's in their index configurations. Therefore, it follows that the total number of equations due to the tracelessness condition will be the same as the number of increments we can make between the even integers from 0 to p, plus the number of increments we can make between the odd integers from 0 to p, as shown in Figure 3.3 for the components of a rank-4 tensor.

For even values of p there will be $p/2+1$ even integers and $p/2$ odd integers between 0 and p. Therefore, we will have $p/2$ increments between the even integers and $p/2-1$ increments between the odd integers. For odd values of p, there will be $(p+1)/2$ even integers and $(p+1)/2$ odd integers between 0 and p, with $(p-1)/2$ increments for each of the sets. Therefore, in either case the number of equations that we get from the trace will be

$$N_T = \frac{p}{2} - 1 + \frac{p}{2} = \frac{p-1}{2} + \frac{p-1}{2} = p - 1\,.$$

Finally, putting everything together, the total number of unique constraint equations we get from the symmetry and tracelessness conditions is

$$N_{const} = N_S + N_T = 2^p - p - 1 + p - 1 = 2^p - 2\,.$$

Subtracting this from the total number of components gives us

$$N_{indep} = 2^p - N_{const} = 2^p - (2^p - 2) = 2$$

which is what we wanted to show.

With the number of independent components of $q^{(p)}$ established, we can now proceed to compute the exact form of those components, from which the structure of the whole tensor will follow by virtue of equations (3.3) and (3.4). Once we have the exact form of the two independent components, we will also immediately be able to verify the invariance of $q^{(p)}$ under rotations by $2\pi/p$.

The way in which we will go about finding the explicit form of the two independent components of $q^{(p)}$ is to first compute how a general fully symmetric fully traceless tensor transforms under an arbitrary rotation of the coordinate system, which will allow us to write a general expression for the components of such a tensor, and once we have that it will be a simple matter to compute the exact form of the components of $q^{(p)}$.

3.1.2 Rotation of a fully symmetric, fully traceless tensor

Given a rank-p tensor A which is fully symmetric and fully traceless in the sense of equations (3.3) and (3.4), we want to examine how it transforms under an arbitrary rotation of the coordinate system. This transformation is of course given by the standard rotation matrix in two dimensions

$$R = \begin{pmatrix} \cos\alpha & -\sin\alpha \\ \sin\alpha & \cos\alpha \end{pmatrix}$$

where α is the angle of rotation. By the standard rules of tensor algebra, that this transformation will be given by

$$A_{i'_1 i'_2 \ldots i'_p} = R_{i'_1 i_1} R_{i'_2 i_2} \ldots R_{i'_p i_p} A_{i_1 i_2 \ldots i_p}\,. \tag{3.7}$$

As we've just shown in the previous section, a fully symmetric fully traceless tensor will always have only two independent components, which means that we only need to compute the transformation above for those two components.

If we denote a generic component of A by $A_{\pi^k_1 \pi^k_2 .. \pi^k_p}$, where, like in the previous section, π^k is some permutation of a fixed number k of 2's and $p-k$ 1's, and we let $A_{11\ldots1} = a$ and $A_{21\ldots1} = b$ be the two independent components of A, then the recursive relation in eq. (3.6) will impose the following cyclic relations on the components of A:

$$k \bmod 4 = 0 \quad \Leftrightarrow \quad A_{\pi^k_1 \pi^k_2 \ldots \pi^k_p} = a\,, \tag{3.8a}$$

$$k \bmod 4 = 1 \quad \Leftrightarrow \quad A_{\pi^k_1 \pi^k_2 \ldots \pi^k_p} = b\,, \tag{3.8b}$$

$$k \bmod 4 = 2 \quad \Leftrightarrow \quad A_{\pi^k_1 \pi^k_2 \ldots \pi^k_p} = -a\,, \tag{3.8c}$$

$$k \bmod 4 = 3 \quad \Leftrightarrow \quad A_{\pi^k_1 \pi^k_2 \ldots \pi^k_p} = -b\,, \tag{3.8d}$$

This will be of great use to us, because it will allow us to compute the contractions in eq. (3.7) by summing over permutations of indices of the components of A rather than summing over specific index configurations like we would normally have to do. We will see this feature as a recurring theme throughout all calculations that involve the order parameter tensor, so we will present them in some detail here.

To compute the transformation of A under a rotation of the coordinate system, we will begin by computing the component $A_{1'1'\ldots1'}$:

$$\begin{aligned}
A_{1'1'\ldots1'} &= R_{1'i_1}R_{1'i_2}\ldots R_{1'i_p}A_{i_1i_2\ldots i_p} \\
&= \sum_{\{\pi^0\}} R_{1'\pi_1^0}R_{1'\pi_2^0}\ldots R_{1'\pi_p^0}A_{\pi_1^0\pi_2^0\ldots\pi_p^0} \\
&+ \sum_{\{\pi^1\}} R_{1'\pi_1}R_{1'\pi_2}\ldots R_{1'\pi_p}A_{\pi_1\pi_2\ldots\pi_p} \\
&+ \ldots \\
&+ \sum_{\{\pi^{p-1}\}} R_{1'\pi_1^{p-1}}R_{1'\pi_2^{p-1}}\ldots R_{1'\pi_p^{p-1}}A_{\pi_1^{p-1}\pi_2^{p-1}\ldots\pi_p^{p-1}} \\
&+ \sum_{\{\pi^p\}} R_{1'\pi_1^p}R_{1'\pi_2^p}\ldots R_{1'\pi_p^p}A_{\pi_1^p\pi_2^p\ldots\pi_p^p}\,,
\end{aligned}$$

From here we can use the cyclic relations in eq. (3.8) to gather all terms that contain a factor of $\pm a$ and all terms that contain a factor of $\pm b$. Furthermore, we note that in any sum over π^k each summand will have k factors of $R_{1'2} = -\sin\alpha$ and $p-k$ factors of $R_{1'1} = \cos\alpha$. This means that we get

$$\begin{aligned}
A_{1'1'\ldots1'} &= \sum_{\{\pi^0\}}(-\sin\alpha)^0(\cos\alpha)^{p-0}a \\
&+ \sum_{\{\pi^1\}}(-\sin\alpha)^1(\cos\alpha)^{p-1}b \\
&- \sum_{\{\pi^2\}}(-\sin\alpha)^2(\cos\alpha)^{p-2}a \\
&+ \ldots \\
&- \sum_{\{\pi^{p-1}\}}(-\sin\alpha)^3(\cos\alpha)^{p-3}A_{22\ldots1} \\
&+ \sum_{\{\pi^p\}}(-\sin\alpha)^p(\cos\alpha)^{p-p}A_{22\ldots2} \\
&= \left(\binom{p}{0}(\cos\alpha)^{p-0}(-\sin\alpha)^0 - \binom{p}{2}(\cos\alpha)^{p-2}(-\sin\alpha)^2 + \ldots\right)a \\
&+ \left(\binom{p}{1}(\cos\alpha)^{p-1}(-\sin\alpha)^1 - \binom{p}{3}(\cos\alpha)^{p-3}(-\sin\alpha)^3 + \ldots\right)b\,,
\end{aligned}$$

or

$$\begin{aligned}
A_{1'1'\ldots1'} &= \left(\binom{p}{0}(\cos\alpha)^{p-0}(\sin\alpha)^0 - \binom{p}{2}(\cos\alpha)^{p-2}(\sin\alpha)^2 + \ldots\right)a \\
&- \left(\binom{p}{1}(\cos\alpha)^{p-1}(\sin\alpha)^1 - \binom{p}{3}(\cos\alpha)^{p-3}(\sin\alpha)^3 + \ldots\right)b\,. \qquad (3.9)
\end{aligned}$$

We omit writing the components $A_{22\ldots1}$ and $A_{22\ldots2}$ explicitly as $\pm a$ or $\pm b$ because the specific values of those components will depend on the value of p mod 4. We also don't write the last terms in the parentheses in the last two equalities even though the sums are finite, because where the terms with $A_{22\ldots1}$ and $A_{22\ldots2}$ end up depends on whether p is even or odd.

Meanwhile, the binomial coefficients come from the fact that when we sum over permutations of indices, each set of permutations will give us a number of terms that are all the same term. That number is simply the number of permutations of the indices, which is given precisely by the binomial coefficient.

What we are left with, then, is two terms in eq. (3.9) that are proportional to some kind of polynomials in $\sin\alpha$ and $\cos\alpha$. To determine what these polynomials are, we can start by examining the exponential $e^{in\alpha}$. Using Euler's formula, we can write this as

$$e^{in\alpha} = \left(e^{i\alpha}\right)^n = (\cos\alpha + i\sin\alpha)^n = \sum_{j=0}^{n} \binom{n}{j} (\cos\alpha)^{n-j} (i\sin\alpha)^j \,.$$

Similarly

$$e^{-in\alpha} = \sum_{j=0}^{n} \binom{n}{j} (\cos\alpha)^{n-j} (-i\sin\alpha)^j \,.$$

Now, we know that we can express sine and cosine in terms of complex exponentials, which in this case means that we can write

$$\cos(n\alpha) = \frac{e^{in\alpha} + e^{-in\alpha}}{2} = \sum_{j=0}^{n} \binom{n}{j} (\cos\alpha)^{n-j} (\sin\alpha)^j \frac{\left(i^j + (-i)^j\right)}{2} \,,$$

$$\sin(n\alpha) = \frac{e^{in\alpha} - e^{-in\alpha}}{2i} = \sum_{j=0}^{n} \binom{n}{j} (\cos\alpha)^{n-j} (\sin\alpha)^j \frac{\left(i^j - (-i)^j\right)}{2i} \,.$$

One thing we can immediately note about these expressions is that the factors with the imaginary units always evaluate to 0, 1 or -1 in both expressions[5]. For example, for the first expression we have

$$\begin{aligned}
j &= 0: \ \frac{i^j + (-i)^j}{2} = \frac{i^0 + (-i)^0}{2} = \frac{1+1}{2} = 1 \,, \\
j &= 1: \ \frac{i^j + (-i)^j}{2} = \frac{i^1 + (-i)^1}{2} = \frac{i-i}{2} = 0 \,, \\
j &= 2: \ \frac{i^j + (-i)^j}{2} = \frac{i^2 + (-i)^2}{2} = \frac{-1-1}{2} = -1 \,, \\
j &= 3: \ \frac{i^j + (-i)^j}{2} = \frac{i^3 + (-i)^3}{2} = \frac{-i+i}{2} = 0 \,, \\
j &= 4: \ \frac{i^j + (-i)^j}{2} = \frac{i^4 + (-i)^4}{2} = \frac{1+1}{2} = 1 \,, \\
&\vdots
\end{aligned}$$

and similarly for the second expression. This means that we can write

$$\begin{aligned}
\cos(n\alpha) &= \sum_{k=0}^{\left\lfloor \frac{n}{2} \right\rfloor} \binom{n}{2k} (-1)^k (\cos\alpha)^{n-2k} (\sin\alpha)^{2k} \\
&= \binom{n}{0} (\cos\alpha)^{n-0} (\sin\alpha)^0 - \binom{n}{2} (\cos\alpha)^{n-2} (\sin\alpha)^2 + \ldots \,,
\end{aligned}$$

$$\begin{aligned}
\sin(n\alpha) &= \sum_{k=0}^{\left\lfloor \frac{n}{2} \right\rfloor} \binom{n}{2k+1} (-1)^k (\cos\alpha)^{n-2k-1} (\sin\alpha)^{2k+1} \\
&= \binom{n}{1} (\cos\alpha)^{n-1} (\sin\alpha)^1 - \binom{n}{3} (\cos\alpha)^{n-3} (\sin\alpha)^3 + \ldots
\end{aligned}$$

[5] We can think of the two factors as being simply a discrete sine and cosine; with $i = e^{i\pi/2}$, it follows that $(i^j + (-i)^j)/2 = \cos((\pi/2)j)$ and $(i^j - (-i)^j)/2 = \sin((\pi/2)j)$, and with j being an integer the expressions will always evaluate to either 0 or ± 1.

Setting $n = p$, we can immediately see that we have

$$A_{1'1'\ldots1'} = a\cos(p\alpha) - b\sin(p\alpha)\,.$$

The calculation for $A^{(p)}_{2'1'\ldots1'}$ is analogous to the one for $A_{1'1'\ldots1'}$, and is shown in Appendix B, with the result being

$$A_{2'1'\ldots1'} = a\sin(p\alpha) + b\cos(p\alpha)\,.$$

These expressions are manifestly invariant under rotations by $2\pi/p$, and with these two components being the two components from which we can construct the whole of A, it follows that A - and indeed any fully symmetric, fully traceless tensor - must also be invariant under rotations by $2\pi/p$.

If we set the parameters a and b to 1 and 0 respectively, which amounts to fixing an arbitrary initial direction for our coordinate system such that $A_{1'1'\ldots1'} = \cos(p\alpha)$ and $A_{2'1'\ldots1'} = \sin(p\alpha)$, then from the cyclic relations in eq. (3.8) it follows that we can express A as

$$A = \sum_{k=0}^{\lfloor \frac{p}{2} \rfloor} \left\{ \sum_{\{\pi^{2k}\}} (-1)^k \cos(p\alpha)\, \mathbf{e}_{\pi_1^{2k}} \otimes \ldots \otimes \mathbf{e}_{\pi_p^{2k}} + \sum_{\{\pi^{2k+1}\}} (-1)^k \sin(p\alpha)\, \mathbf{e}_{\pi_1^{2k+1}} \otimes \ldots \otimes \mathbf{e}_{\pi_p^{2k+1}} \right\}. \tag{3.10}$$

3.1.3 The components of $q^{(p)}$

Now that we have the general form of a fully symmetric, fully traceless tensor in eq. (3.10), it is a straightforward matter to compute the exact form of the microscopic p-atic order parameter tensor $q^{(p)}$. From the definition in eq. (3.2) and the preceding discussions it readily follows that we must have

$$\left[\!\left[\left(\boldsymbol{\nu}^{(p)}\right)^{\otimes p} \right]\!\right] = NA\,,$$

where A is the tensor from eq. (3.10), whose phase can now be related to that of $\boldsymbol{\nu}^{(p)}$ via[6]

$$p\alpha = p\vartheta_p\,.$$

To compute the proportionality constant N, we can begin by computing the norm of A, given simply as the sum of the squares of all its components:

$$\begin{aligned}
|A|^2 \;\equiv\; A_{k_1\ldots k_p}A_{k_1\ldots k_p} \;&=\; \sum_{k=0}^{p}\sum_{\{\pi^k\}} A_{\pi_1^k\ldots\pi_p^k}A_{\pi_1^k\ldots\pi_p^k} \\
&= \sum_{\{\pi^0\}} A_{\pi_1^0\ldots\pi_p^0}A_{\pi_1^0\ldots\pi_p^0} + \sum_{\{\pi^1\}} A_{\pi_1^1\ldots\pi_p^1}A_{\pi_1^1\ldots\pi_p^1} + \ldots + \sum_{\{\pi^p\}} A_{\pi_1^p\ldots\pi_p^p}A_{\pi_1^p\ldots\pi_p^p} \\
&= \sum_{k=0}^{\lfloor \frac{p}{2} \rfloor} \left\{ \binom{p}{2k} \cos^2(p\vartheta_p) + \binom{p}{2k+1} \sin^2(p\vartheta_p) \right\} \;=\; 2^{p-1}\left(\cos^2(p\vartheta_p) + \sin^2(p\vartheta_p)\right) \;=\; 2^{p-1}\,.
\end{aligned}$$

This gives us

$$\left| \left[\!\left[\left(\boldsymbol{\nu}^{(p)}\right)^{\otimes p} \right]\!\right] \right|^2 = 2^{p-1}N^2\,,$$

which means that we must have

$$\left|q^{(p)}\right|^2 = 2^{p-2}\cdot 2^{p-1}N^2 = 2^{2p-3}N^2\,.$$

As a matter of convention, we want to define our microscopic order parameter tensor to have a norm of $1/2$ for all p, i.e.

$$\left|q^{(p)}\right|^2 = \frac{1}{2} \;\;\forall\;\; p\,.$$

This gives us

$$\left|q^{(p)}\right|^2 = 2^{2p-3}N^2 = \frac{1}{2} \;\Rightarrow\; N^2 = 2^{2-2p} \;\Rightarrow\; N = 2^{1-p}\,.$$

[6] One way in which we can think of this is that we define a coordinate system such that $\boldsymbol{\nu}^{(p)}$ is initially oriented along the x-axis, and letting the coordinate system rotate in such a way that $\boldsymbol{\nu}^{(p)}$ is always lying along the rotating x-axis and the angle of rotation α of the coordinate system is always equal to the phase ϑ_p of $\boldsymbol{\nu}^{(p)}$.

which means that

$$q^{(p)} \equiv \sqrt{2^{p-2}}\left[\!\left[\left(\boldsymbol{\nu}^{(p)}\right)^{\otimes p}\right]\!\right] = \sqrt{2^{p-2}}\cdot 2^{1-p}A$$

$$= \sqrt{2^{-p}}\sum_{k=0}^{\lfloor \frac{p}{2} \rfloor}\left\{\sum_{\{\pi^{2k}\}}(-1)^k\cos\left(p\vartheta_p\right)\mathbf{e}_{\pi_1^{2k}}\otimes\ldots\otimes\mathbf{e}_{\pi_p^{2k}} + \sum_{\{\pi^{2k+1}\}}(-1)^k\sin\left(p\vartheta_p\right)\mathbf{e}_{\pi_1^{2k+1}}\otimes\ldots\otimes\mathbf{e}_{\pi_p^{2k+1}}\right\}.$$

From this it follows that the components of $q^{(p)}$ can be expressed as

$$q^{(p)}_{\pi_1^k\ldots\pi_p^k} = \begin{cases} \sqrt{2^{-p}}\cos\left(p\vartheta_p\right), & k \bmod 4 = 0 \\ \sqrt{2^{-p}}\sin\left(p\vartheta_p\right), & k \bmod 4 = 1 \\ -\sqrt{2^{-p}}\cos\left(p\vartheta_p\right), & k \bmod 4 = 2 \\ -\sqrt{2^{-p}}\sin\left(p\vartheta_p\right), & k \bmod 4 = 3 \end{cases} \tag{3.11}$$

where π^k is, as before, an arbitrary permutation of k 2's and $p-k$ 1's.

With this we finally have the entire structure of the microscopic order parameter tensor. Despite having only two free components, which, as we have just seen are what embodies the $2\pi/p$ rotational symmetry of the p-atic order parameter tensor, the way in which those components are arranged to produce the full rank-p order parameter tensor gives it additional properties which enable it to carry a wealth of more subtle geometric information about the system, such as splay, bend and twist [14], which can be used to extract information about various kinds of distortions in the ordering of the system. Therefore, it should come as no surprise that a tensorial formulation of the hydrodynamics of p-atics has enjoyed a great deal of popularity over the decades. Nevertheless, this approach is not without disadvantages, and one of our goals in this thesis is to address some of them.

In a comprehensive hydrodynamic theory of p-atic liquid crystals in two dimensions, most of the quantities of interest would either be scalars, vectors or rank-2 tensors, meaning that any dynamical variable in such a theory would in general have at most four components. The p-atic order parameter tensor, with its 2^p components would be the only dynamical variable with a number of components disproportionately larger than that of any of the other dynamical variables (Fig. 3.4), which means that in order for us to properly incorporate it into a hydrodynamic theory, we would need to construct all the appropriate contractions of the order parameter tensor with the other dynamical variables, itself or gradient operators. What is more, we would need to do this in a way which can accommodate the changing number of components of the order parameter tensor for different values of p without affecting the resulting dynamics. It should go without saying that this procedure can quickly become a major source of not only computational, but also conceptual complication, which we would like to mitigate by formulating the dynamics of p-atic liquid crystals using only the two independent components of the p-atic order parameter tensor instead. Although disregarding the 2^p-2 remaining components of the order parameter tensor comes at the cost of losing the finer details of the geometry of the p-atic order parameter and its topological defects, we want to argue that the essential aspects of the physics and material properties of p-atic liquid crystals - namely the dynamics of their topological defects - can still be captured using only the two independent components of the order parameter tensor.

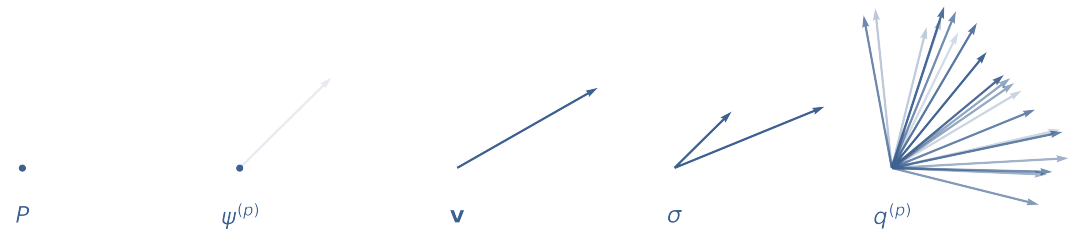

Figure 3.4: Schematic representation of the various dynamical variables that we come across in the study of the hydrodynamics of p-atics, arranged in order of increasing number of components. On the far left is a simple scalar, such as the isotropic pressure, which has no sense of directionality associated with it. Next to it is the scalar order parameter we would like to construct. Being a complex scalar, it will have a sense of directionality associated with it though its phase, as indicated by the faded arrow. Depicted next to the scalar order parameter is a vector with only two components in two dimensions. Next to the vector again is a rank-2 tensor with four components in two dimensions, an example of which might be the stress tensors which appear when we couple the order parameter to a flow. To the far right is an illustration of p-atic order parameter tensor, which will in general have considerably more components than any of the other dynamical variables.

To do this, we will first need to construct an order parameter which can carry the information in the two independent

components of $q^{(p)}$ as a single object, and the most straightforward way to do this is to employ the other commonly used form of a p-atic order parameter, namely a complex scalar, which we will want to consider next.

3.1.4 Complex scalar order parameter

The simplest way in which we could construct a complex scalar p-atic order parameter is to use the explicit form of the components of the order parameter tensor that we have already derived in eq. (3.11). Using $q^{(p)}_{11\ldots1}$ and $q^{(p)}_{21\ldots1}$ as the independent components, we can define a microscopic complex scalar order parameter as

$$\psi_p \equiv \sqrt{2^p}\left(q^{(p)}_{11\ldots1} + iq^{(p)}_{21\ldots1}\right) , \tag{3.12}$$

where we include the prefactor $\sqrt{2^p}$ for convention such that ψ_p has unit magnitude for any p. Using the expressions in eq. (3.11), we get

$$\psi_p = \cos\left(p\vartheta_p\right) + i\sin\left(p\vartheta_p\right) = e^{ip\vartheta_p} . \tag{3.13}$$

Now, although defining the complex scalar order parameter from the two independent components of the order parameter tensor is perfectly legitimate, we could also construct ψ_p without considering the tensorial order parameter at all, but by only considering the symmetry of p-atic particles instead. As a point of interest, as well as for the sake of completeness, we will also take a look at this second way of constructing the scalar p-atic order parameter. This should give us another perspective on why the mapping of the order parameter tensor to a complex scalar in eq. (3.12) and the resulting expression in eq. (3.13) is reasonable, as well as tying everything we've done so far in this section to the discussions in Chapter 2, thereby allowing us to also throw light on one final noteworthy aspect of the p-atic order parameter (tensor or scalar), namely the relationship between its phase and the particle direction ϑ_p.

Let us go back to Figure 3.1 for a moment. It is quite clear from the geometry of the nematic particle that whatever orientation it is in, we only need to turn it half a revolution in order to get it to an orientation that is indistinguishable from the initial one. To be more concrete, if we start the particle off parallel to the y-axis, with $\boldsymbol{\nu}^{(2)}$ pointing in the negative y direction, and then let the particle rotate in the standard sense (i.e. we let ϑ_2 increase), then as soon as it is parallel to the y-axis again and $\boldsymbol{\nu}^{(2)}$ is pointing in the positive y direction, the particle will have swept through all possible orientations it can have. The implication of this for the director $\boldsymbol{\nu}^{(2)}$ is that if we let ϑ_2 increase any further such that $\boldsymbol{\nu}^{(2)}$ enters the second quadrant, we will obtain no new orientations of the particle, which means that all values of ϑ_2 for which $\boldsymbol{\nu}^{(2)}$ lies in the second and third quadrants are redundant. Therefore, in order for $\boldsymbol{\nu}^{(2)}$ to only take on values that correspond to all the *unique* orientations of the nematic particle, we restrict the range of values of ϑ_2 to the interval $[-\pi/2, \pi/2]$, as indicated by the bold dashed line in the right plot in Figure 3.1.

By exactly the same reasoning, we can infer that the same will be true for the case of $p = 3$ - as can be seen in the first and second columns of plots in Figure 3.5 [7] - and indeed for any value of p; we will always have to restrict the values of ϑ_p to the interval $[-\pi/p, \pi/p]$ in order for every value of $\boldsymbol{\nu}^{(p)}$ to correspond to one and only one unique orientation of a general p-atic particle.

This feature of $\boldsymbol{\nu}^{(p)}$ makes using it directly as our p-atic order parameter somewhat impractical, because whatever dynamical equations we might formulate using $\boldsymbol{\nu}^{(p)}$, we would have no simple way of imposing the restriction on the range of values of ϑ_p. For all the equations would know, $\boldsymbol{\nu}^{(p)}$ would always be simply

$$\boldsymbol{\nu}^{(p)} = \left(\cos\vartheta_p, \sin\vartheta_p\right) ,$$

and there would be no intrinsic feature of the equations that would prevent ϑ_p from taking values outside the interval $[-\pi/p, \pi/p]$ and thus reintroduce the very ambiguities that we wanted to avoid by restricting the range of values of ϑ_p in the first place. What we want, then, is to construct an order parameter that takes on values over the whole circle, i.e. with a phase $\theta_p \in [-\pi, \pi]$, and which to each point on the circle associates one and only one unique orientation of the p-atic particle in a way that makes it invariant under rotations by $2\pi/p$.[8] In other words, we want an object that to each direction of the director $\boldsymbol{\nu}^{(p)}$ associates some other direction in a unique way, and in a way that endows it with the discrete rotational symmetry of $2\pi/p$.

One valid candidate for such an object would be a complex scalar, and so we define a complex scalar order parameter ψ_p as

$$\psi_p \equiv e^{i\theta_p} , \tag{3.14}$$

[7] See also supplementary figures C.6-C.8

[8] Were it not for the requirement of invariance under rotations by $2\pi/p$, we could in principle construct any two-component object as our order parameter, as long as its phase grows strictly monotonously with ϑ_p.

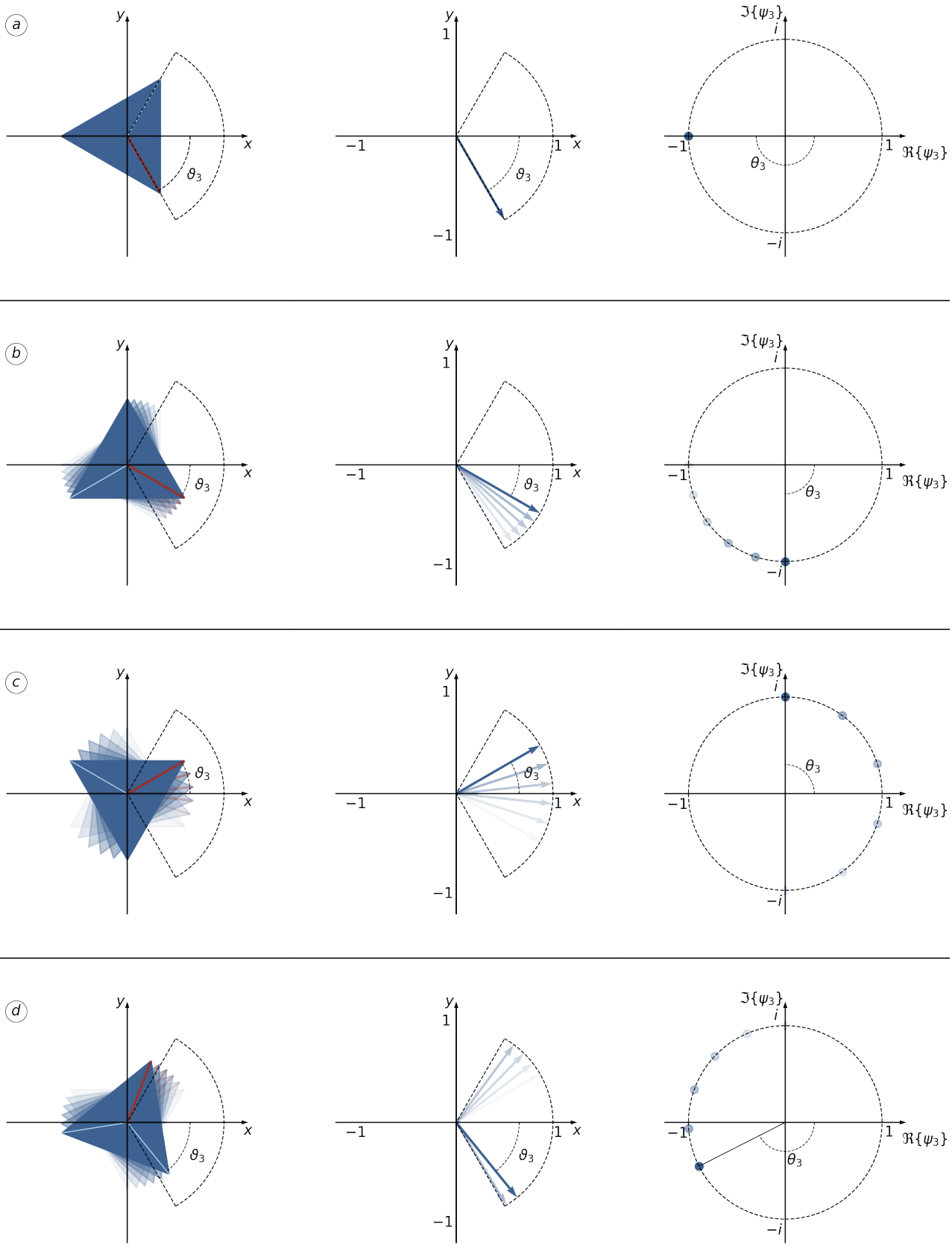

Figure 3.5: Illustration of the relationship between the orientation of a triatic ($p = 3$) particle (left column), the corresponding director $\boldsymbol{\nu}^{(3)}$ (middle column), and the complex scalar order parameter ψ_3 (right column). We can see that as the particle rotates, the director $\boldsymbol{\nu}^{(3)}$ follows suit up to a certain point. Once the corner of the particle that initially started at $-\pi/3$ (indicated by the red line) passes $\pi/3$ (row d), the particle, naturally, just continues to rotate as normal. The director, on the other hand - because of the restriction on the range of values of its phase - makes a jump back to $-\pi/3$, consistent with the fact that after the first corner of the particle passes $\pi/3$ the particle reaches configurations that are indistinguishable from the ones it has already had. Meanwhile the complex order parameter ψ_3, because of the way we define it, makes no such jump. It simply rotates around the unit circle whatever the orientation of the particle is, but - crucially - while still retaining the information about the particle's orientation due to the way it is defined.

where

$$\theta_p \equiv p\vartheta_p \tag{3.15}$$

is the order parameter phase. With this expression for the order parameter phase θ_p we see more explicitly the fact that the order parameter phase doesn't represent anything physical - as is also evident from Figure 3.5. The only quantity with a direct physical interpretation is the phase ϑ_p of the unit director $\boldsymbol{\nu}^{(p)}$. As θ_p is a scaled version of ϑ_p, the direction of ψ_p doesn't directly represent the orientation of anything physical since it will in general be different than the direction of $\boldsymbol{\nu}^{(p)}$. Nevertheless, what θ_p does give us is the fulfillment of the two requirements that we make on ψ_p; it makes ψ_p invariant under rotations by $2\pi/p$:

$$\psi_p = e^{i\theta_p} = e^{ip\vartheta_p} \to e^{ip\left(\vartheta_p + \frac{2\pi}{p}\right)} = e^{ip\vartheta_p} e^{i2\pi} = e^{ip\vartheta_p} = \psi_p \,,$$

and it lies in the interval $[-\pi, \pi]$:

$$\vartheta_p \in \left[-\frac{\pi}{p}, \frac{\pi}{p}\right] \Rightarrow \theta_p = p\vartheta_p \in p\left[-\frac{\pi}{p}, \frac{\pi}{p}\right] = [-\pi, \pi] \,.$$

At this point, it might seem like we are just going around in circles: we begin with a unit vector - $\boldsymbol{\nu}^{(p)}$ - which we say we cannot use as our p-atic order parameter, only to end up with an object - ψ_p - that is perfectly mappable to a unit vector, which we claim that we *can* use as our order parameter. This finally brings us to a subtle but crucial point for our whole theory.

Naïvely, we might be tempted to think that the restriction on the range of values of ϑ_p means that we would have different order parameter spaces - and therefore different order parameters - for different values of p. After all, $\boldsymbol{\nu}^{(p)}$ takes its values on different circle sections for different values of p, so it wouldn't be too far fetched to think that we might need different order parameters for each value of p. However, the crucial observation is that due to the dihedral symmetry of p-atic particles, $\boldsymbol{\nu}^{(p)}$ doesn't just take on values on sections of circles, but it takes on values on sections of circles *with the endpoints identified*. These spaces are all homeomorphic to a circle - the order parameter space corresponding to ψ_p - for any value of p, and it is precisely this feature of p-atic particles and their corresponding unit directors $\boldsymbol{\nu}^{(p)}$ that allows us to define a single order parameter which always takes its values on the whole circle, and which we can therefore use in any dynamical equations that we may formulate without needing to impose any additional constraints on its phase like we would for $\boldsymbol{\nu}^{(p)}$. In other words, the dihedral symmetry of p-atic particles is what allows us to use the same theoretical framework for describing *all* p-atics, and what the preceding argument shows us is exactly how this comes about.

Now that we have our microscopic order parameter, it is a straightforward matter to coarse-grain it in order to obtain a macroscopic one, which we can use to begin formulating dynamical equations for p-atics.

3.1.5 Coarse-graining of the microscopic order parameter

As the final step in the construction of the p-atic order parameter, we want to coarse-grain the microscopic expressions we arrived at in the previous sections to obtain macroscopic quantities which we can use as thermodynamic variables for which we can formulate dynamical equations.

Up to this point, all our considerations and analyses were done on the microscopic scale of a single p-atic particle with orientation ϑ_p with respect to some reference direction. However, our real goal is to describe macroscopic collections of p-atic particles, in which case the microscopic order parameter ψ_p will be

$$\psi_p(\mathbf{r}) = e^{i\theta_p(\mathbf{r})} = e^{ip\vartheta_p(\mathbf{r})} = e^{ip\sum_k \vartheta_p^{(k)}\delta(\mathbf{r}-\mathbf{r}_k)} = \prod_k e^{ip\vartheta_p^{(k)}\delta(\mathbf{r}-\mathbf{r}_k)} \,, \tag{3.16}$$

where $\vartheta_p^{(k)}$ is the orientation of the p-atic particle located at position $\mathbf{r}_k$. The macroscopic order parameter Ψ_p can then be obtained by simply taking the ensemble average of ψ_p. Therefore, we define the macroscopic order parameter Ψ_p as

$$\Psi_p(\mathbf{r}) \equiv \langle \psi_p(\mathbf{r}) \rangle \equiv \frac{1}{N!h^{2N}} \int \frac{e^{-\beta H(\mathbf{R})}}{Z_N} \psi_p(\mathbf{r}) \, d\mathbf{R} = \frac{1}{N!h^{2N}} \int \frac{e^{-\beta H(\mathbf{R})}}{Z_N} e^{ip\sum_k \vartheta_p^{(k)}\delta(\mathbf{r}-\mathbf{r}_k)} \, d\mathbf{R} \,, \tag{3.17}$$

where

$$Z_N \equiv \frac{1}{N!h^{2N}} \int e^{-\beta H(\mathbf{R})} \, d\mathbf{R} \tag{3.18}$$

is the canonical partition function, with $H(\mathbf{R})$ being the Hamiltonian governing the microscopic interactions of the p-atic particles. The explicit evaluation of both integrals is clearly dependent on the specific form of the Hamiltonian for our system, which can be quite complicated, making the integrals difficult to evaluate explicitly. However, the most important issue for our present purposes is the correspondence between the tensorial and microscopic

order parameters, as well as the relationship between the director phase ϑ_p and the order parameter phase θ_p, and that these relationships persist to the macroscopic scale and remain unaffected by the coarse-graining process. Luckily, we can argue that this will be the case without evaluating the integrals in eq.'s (3.17) and (3.18) explicitly.

The multi-particle microscopic order parameter ψ_p is a granular quantity in that it only has non-zero values at the particle locations $\mathbf{r}_k$ by virtue of the delta functions in eq. (3.16). When we compute the ensemble average of ψ_p, this granularity will get smoothed out by the integration over all possible values of $\mathbf{r}_k$, which will result in a macroscopic order parameter Ψ_p that is a smooth function over all of space. Furthermore, because ψ_p is a unit complex number, its ensemble average must of course also be a complex number, which means that we must have

$$\Psi_p(\mathbf{r}) = |\Psi_p|(\mathbf{r})\, e^{i\theta_p(\mathbf{r})}\,, \tag{3.19}$$

where $\theta_p(\mathbf{r})$ now represents the average[9] orientation of particles around the point $\mathbf{r}$.

Meanwhile, the magnitude $|\Psi_p|(\mathbf{r})$ of Ψ_p represents a measure of the average degree of alignment of particles in some neighborhood around $\mathbf{r}$. In a maximally disordered state the values of ψ_p around any given point $\mathbf{r}$ would be evenly distributed around the unit circle in the complex plane, meaning that their average would be zero. In other words, in a maximally disordered state

$$\Psi_p(\mathbf{r}) = 0\,,$$

from which it follows that

$$|\Psi_p|(\mathbf{r}) = 0$$

for a maximally disordered state. For any other state the particles will have some degree of net alignment, and therefore the values of ψ_p around a given point $\mathbf{r}$ will no longer be evenly distributed around the unit circle in the complex plane, but will instead distributed around some preferred direction. Consequently, the magnitudes of ψ_p would no longer average to zero, but will instead average to some non-zero value $|\Psi_p|(\mathbf{r})$. From this it directly follows that there must be some maximum value of $|\Psi_p|(\mathbf{r})$ which occurs in the state where the system is maximally ordered, with all particles in the system being oriented in the same direction. For obvious reasons, we often refer to this state as the *equilibrium state* of the system, and the corresponding magnitude of the order parameter as the *equilibrium magnitude*.[10]

As for the correspondence between θ_p and ϑ_p, the simplest way to argue that the relationship in eq. (3.15) will be maintained after coarse-graining is that the coarse-graining procedure can be applied separately to the microscopic order parameter $\psi_p(\mathbf{r})$ and to the microscopic unit director $\boldsymbol{\nu}^{(p)}$ mapped to its own complex scalar $e^{i\vartheta_p}$. Once this is done, one can go through the same arguments we used on the microscopic scale to arrive at the identity in eq. (3.15).

We can perform the exact same coarse-graining procedure for the tensorial order parameter, and define a macroscopic order parameter tensor $Q^{(p)}$ as

$$Q^{(p)} \equiv \left\langle q^{(p)} \right\rangle \equiv \frac{1}{N!h^{2N}} \int \frac{e^{-\beta H(\mathbf{R})}}{Z_N} q^{(p)}\, d\mathbf{R}\,,$$

which we can also express component-wise:

$$Q^{(p)}_{k_1\ldots k_p} \equiv \left\langle q^{(p)}_{k_1\ldots k_p} \right\rangle \equiv \frac{1}{N!h^{2N}} \int \frac{e^{-\beta H(\mathbf{R})}}{Z_N} q^{(p)}_{k_1\ldots k_p}\, d\mathbf{R}\,. \tag{3.20}$$

We have already established that on the microscopic scale we can relate the scalar and tensorial order parameters to each other via eq. (3.12), and combining equations (3.11) and (3.13) it is clear that we must have

$$q^{(p)}_{\pi^k_1\ldots\pi^k_p} = \begin{cases} \sqrt{2^{-p}}\psi_R\,, & k \bmod 4 = 0 \\ \sqrt{2^{-p}}\psi_I\,, & k \bmod 4 = 1 \\ -\sqrt{2^{-p}}\psi_R\,, & k \bmod 4 = 2 \\ -\sqrt{2^{-p}}\psi_I\,, & k \bmod 4 = 3 \end{cases}, \tag{3.21}$$

Inserting this into eq. (3.20), we get

$$Q^{(p)}_{\pi^k_1\ldots\pi^k_p} = \begin{cases} \sqrt{2^{-p}} \frac{1}{N!h^{2N}} \int \frac{e^{-\beta H(\mathbf{R})}}{Z_N} \psi_R\, d\mathbf{R}\,, & k \bmod 4 = 0 \\ \sqrt{2^{-p}} \frac{1}{N!h^{2N}} \int \frac{e^{-\beta H(\mathbf{R})}}{Z_N} \psi_I\, d\mathbf{R}\,, & k \bmod 4 = 1 \\ -\sqrt{2^{-p}} \frac{1}{N!h^{2N}} \int \frac{e^{-\beta H(\mathbf{R})}}{Z_N} \psi_R\, d\mathbf{R}\,, & k \bmod 4 = 2 \\ -\sqrt{2^{-p}} \frac{1}{N!h^{2N}} \int \frac{e^{-\beta H(\mathbf{R})}}{Z_N} \psi_I\, d\mathbf{R}\,, & k \bmod 4 = 3 \end{cases}.$$

[9] Although we interpret $\theta_p(\mathbf{r})$ as the average orientation of particles around $\mathbf{r}$, it is not actually the same as the ensemble average of the microscopic θ_p, since in general $\langle e^{i\theta_p}\rangle \neq e^{i\langle\theta_p\rangle}$.

[10] Sometimes, this is also referred to as the ground state magnitude.

Now, because computing the ensemble average is a linear operation, then we must have

$$\Psi_p = \Psi_R + i\Psi_I \equiv \langle \psi_p \rangle = \langle \psi_R + i\psi_I \rangle = \langle \psi_R \rangle + i \langle \psi_I \rangle \ .$$

Therefore, we must have

$$Q^{(p)}_{\pi^k_1 \ldots \pi^k_p} = \begin{cases} \sqrt{2^{-p}} \frac{1}{N! h^{2N}} \int \frac{e^{-\beta H(\mathbf{R})}}{Z_N} \psi_R \, d\mathbf{R} \, , & k \bmod 4 = 0 \\ \sqrt{2^{-p}} \frac{1}{N! h^{2N}} \int \frac{e^{-\beta H(\mathbf{R})}}{Z_N} \psi_I \, d\mathbf{R} \, , & k \bmod 4 = 1 \\ -\sqrt{2^{-p}} \frac{1}{N! h^{2N}} \int \frac{e^{-\beta H(\mathbf{R})}}{Z_N} \psi_R \, d\mathbf{R} \, , & k \bmod 4 = 2 \\ -\sqrt{2^{-p}} \frac{1}{N! h^{2N}} \int \frac{e^{-\beta H(\mathbf{R})}}{Z_N} \psi_I \, d\mathbf{R} \, , & k \bmod 4 = 3 \end{cases} = \begin{cases} \sqrt{2^{-p}} \Psi_R \, , & k \bmod 4 = 0 \\ \sqrt{2^{-p}} \Psi_I \, , & k \bmod 4 = 1 \\ -\sqrt{2^{-p}} \Psi_R \, , & k \bmod 4 = 2 \\ -\sqrt{2^{-p}} \Psi_I \, , & k \bmod 4 = 3 \end{cases} ,$$

and with this we see that the relationship between the scalar and tensorial order parameters is indeed maintained to the macroscopic scale.

With our order parameter fully constructed, we now want to take a brief look at one final aspect of the p-atic order parameter before we move on to the energetics of p-atics, namely p-atic topological defects.

3.1.6 Elementary defects in p-atics

In Chapter 2 we saw how topological point defects, which are characterized by their associated winding numbers, or topological charges, naturally arise in systems with broken $O(2)$ symmetry, and because p-atic liquid crystals are just such a class of systems, we would expect them to exhibit the same kind of defects.

On first instinct, one might object that the arguments we made in Chapter 2 would be of little use to us here with a complex scalar order parameter, since all of our analyses in that chapter were based on vectorial order parameters. However, although the complex numbers are not isomorphic to a (real) two-dimensional vector space[11], complex scalars and two-dimensional vectors do have some properties in common - the crucial ones for us being that both have a meaningful notion of a magnitude and a phase associated with them. This means that although the complex numbers are not isomorphic to a two-dimensional vector space, we can still visualize the value of complex numbers (complex scalar fields) with real two-dimensional vectors (vector fields), which again means that both types of object can be used to represent the order parameter of a system with broken $O(2)$ symmetry. In other words, even though the complex numbers and two-dimensional vector spaces are not themselves isomorphic to each other, the order parameter spaces corresponding to each type of order parameter *are*! We can see this formally with the map

$$\Psi_p \to \mathbf{\Psi}_p = (\Re\{\Psi_p\}, \Im\{\Psi_p\}) \ ,$$

and the inverse map

$$\mathbf{\Psi}_p \to \Psi_p = \Psi_x + i\Psi_y \, .$$

These two maps clearly constitute a bijection, and by extension an isomorphism between the order parameter space of a complex scalar and the order parameter space of a real two-dimensional vector.

This is, of course, good news for us, because it means that all the discussions from Chapter 2 are perfectly applicable to p-atic liquid crystals and the complex order parameter that we have constructed.

For the purposes of this thesis, as is also common practice in the field of p-atics, we will only focus our attention on defects with the lowest (non-zero) charge - which we will call *elementary defects* - for the primary reason that any higher charge defects are energetically unstable and will always dissociate into groups of defects with lowest non-zero charge[12].

As we have seen in Chapter 2, the charge of topological point defects in systems with broken $O(2)$ symmetry is given by the winding number of phase singularities in their order parameters. However, in the case of p-atics, the order parameter doesn't really represent anything physical, but is instead an abstract quantity which we use to encode information about the structure and ordering properties of a whole class of systems which may not have anything to do with each other physically. The implication of this is that when we have a defect of charge m_p in

[11] In this context, perhaps the clearest manifestation of that fact is that superpositions of different configurations of complex scalar and real vector fields do not produce the same results. For example, if we have two configurations $\Psi_1 = |\Psi_1| e^{i\theta_1}$ and $\Psi_2 = |\Psi_2| e^{i\theta_2}$ of a complex scalar field, for our purposes their superposition Ψ_T is obtained multiplicatively, i.e. $\Psi_T = \Psi_1 \Psi_2 = |\Psi_1| |\Psi_2| e^{i(\theta_1 + \theta_2)}$, the obvious reason for this being that the phases of the two configurations combine additively, as we would like them to for describing the ordering properties of systems of structured particles. However, if we map the two initial configurations of the complex scalar field to vectors $\mathbf{\Psi}_1$ and $\mathbf{\Psi}_2$ in the usual way: $\mathbf{\Psi}_1 = (\Re\{\Psi_1\}, \Im\{\Psi_1\})$ and $\mathbf{\Psi}_2 = (\Re\{\Psi_2\}, \Im\{\Psi_2\})$, then the only way we could superimpose those two (vector) configurations with each other would be to add them together, which would *not* result in a corresponding map $\mathbf{\Psi}_T = (\Re\{\Psi_T\}, \Im\{\Psi_T\})$.

[12] See supplementary Figure C.1 for a demonstration of this via a numerical solution of eq. (3.29).

the order parameter, the one thing we have to characterize that defect by - namely its charge - would be the same across all p-atic systems even though the exact way in which the defect manifests itself physically will in general be different in different p-atics. Therefore, we would like to define a charge s_p of p-atic defects in a way which reflects the nature of the p-atic system in which it appears.

The natural way to do this is of course to use the phase ϑ_p of the p-atic director $\mathbf{n}^{(p)}$, since it directly represents the physical orientation of the p-atic particles. Therefore, we define

$$s_p \equiv \oint_{\mathcal{M}} d\vartheta_p \,.$$

Now, because of the correspondence in eq. (3.15) between the director phase and the order parameter phase, it follows that we must have

$$s_p \equiv \oint_{\mathcal{M}} d\vartheta_p = \frac{1}{p} \oint_{\mathcal{M}} d\theta_p = \frac{m_p}{p} \,.$$

In Chapter 2, we have already established that m_p must be an integer for an order parameter like Ψ_p, and with p being by definition a natural number it follows from the expression above that for any $p > 1$ the charge s_p of p-atic topological point defects will be *fractional*, which is arguably one of the most distinguishing features of p-atic liquid crystals in the field of ordered media. The way these defects manifest themselves in various p-atics is shown in Figure 3.6 for the cases $p = 1, 2, 3, 4$ and $m_p = \pm 1$.

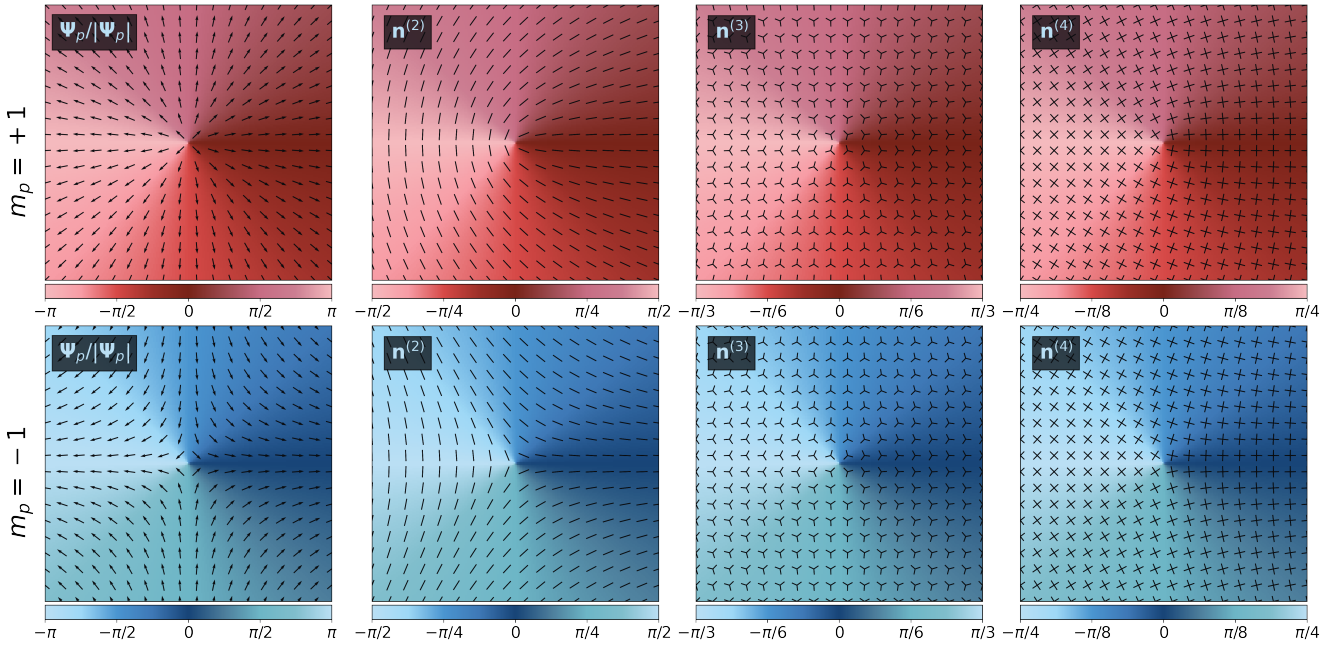

Figure 3.6: Elementary topological defects in p-atics. The leftmost column of plots shows defects with charges $m_p = 1$ (top row) and $m_p = -1$ (bottom row) in the order parameter Ψ_p, while the remaining columns show how these defects manifest themselves in the unit directors of p-atics for $p = 2, 3, 4$. Additionally, because of the relationship between the phase of the order parameter and the phase of the unit director in eq. (3.15), the leftmost column also serves to show how the $m_p = \pm 1$ defects manifest themselves in a polar system, since for those systems $\theta_1 = 1 \cdot \vartheta_1 = \vartheta_1$. The unit directors $\mathbf{n}^{(p)}$ are visualized using p-legged stars in order to emphasize and better visualize the p-fold rotational symmetry of the p-atic particles. The honest-to-God directors can be thought of as being superimposed over the leg which lies within the interval $[-\pi/p, \pi/p]$ on any given p-star. As a particular point of interest, we may note the manifestation of the $\pm 1/2$ nematic defects in the fingerprint in Figure 1.1.

Now that we have established what the exact defects are whose dynamics we want to study, we can plunge into the energetics of p-atics!

3.2 The universality of dry p-atics

We want to begin formulating a description of the dynamics of p-atic liquid crystals, and as a first step to that end, we want to consider the regime where dissipative forces are the dominant influence in our systems. Intuitively, this amounts to considering the state of the system to be changing slowly enough for it to be at inhomogeneous thermodynamic equilibrium at every instant of time, which means that we can think of this process as an extension of the concept of quasi-static processes to inhomogeneous situations. By definition, the regime of energy dissipation is one where the system is losing energy at every instant during its evolution, which allows us to formulate

a time-evolution equation for the p-atic order parameter using the principle of minimization of the free energy functional of the order parameter. For this reason, we often call the resulting dynamics *relaxational dynamics*, and the standard way of obtaining their equations is to set the time derivative of the order parameter proportional to the (negative) functional derivative of the free energy functional[13].

Furthermore, as a first demonstration of the conceptual and computational simplifications we gain by using a complex scalar order parameter, we will also demonstrate that the relaxational dynamics of p-atics just described are universal, which is to say that they do not depend on the value of p. This can be done in two ways: we can either start with a tensorial free energy functional which we reformulate in terms of our complex scalar order parameter, and then use it to derive the dynamical evolution equations, or we can start from the tensorial free energy functional, derive the dynamical equations for the order parameter tensor and then reformulate the result in terms of the complex scalar order parameter. Naturally, both routes should lead us to the same final dynamical equations, and since both approaches are nice exercises in variational calculus, we will demonstrate both explicitly. We will take the former approach here, while the latter is left to Appendix B, where the detailed calculations for both are also presented.

To describe the dynamics of dry p-atics, we begin with the standard Landau free energy functional of the order parameter, which we can express in terms of the order parameter tensor $Q^{(p)}$ as [13]

$$F\left[Q^{(p)}\right] = \int \frac{L_p}{2}\left|\nabla Q^{(p)}\right|^2 + \frac{A_p}{2}\left|Q^{(p)}\right|^2 + \frac{B_p}{4}\left|Q^{(p)}\right|^4 \, d\mathbf{r}\,, \tag{3.22}$$

where L_p, A_p and B_p are phenomenological parameters, with L_p being a measure of the elastic stiffness of the p-atic, while A_p and B_p determine the exact shape of the Mexican hat free energy density, which in turn determines the equilibrium value of the order parameter. In principle, all three parameters can depend on temperature, giving different functional forms to the free energy for different thermal regimes. However, in this thesis we will consider our systems to always be at a fixed temperature, in which case we can regard all three parameters in F_p as constants.[14]

The three terms in the integrand in eq. (3.22) are given as contractions of $Q^{(p)}$ and its gradient with themselves, i.e.

$$\left|\nabla Q^{(p)}\right|^2 = \partial_i Q^{(p)}_{k_1\ldots k_p}\partial_i Q^{(p)}_{k_1\ldots k_p}\,,\quad \left|Q^{(p)}\right|^2 = Q^{(p)}_{k_1\ldots k_p}Q^{(p)}_{k_1\ldots k_p}\,,\ \text{ and }\ \left|Q^{(p)}\right|^4 = \left(Q^{(p)}_{k_1\ldots k_p}Q^{(p)}_{k_1\ldots k_p}\right)^2\,.$$

At a glance, it is not immediately obvious how these expressions all combine with each other to result in the same kind of dynamics for all values of p, as the number of components, and consequently the number of contractions in each expression clearly depend on p. Nevertheless, due to $Q^{(p)}$ only having two independent components, it turns out that we will always have

$$\left|\nabla Q^{(p)}\right|^2 = \frac{1}{2}\left|\nabla\Psi_p\right|^2\,,\quad \left|Q^{(p)}\right|^2 = \frac{1}{2}\left|\Psi_p\right|^2\,,\ \text{ and }\ \left|Q^{(p)}\right|^4 = \frac{1}{4}\left|\Psi_p\right|^4\,,$$

which means that the free energy can be expressed in therms of the scalar order parameter Ψ_p as

$$F\left[\Psi_p\right] = \int \frac{L_p}{4}\left|\nabla\Psi_p\right|^2 + \frac{A_p}{4}\left|\Psi_p\right|^2 + \frac{B_p}{16}\left|\Psi_p\right|^4 \, d\mathbf{r}\,. \tag{3.23}$$

As we've already argued in Section 3.1, Ψ_p is a complex scalar that doesn't change its structure with varying values of p, which means that the free energy in eq. (3.23) will have exactly the same form for any value of p, and so it follows that the dynamics resulting from this free energy functional must be the same for all p. In other words, all dry p-atics must have exactly the same evolution given the same initial conditions, and we see how the complex scalar order parameter helps us expose this feature and make it manifest in our equations in a way that the tensorial order parameter does not.

Before we proceed to derive the dynamical equation for Ψ_p, we will first rewrite the free energy in a slightly different form by conventionally setting

$$L_p \equiv 2K_p\,,\ A_p \equiv -2g_p\,,\ B_p \equiv 4g_p\,,\ K_p, g_p > 0\,, \tag{3.24}$$

which gives us

$$F_p[\Psi_p] = \int \frac{K_p}{2}|\nabla\Psi_p|^2 - \frac{g_p}{2}\left(1 - \frac{1}{2}|\Psi_p|^2\right)|\Psi_p|^2 \, d\mathbf{r}\,. \tag{3.25}$$

[13]One intuitive way of thinking of this is as a continuum generalization of the standard method of setting the time evolution of a dynamical variable proportional to the gradient of some potential. For example, a mass in free fall will move in such a way as to minimize its gravitational potential, and we describe this by setting the time derivative of its momentum proportional to the negative gradient of the gravitational potential.

[14]Specifically, we will regard them as constants with respect to temperature. In principle, they could still depend on the value of p, although, as we will see, that will still have no significant consequence for dry p-atics.

The choice to reduce the coefficients A_p and B_p to a single parameter g_p simply corresponds to fixing the ratio between the contributions of $|\Psi_p|^2$ and $|\Psi_p|^4$ to the local free energy (density).[15] As we will see shortly, this simply fixes the equilibrium value of $|\Psi_p|$ to 1.

To derive a dynamical evolution equation for Ψ_p, we want to use the principle of minimization of the free energy functional in eq. (3.25) - the standard way of doing this being to set the time derivative of Ψ_p proportional to the negative functional derivative of F_p with respect to Ψ_p. Now, from statistical mechanics we know that the functional derivative of the free energy with respect to the order parameter gives us the thermodynamically conjugate field to the order parameter. In the case of p-atics, the thermodynamically conjugate field to the order parameter is known as *molecular field*, and is given as

$$h_p \equiv \frac{\delta F_p}{\delta \Psi_p}\,. \tag{3.26}$$

In other words, the evolution equation for the p-atic order parameter can be obtained by setting its time derivative proportional to the negative of its thermodynamically conjugate field, which we can understand physically by way of analogy.

Suppose we have a gas which is initially at some temperature T_0, and is confined in a movable piston. If we put the piston in contact with a heat source, the gas will naturally start heating up, which will cause its pressure to increase, making the gas expand in the piston. In other words, as the gas heats up, its *pressure* will increase, which will lead to a change in its *volume*. Therefore, if we want to describe the time evolution of the volume in this process, it would not be unreasonable to set the time derivative of the volume proportional to its thermodynamically conjugate variable - the pressure. This is precisely what we do with the p-atic order parameter and the molecular field.

Now, because the order parameter Ψ_p is a complex number, it turns out that the molecular field will be given strictly in terms of Ψ_p^* rather than Ψ_p itself, and because we want to formulate a dynamical equation for Ψ_p only in terms of itself, we define the evolution equation in terms of h_p^* rather than h_p. Therefore, we define the time evolution of Ψ_p as

$$\partial_t \Psi_p \equiv -\Gamma_p h_p^*\,, \tag{3.27}$$

where Γ_p is the dimensionless[16] rotational viscosity. Using the expression for h_p in terms of the free energy in eq. (3.26), gives us

$$\partial_t \Psi_p = -\Gamma_p \frac{\delta F_p}{\delta \Psi_p^*}\,. \tag{3.28}$$

With the dynamical equation for Ψ_p defined in this way, we can immediately see explicitly that it does result in minimization of the free energy. Computing the time derivative of F_p, we get

$$\frac{d}{dt}F_p = \int \frac{\delta F_p}{\delta \Psi_p}\frac{\partial \Psi_p}{\partial t} + \frac{\delta F_p}{\delta \Psi_p^*}\frac{\partial \Psi_p^*}{\partial t}\,d\mathbf{r} \equiv \int -\frac{1}{\Gamma_p}\partial_t\Psi_p^* \cdot \partial_t \Psi_p - \partial_t \Psi_p \cdot \frac{1}{\Gamma_p}\partial_t \Psi_p^*\,d\mathbf{r} = -\frac{2}{\Gamma_p}\int |\partial_t \Psi_p|^2\,d\mathbf{r}\,.$$

The integrand in the last transition is manifestly positive for all times and positions, and so it follows from the overall negative sign in front of the integral that the time derivative of the free energy on the whole is negative for all t, meaning that the definition of the dynamical equation eq. (3.27) does indeed result in minimization of the free energy.

With F_p given in eq. (3.25), we can readily compute the variational with respect to Ψ_p to obtain the final dynamical equation. This is done in detail in Appendix B, and the result is

$$\partial_t \Psi_p = \Gamma_p \left(\frac{K_p}{2}\nabla^2 \Psi_p + \frac{g_p}{2}\left(1 - |\Psi_p|^2\right)\Psi_p \right)\,. \tag{3.29}$$

With this evolution equation we can describe the dynamics of any dry p-atic with any initial conditions, and we will take a few moments to examine some of the key properties of those dynamics next.

In Figure 3.7, we can see a time series of the relaxation of the order parameter, which was obtained by a numerical solution of eq. (3.29) over a square domain with periodic boundary conditions.[17] The order parameter was started

[15] This in turn - in light of the dependence of L_p, A_p and B_p on temperature - corresponds to considering the system at some fixed temperature such that the ratio of A_p to B_p is -2.

[16] In general, it will be assumed that all the quantities in the main text are dimensionless unless otherwise stated. For a discussion on the rescaling of dynamical variables, see Appendix A.

[17] Unless otherwise stated, all numerical solution of the equations of motion in this and the next chapter are done on a 256×256 grid, with $dt = 0.1$ in units of τ and $dx = dy = 1$ in units of L, with τ and L defined in Appendix A.

off in a random configuration, and the material parameters were set as $K_p = 10$ and $g_p = 1$.

Using a random initial configuration for the order parameter can be interpreted physically as starting the system off in a maximally disordered state. By the reasoning we used to formulate the dynamical equation for Ψ_p, we would expect the system to find its way to an ordered state from that initial configuration, which is indeed what we see in Figure 3.7. In particular, because we arrived at eq. (3.29) using a principle of *minimization* of the free energy, it follows that we should expect the system to keep ordering itself until it reaches a maximally ordered, or *uniform* state, in which the order parameter can be expressed as

$$\Psi_{p,0} = |\Psi_p|_0 \, e^{i\theta_{p,0}} \,,$$

where $|\Psi_p|_0$ and $\theta_{p,0}$ are both constants. The equilibrium magnitude $|\Psi_p|_0$ can easily be found from eq. (3.29). In equilibrium we must by definition have $\partial_t \Psi_p = 0$. Furthermore, in a uniform state, where both the magnitude and phase of Ψ_p are constant, we will also have $\nabla^2 \Psi_{p,0} = 0$, which means that in the equilibrium state, we must have

$$\frac{g_p}{2}\left(1 - |\Psi_p|_0^2\right)\Psi_{p,0} = 0 \;\rightarrow\; |\Psi_p|_0 = 1 \,.$$

We can verify this numerically also, which is shown in Figure C.2 for the same evolution as in Figure 3.7.

We note, as we have just seen explicitly also, that the dynamical equation for Ψ_p cannot be used to determine the equilibrium *phase* of the order parameter. The reason for this is that the equilibrium phase depends on the route by which the system relaxes to the ground state, and this can only be found by integration of eq. (3.29).

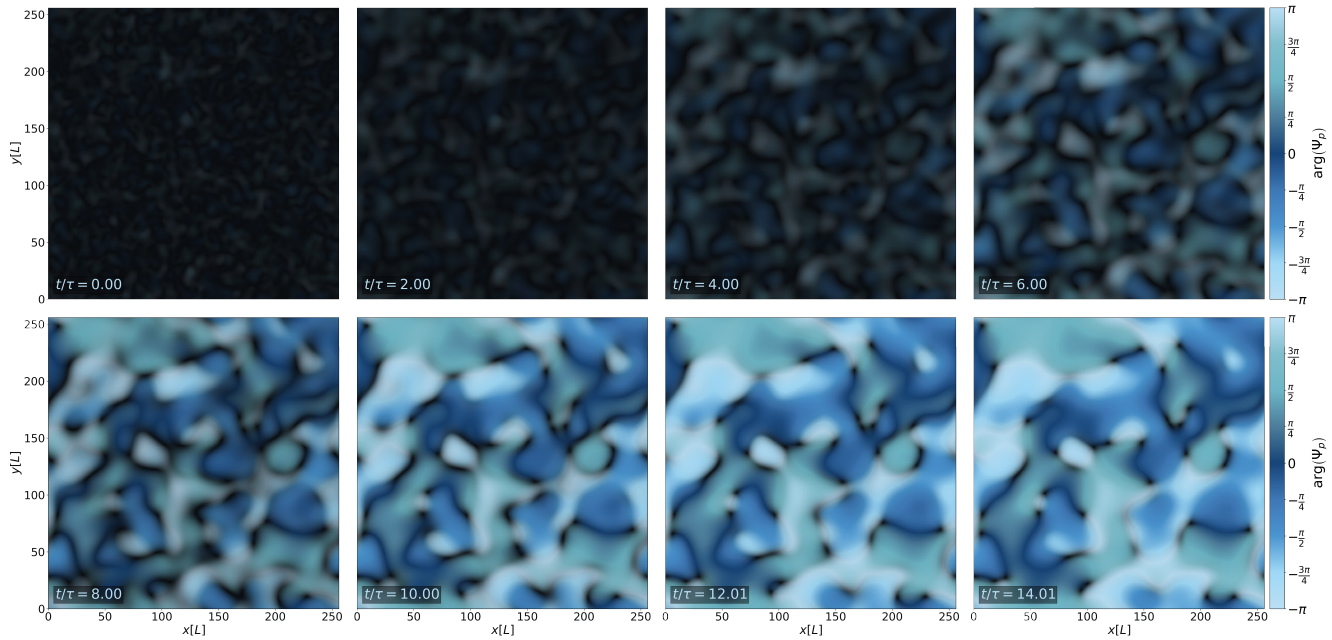

Figure 3.7: Time series of the relaxation of the p-atic order parameter over a 256×256 square grid with periodic boundary conditions. The color of the plot represents the phase of Ψ_p, while the magnitude is visualized by the intensity of the color, where the opacity increases with increasing values of $|\Psi_p|$ and $|\Psi_p| = 0$ corresponds to no intensity (black). The time series demonstrates the relaxation of the order parameter, where the system is started off in a maximally disordered state (top left plot) and evolves to a more ordered state (bottom right plot). Given enough time, the system will reach its equilibrium in a maximally ordered state, which can be seen in the time series for the evolution of the magnitude $|\Psi_p|$ from the same initial conditions, shown in Supplementary Figure C.2.

An interesting feature of the way we solve the dynamical equations for the dry p-atics is the fact that no matter what initial configuration we set for the order parameter, the system will always evolve to a maximally ordered, spatially uniform state, which can be seen explicitly in Figure C.2. The reason for this is that we use periodic boundary conditions to solve the evolution equation for the order parameter, which effectively means that the domain over which we solve the equation has the topology of a torus. As it turns out, this topology is incompatible with having an isolated defect in the system, which we can understand as follows.

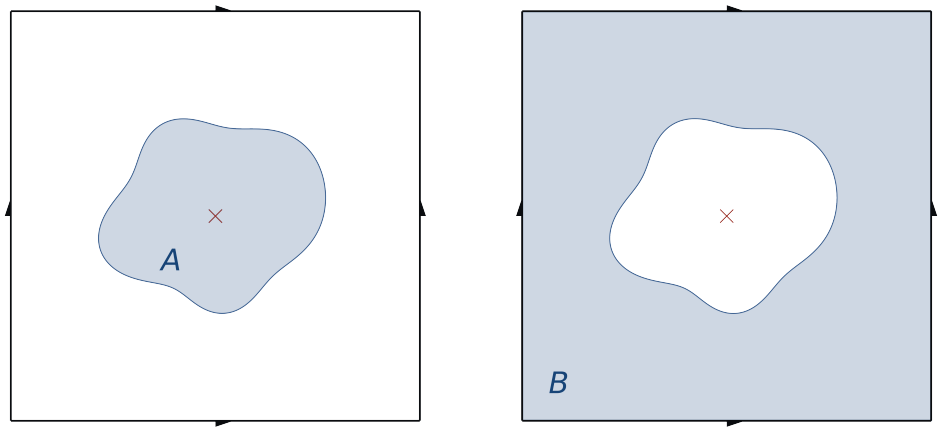

Figure 3.8: An isolated defect - marked by the red cross - in a square domain with periodic boundary conditions. The regions A and B are delimited by an integration contour for determining the winding number of the defect.

Suppose we have a square domain with periodic boundary conditions with a single defect in it, as shown in Figure 3.8. Then, as usual, we can define an integration contour around that defect to compute its winding number. Whatever integration contour we define, it will, naturally, divide the domain into two subdomains A and B, also indicated in Figure 3.8. However, because of the periodic boundary conditions, there is no unambiguous way to define which of the two regions A and B is inside the contour and which is outside. This means that the isolated defect can be considered to be both inside and outside the integration contour at the same time, and consequently, that the calculation of its winding number should be zero and non-zero. The resolution of this contradiction is that no isolated defects can ever appear in a square domain with periodic boundary conditions. Instead, defects must always appear in groups with net charge of zero.

With the essential features of the dry p-atics covered, we want to take one final step and couple the evolution of the order parameter to the evolution of a flow field. This will significantly increase the complexity of the theory, as a coupling between the order parameter and the flow field introduces a whole host of new phenomena which affect the physical description of the system. One such phenomenon is the emergence of various forms of hydrodynamic stress which are unique to the p-atic liquid crystals as they fundamentally depend on the structure of the p-atic particles. In the following, we will want to examine some of these forms of stress and how they affect the flow induced by a single defect in the system.

Chapter 4

Coupling with the flow

In this chapter we want to relax the requirement that dissipative forces are the dominant influence on the dynamics of p-atic systems. As a result, in this regime we expect there to be a flow of matter in the system, which will in turn require us to couple the evolution of the order parameter with the evolution of the flow velocity in order to obtain a proper description of the system's dynamics. As in any continuous medium, the driving influences that affect the dynamics are the various forms of hydrodynamic stresses, whose complexity is increased in p-atic liquid crystals due to the structured nature of p-atic particles.

A complete description of the physics of p-atic liquid crystals in these regimes is too far beyond the scope of this thesis, and we will therefore restrict our attention to one specific aspect of coupling of the order parameter to the flow. As in any hydrodynamic system, one of the major driving influences on the dynamics are the hydrodynamic stresses whose properties and origin depend on the nature of the system. Due to the structure and geometry of their particles, p-atic liquid crystals exhibit unique forms of hydrodynamic stresses which are fundamentally dependent on the p-atic order parameter. Therefore, it should go without saying that an understanding of these stresses and the nature of their dependence on the order of the p-atic, in other words the value of p, is essential for understanding the physics of p-atics on the whole.

In this chapter, we want to examine the way these stresses affect the interplay of p-atic topological defects and the flow of matter in the system. In particular, we want to compute the flow profiles induced by a single p-atic defect in the system, which we will do for the elementary defects discussed in Section 3.1.6.

Furthermore, we will do all the calculations using the complex scalar order parameter we constructed in the previous chapter. Of particular interest will be the expressions for the hydrodynamic stresses that are specific to the p-atics in terms of the complex scalar order parameter, since these are currently found in the literature only in terms of the tensorial order parameter.

4.1 The dynamical equations

As our starting point we will use the dynamical equations for the flow velocity and the order parameter which are given in Ref. [15] as:

$$\rho \frac{D\mathbf{v}}{Dt} = \nabla \cdot \sigma \,,$$

$$\frac{DQ^{(p)}}{Dt} = \Gamma_p H^{(p)} + p \left[\!\!\left[Q^{(p)} \cdot \boldsymbol{\omega} \right]\!\!\right] + \lambda_p \left[\!\!\left[\nabla^{\otimes(p-2)} \mathbf{u} \right]\!\!\right] + \overline{\lambda}_p \operatorname{tr}(\mathbf{u})\, Q^{(p)} + \nu_p \left[\!\!\left[\nabla^{\otimes(p \bmod 2)} \mathbf{u}^{\otimes \lfloor p/2 \rfloor} \right]\!\!\right] ,$$

where, as in Chapter 3, the brackets $[\![\cdots]\!]$ make their argument symmetric and traceless, $H^{(p)}$ is the molecular tensor as defined in eq. (B.1) describing the relaxation of the p-atic free energy, and λ_p, $\overline{\lambda}_p$ and ν_p are material constants. The tensors $\boldsymbol{\omega}$ and $\mathbf{u}$ are respectively the vorticity and strain rate tensors, and are defined as

$$\boldsymbol{\omega} \equiv \frac{1}{2}\left(\nabla \mathbf{v} - (\nabla \mathbf{v})^T\right) \text{ and } \mathbf{u} \equiv \frac{1}{2}\left(\nabla \mathbf{v} + (\nabla \mathbf{v})^T\right) ,$$

or, in component form

$$\omega_{ij} \equiv \frac{1}{2}\left(\partial_i v_j - \partial_j v_i\right) , \; u_{ij} \equiv \frac{1}{2}\left(\partial_i v_j + \partial_j v_i\right) .$$

The dot product in the second term in the evolution equation for the order parameter tensor denotes a contraction of the last index of $Q^{(p)}$ with the first index of $\boldsymbol{\omega}$, such that

$$\left(Q^{(p)} \cdot \boldsymbol{\omega}\right)_{k_1 \ldots k_p} = Q^{(p)}_{k_1 \ldots k_{p-1} i} \omega_{i k_p} \,.$$

The operator $\nabla^{\otimes p}$ is simply the p'th tensorial power of the gradient operator with itself, such that

$$\nabla^{\otimes p} = \mathbf{e}_{k_1} \otimes \ldots \otimes \mathbf{e}_{k_p} \partial_{k_1} \ldots \partial_{k_p} \,,$$

where, by convention

$$\nabla^{\otimes 0} \equiv 1 \,.$$

Meanwhile, the stress tensor σ in the evolution equation for the velocity contains all the forms of stress which may arise as a result of the flow and interactions between the flow and the order parameter. Before we proceed to examine the stress tensor more closely, we will modify the evolution equation for the flow velocity by adding an additional dampening term to describe friction with a substrate, so that

$$\rho \frac{D\mathbf{v}}{Dt} = -\gamma \mathbf{v} + \nabla \cdot \sigma \,,$$

with γ the friction coefficient. Furthermore, we will also want to examine the flow in the regime of low Reynolds number, which effectively means that

$$\frac{D\mathbf{v}}{Dt} \approx \partial_t \mathbf{v} \,.$$

This gives us the final evolution equation for the flow velocity:

$$\rho \partial_t \mathbf{v} = -\gamma \mathbf{v} + \nabla \cdot \sigma \,. \tag{4.1}$$

For the remainder of this chapter, we will want to consider the steady-state solution of this equation and examine the influence of the various kinds of stresses that arise from the interactions of the flow with the order parameter when we have a single defect of charge $\pm 1/p$ in our system.

4.1.1 Decomposition of the stress

The standard way of decomposing the total stress σ is to divide it into a static part $\sigma^{(s)}$ and a dynamic part $\sigma^{(d)}$ such that

$$\sigma = \sigma^{(s)} + \sigma^{(d)} \,.$$

The static stress is given as

$$\sigma^{(s)} = -P\mathbb{I} + \sigma^{(e)} \,,$$

where the first term describes the contribution of the isotropic pressure to the total stress, while $\sigma^{(e)}$ is the elastic stress which results from a static distortion of the order parameter, and is given as

$$\sigma^{(e)}_{ij} = -L_p \partial_i Q^{(p)}_{k_1 \ldots k_p} \partial_j Q^{(p)}_{k_1 \ldots k_p} \,. \tag{4.2}$$

Meanwhile, the dynamic stress is customarily further decomposed into a dissipative viscous contribution $\sigma^{(v)}$, and a conservative, reactive contribution $\sigma^{(r)}$, so that

$$\sigma^{(d)} = \sigma^{(v)} + \sigma^{(r)}$$

The viscous stress is given as

$$\sigma^{(v)} = 2\eta \left[\!\left[\mathbf{u}\right]\!\right] \,,$$

where η is the shear viscosity. With $\mathbf{u}$ being by definition a symmetric tensor, it follows that the only effect of the operator $[\![\cdots]\!]$ is to make $\mathbf{u}$ traceless. However, for this entire chapter, we will work under the assumption of incompressible flow such that $\nabla \cdot \mathbf{v} = 0$. This means that

$$\operatorname{tr} \mathbf{u} = \frac{1}{2} \cdot 2 \partial_i v_i = 0 \,.$$

Therefore, we can express the viscous stress in component form as

$$\sigma^{(v)}_{ij} = \eta \left(\partial_i v_j + \partial_j v_i\right) \,.$$

Meanwhile, the reactive stress is given as

$$\sigma^{(r)} = \lambda_p (-1)^{p-1} \nabla^{\otimes (p-2)} \odot H^{(p)} + \frac{p}{2} \left(Q^{(p)} \cdot H^{(p)} - H^{(p)} \cdot Q^{(p)}\right) \,. \tag{4.3}$$

The operator $\odot$ represents a full contraction of corresponding indices of the tensors on which it acts. In this particular case, the derivative operator on the left has two indices less than the molecular tensor, which leaves two free indices to correspond with the two free indices in a stress tensor. Meanwhile, the dot products between the order parameter and the molecular tensor in the parenthesis in the second term represent a contraction of $p-1$ indices in each of the tensors, leaving a total of two free indices for these terms also. In other words, in component form, the reactive stress can be expressed as

$$\sigma_{ij}^{(r)} = \lambda_p(-1)^{p-1}\partial_{k-1}...\partial_{k_{p-2}}H^{(p)}_{k_1...k_{p-2}ij} + \frac{p}{2}\left(Q^{(p)}_{k_1...k_{p-1}i}H^{(p)}_{k_1...k_{p-1}j} - H^{(p)}_{k_1...k_{p-1}i}Q^{(p)}_{k_1...k_{p-1}j}\right) . \tag{4.4}$$

With these expressions for the stresses, we clearly see that only the elastic and reactive stresses have an explicit dependence on the exact structure of the p-atic systems. We want to examine how these stresses affect the dynamics of individual defects. For later convenience, we will split the reactive stress $\sigma^{(r)}$ into two terms $\sigma^{(r,1)}$ and $\sigma^{(r,2)}$ such that

$$\sigma^{(r)} = \sigma^{(r,1)} + \sigma^{(r,2)} ,$$

where

$$\sigma^{(r,1)} = \lambda_p(-1)^{p-1}\partial_{k-1}...\partial_{k_{p-2}}H^{(p)}_{k_1...k_{p-2}ij} , \tag{4.5}$$

and

$$\sigma^{(r,2)} = \frac{p}{2}\left(Q^{(p)}_{k_1...k_{p-1}i}H^{(p)}_{k_1...k_{p-1}j} - H^{(p)}_{k_1...k_{p-1}i}Q^{(p)}_{k_1...k_{p-1}j}\right) . \tag{4.6}$$

4.2 Defect induced flows

We want to examine how a single p-atic defect affects the velocity flow field under the influence of the various forms of stress discussed in the previous section. To begin with, we will reformulate eq. (4.1) and cast it in a more familiar form which will help us isolate the contributions to the stress which are specific to p-atics. Specifically, we want to re-write eq. (4.1) using the explicit expressions for the static and viscous stresses in terms of the isotropic pressure and velocity gradients respectively. In other words, we want to use that

$$\sigma_{ij} = \sigma_{ij}^{(s)} + \sigma_{ij}^{(d)} = -P\delta_{ij} + \sigma_{ij}^{(e)} + \eta\left(\partial_i v_j + \partial_j v_i\right) + \sigma_{ij}^{(r)} .$$

Inserting into eq. (4.1), we now get in component form

$$\begin{aligned}
\rho\partial_t v_i &= -\gamma v_i + \partial_j\left(-P\delta_{ij} + \eta\left(\partial_i v_j + \partial_j v_i\right) + \sigma_{ij}^{(e)} + \sigma_{ij}^{(r)}\right) \\
&= -\gamma v_i - \partial_i P + \eta\left(\partial_i\partial_j v_j + \partial_j\partial_j v_i\right) + \partial_j\sigma_{ij}^{(e)} + \partial_j\sigma_{ij}^{(r)} \\
&= -\gamma v_i - \partial_i P + \eta\nabla^2 v_i + \partial_j\sigma_{ij}^{(e)} + \partial_j\sigma_{ij}^{(r)} ,
\end{aligned}$$

where we use that $\partial_j v_j = 0$ under the assumption of incompressibility.

This gives us the final evolution equation

$$\rho\partial_t\mathbf{v} = \eta\nabla^2\mathbf{v} - \gamma\mathbf{v} - \nabla P + \nabla\cdot\sigma^{(e)} + \nabla\cdot\sigma^{(r)} .$$

The only terms in the evolution equation which could potentially depend on p are the elastic stress, and the two terms in the reactive stress, and to better expose their dependence on p, we want to re-write them in terms of the complex scalar order parameter Ψ_p. For the elastic stress we have

$$\sigma_{ij}^{(e)} = -\frac{L_p}{2}\left(\partial_i\Psi_R\partial_j\Psi_R + \partial_i\Psi_I\partial_j\Psi_I\right) , \tag{4.7}$$

and for the second term in the reactive stress we have

$$\sigma_{ij}^{(r,2)} = \frac{pL_p}{4}\left(\Psi_i\nabla^2\Psi_j - \Psi_j\nabla^2\Psi_i\right) , \quad i\in\{R,I\} . \tag{4.8}$$

These terms are fully general, and hold for any configuration of the order parameter. What is more, neither term changes its functional form with varying values of p, which means that these contributions to the stress are the same for all p-atics. The last remaining term - the first term in $\sigma^{(r)}$, however, does change its functional form with p. Its general expression will be more complicated due to the nonlinear terms in the order parameter that are contained in $H^{(p)}$, so we want to consider the first term in the reactive stress in the far-field, where the nonlinear

terms in $H^{(p)}$ vanish. Then we can compute the first term of the reactive stress explicitly for a few specific values of p, and the results are

$$p=2: \quad \sigma^{(r,1)} = -\frac{\lambda_2 L_2}{2}\begin{pmatrix} \nabla^2\Psi_R & \nabla^2\Psi_I \\ \nabla^2\Psi_I & -\nabla^2\Psi_R \end{pmatrix}, \tag{4.9a}$$

$$p=3: \quad \sigma^{(r,1)} = -\frac{\lambda_3 L_3}{2\sqrt{2}}\begin{pmatrix} \partial_x\nabla^2\Psi_R + \partial_y\nabla^2\Psi_I & \partial_x\nabla^2\Psi_I - \partial_y\nabla^2\Psi_R \\ \partial_x\nabla^2\Psi_I - \partial_y\nabla^2\Psi_R & -\partial_x\nabla^2\Psi_R - \partial_y\nabla^2\Psi_I \end{pmatrix}, \tag{4.9b}$$

$$p=4: \quad \sigma^{(r,1)} = -\frac{\lambda_4 L_4}{4}\begin{pmatrix} \partial_x^2\nabla^2\Psi_R - \partial_y^2\nabla^2\Psi_R + 2\partial_x\partial_y\Psi_I & \partial_x^2\Psi_I - \partial_y^2\Psi_I - 2\partial_x\partial_y\Psi_R \\ \partial_x^2\Psi_I - \partial_y^2\Psi_I - 2\partial_x\partial_y\Psi_R & -\partial_x^2\nabla^2\Psi_R + \partial_y^2\nabla^2\Psi_R - 2\partial_x\partial_y\Psi_I \end{pmatrix}. \tag{4.9c}$$

Now that we have the explicit expressions for all the forms of stress, we want to consider their influence on the steady state flow when we have a single defect centered at the origin. In the steady-state we have, by definition, $\partial_t \mathbf{v} = 0$, which means that the velocity field will be given by the the equation

$$\eta\nabla^2\mathbf{v} - \gamma\mathbf{v} = -\left(\nabla\cdot\sigma^{(e)} + \nabla\cdot\sigma^{(r,1)} + \nabla\cdot\sigma^{(r,2)}\right) \tag{4.10}$$

This equation will be solved in a variety of regimes, as determined by the coefficients η and γ. The solutions will be obtained numerically using a finite difference approximation with Dirichlet boundary conditions on a 128×128 grid. The results are shown in the figures below. In each figure, the plots with red streamlines show the flow field induced by the $+1/p$ defect, while the plots with blue streamlines show the flow field induced by the $-1/p$ defect.

No friction

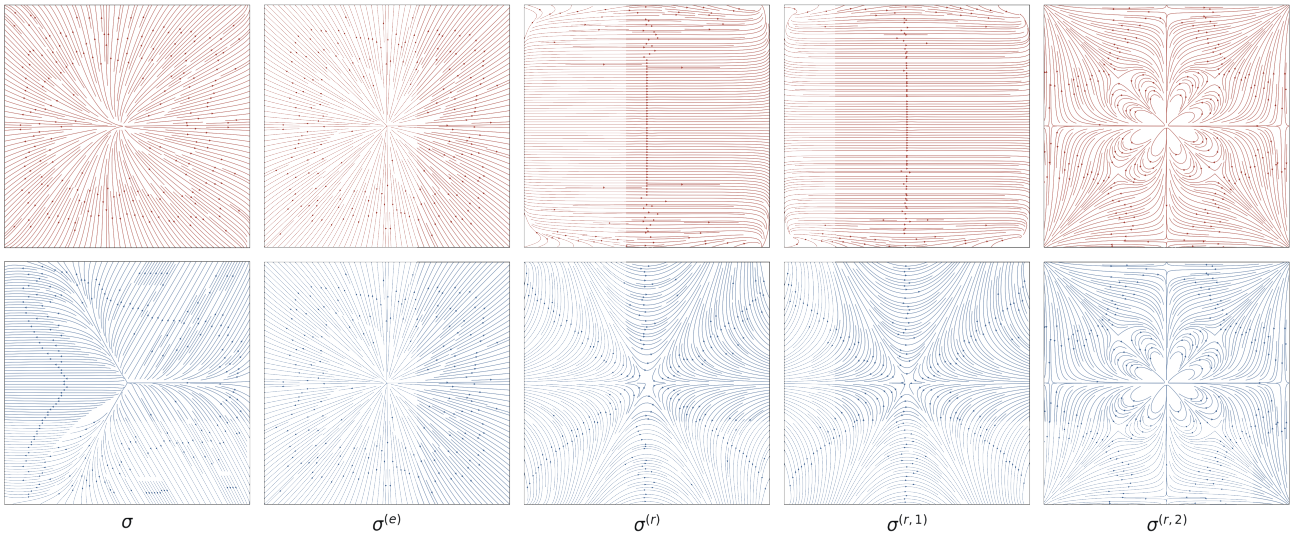

Figure 4.1: $p=2$, $\eta=1$, $\gamma=0$.

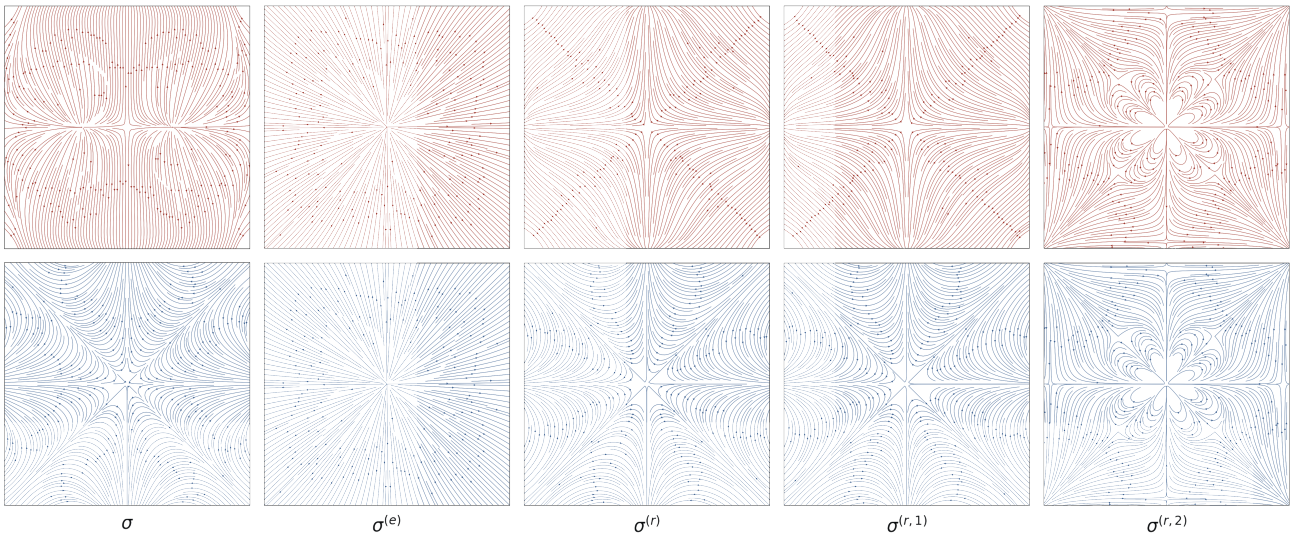

Figure 4.2: $p = 3$, $\eta = 1$, $\gamma = 0$.

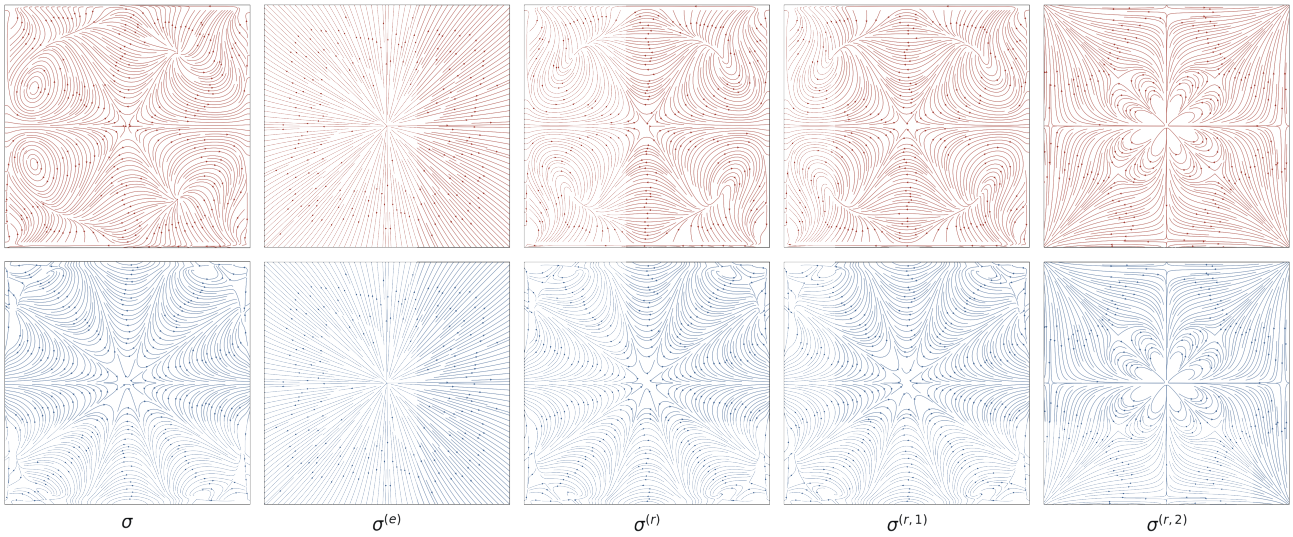

Figure 4.3: $p = 4$, $\eta = 1$, $\gamma = 0$.

No viscosity

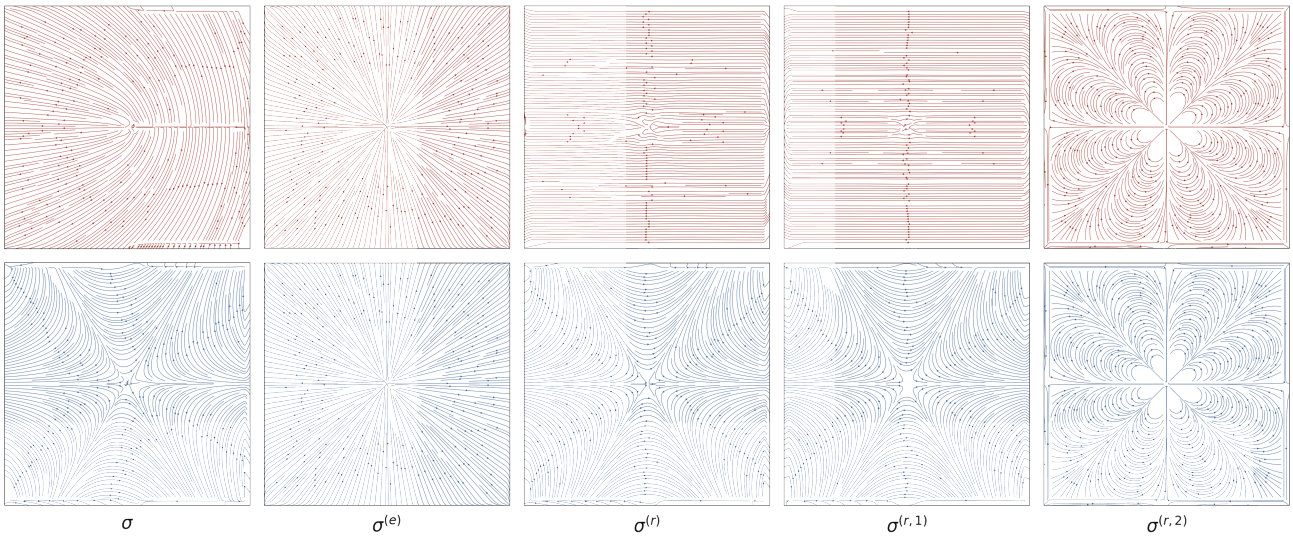

Figure 4.4: $p = 2$, $\eta = 0$, $\gamma = 1$.

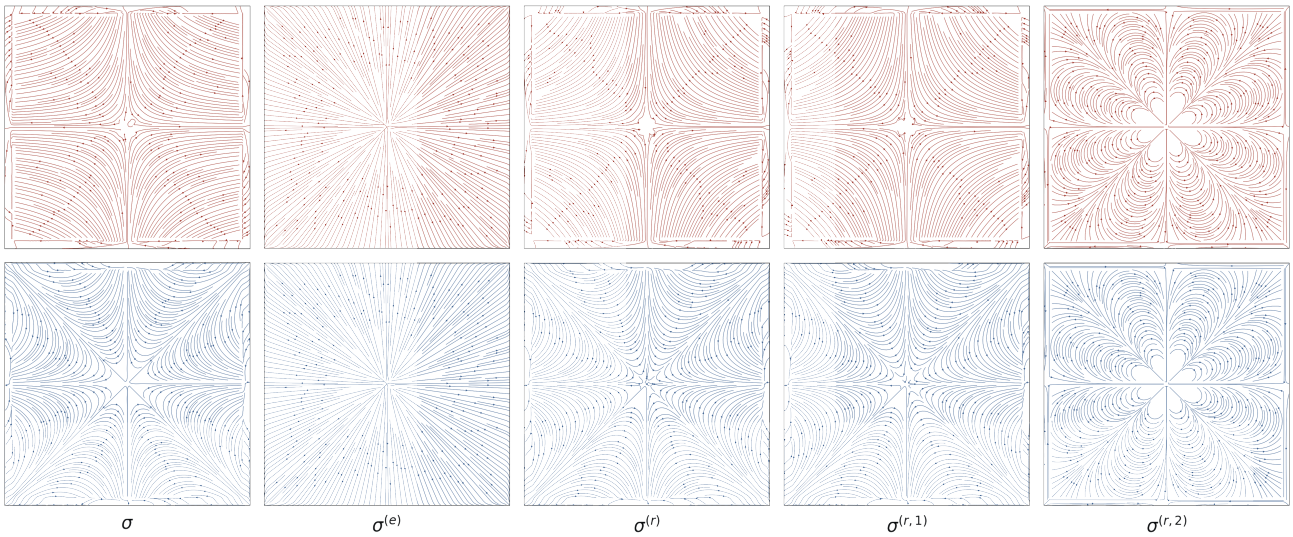

Figure 4.5: $p = 3$, $\eta = 0$, $\gamma = 1$.

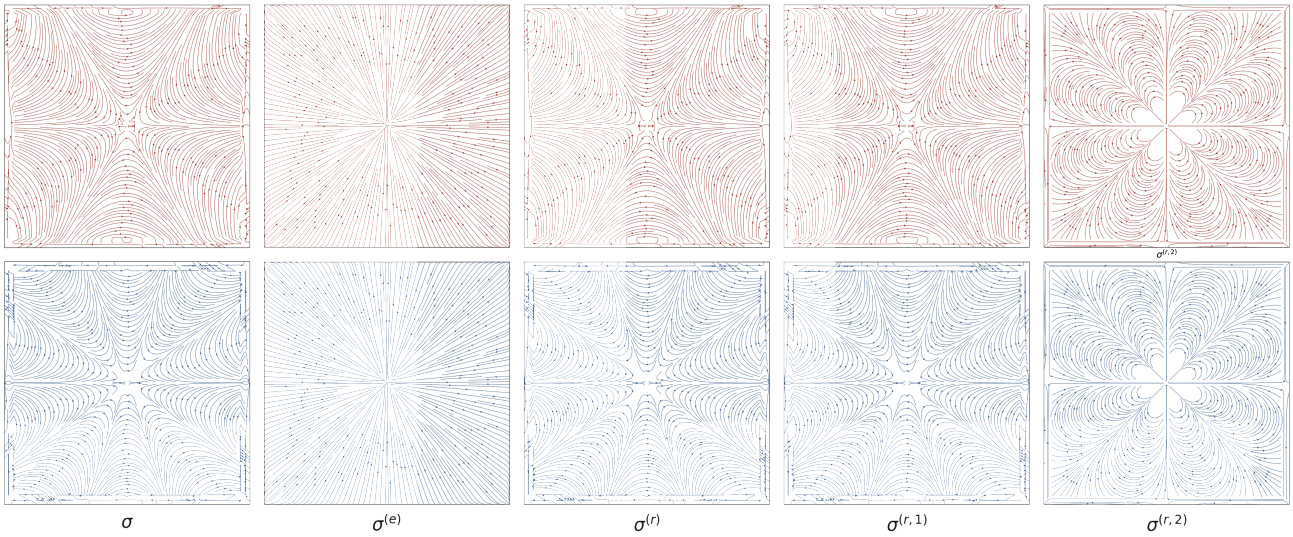

Figure 4.6: $p = 4$, $\eta = 0$, $\gamma = 1$.

Friction and viscosity

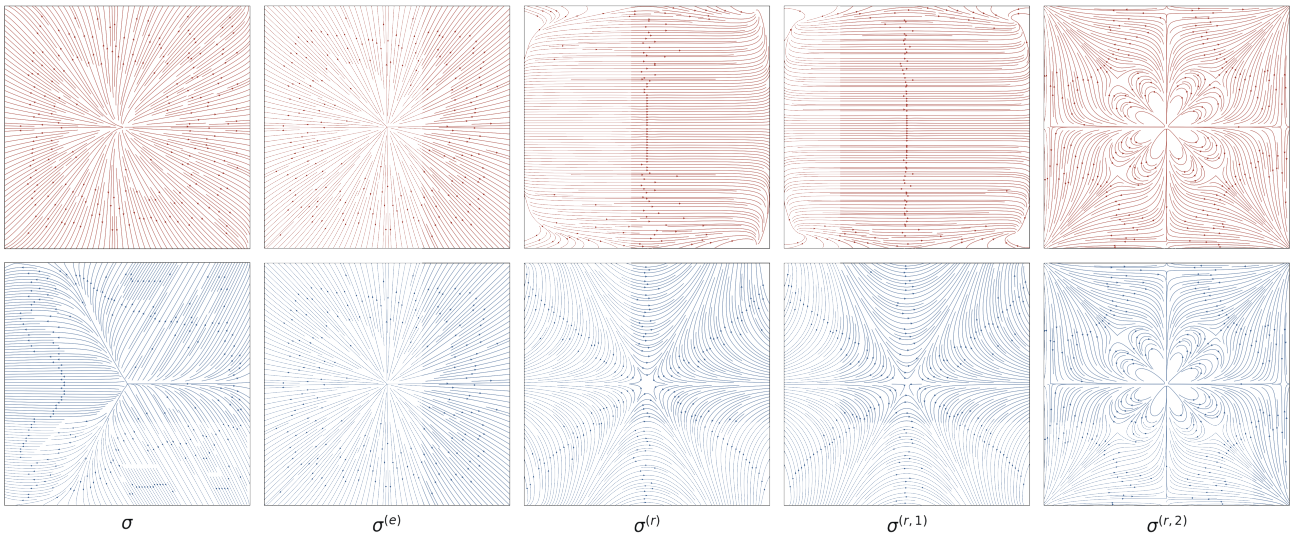

Figure 4.7: $p = 2$, $\eta = 1$, $\gamma = 1$.

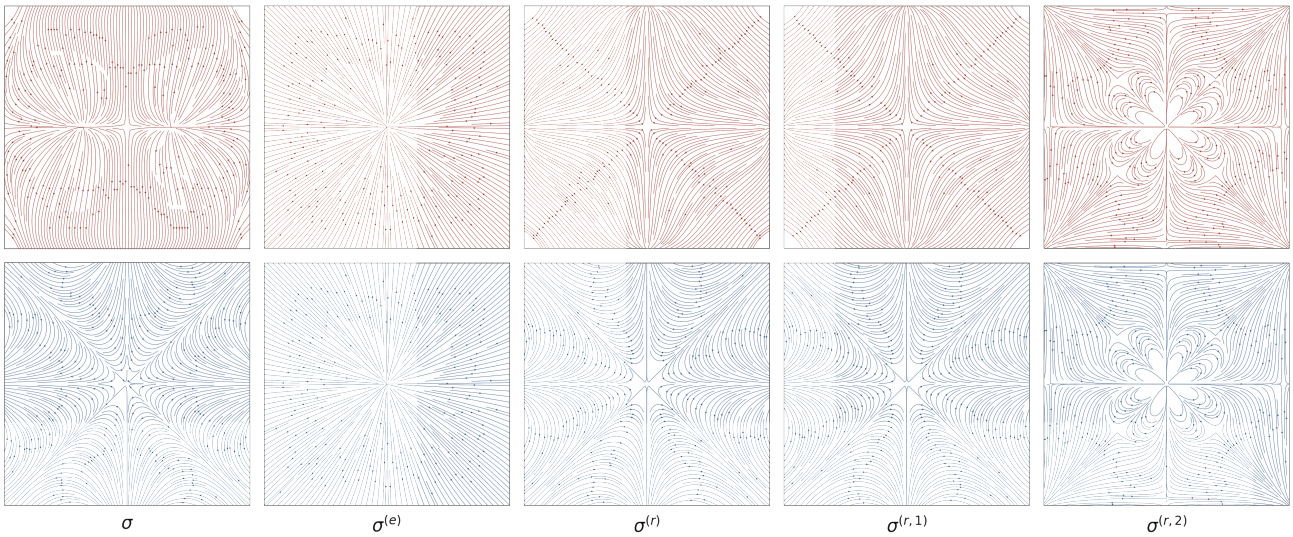

Figure 4.8: $p = 3$, $\eta = 1$, $\gamma = 1$.

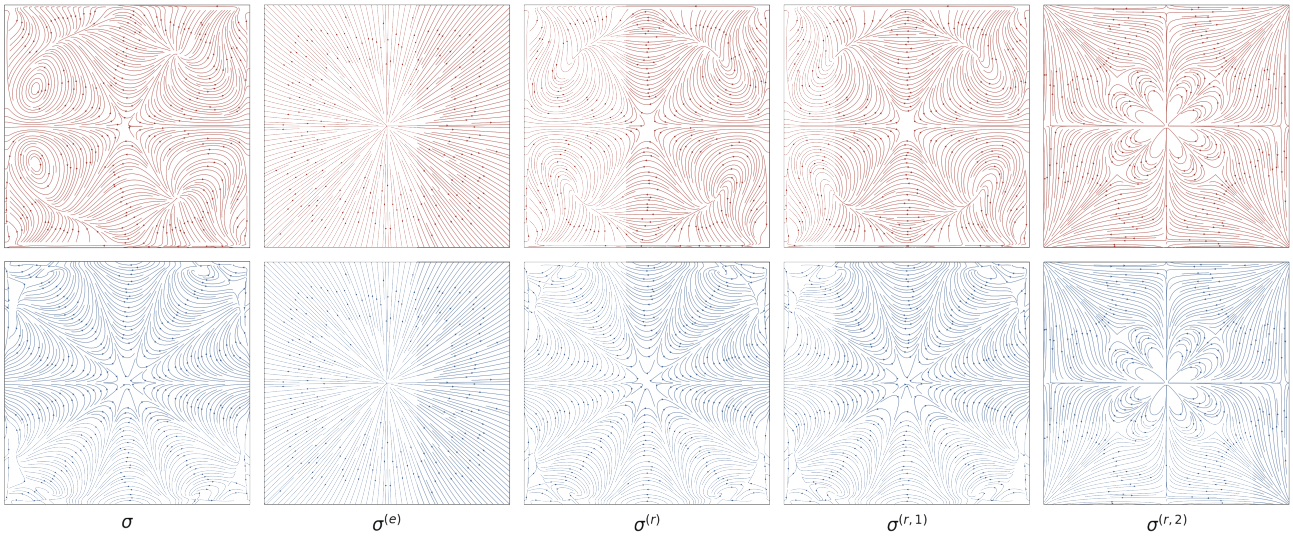

Figure 4.9: $p = 4$, $\eta = 1$, $\gamma = 1$.

Friction dominated

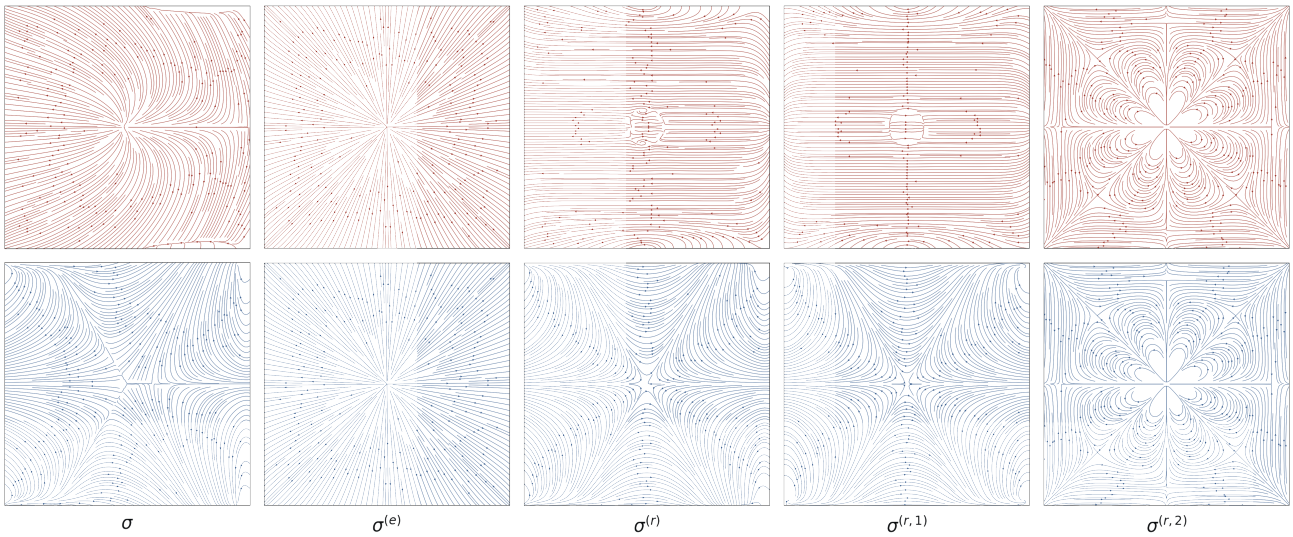

Figure 4.10: $p = 2$, $\eta = 1$, $\gamma = 100$.

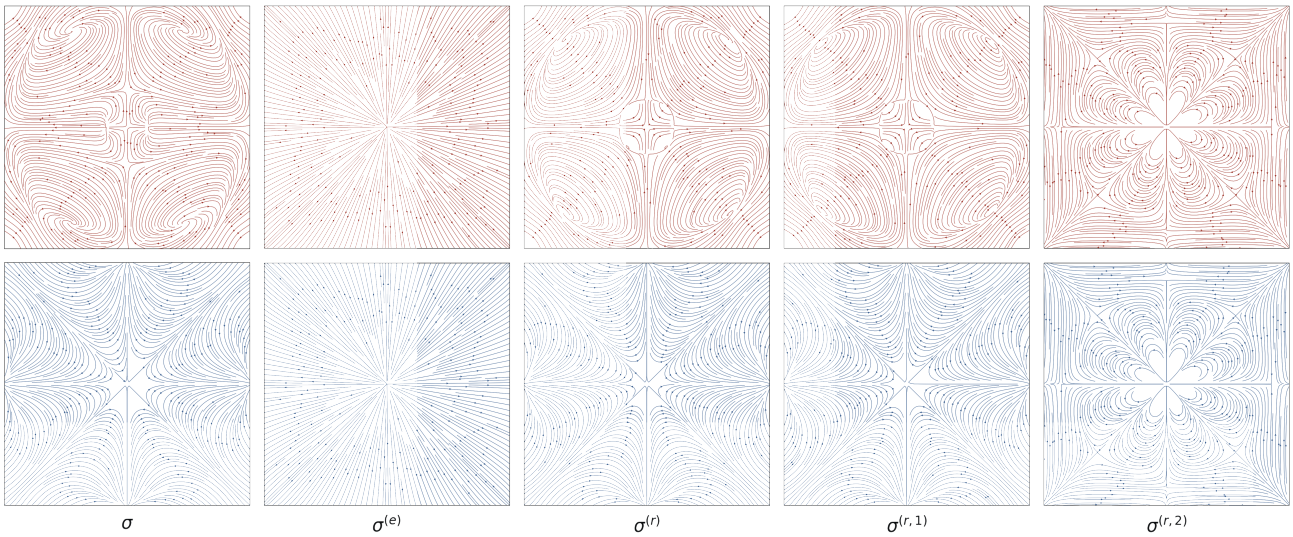

Figure 4.11: $p = 3$, $\eta = 1$, $\gamma = 100$.

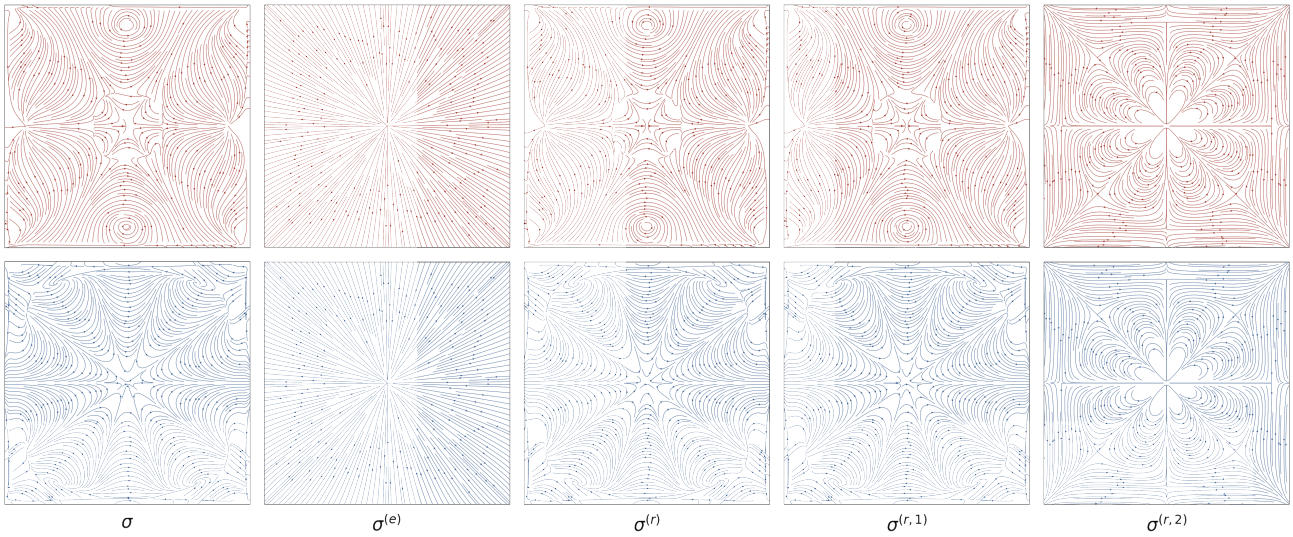

Figure 4.12: $p = 4$, $\eta = 1$, $\gamma = 100$.

Viscosity dominated

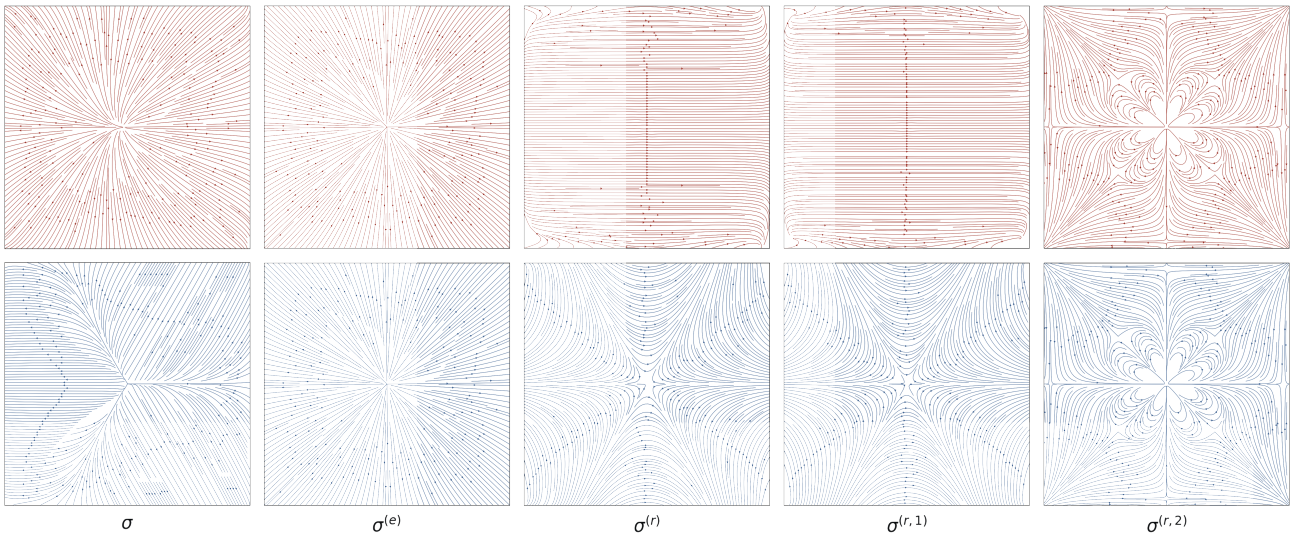

Figure 4.13: $p = 2$, $\eta = 100$, $\gamma = 1$.

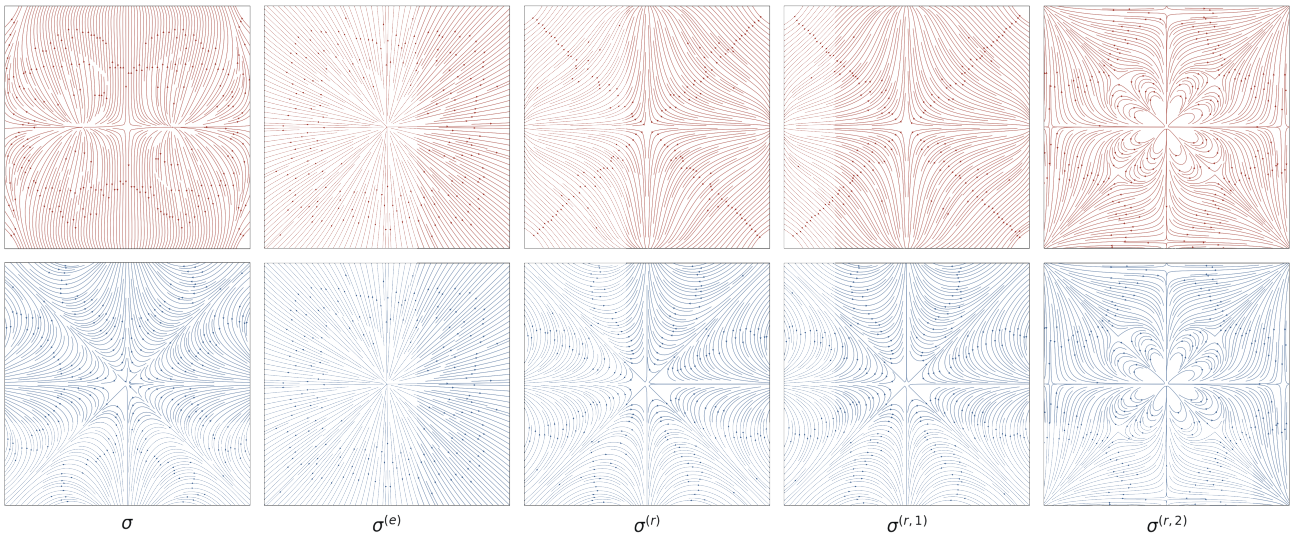

Figure 4.14: $p = 3$, $\eta = 100$, $\gamma = 1$.

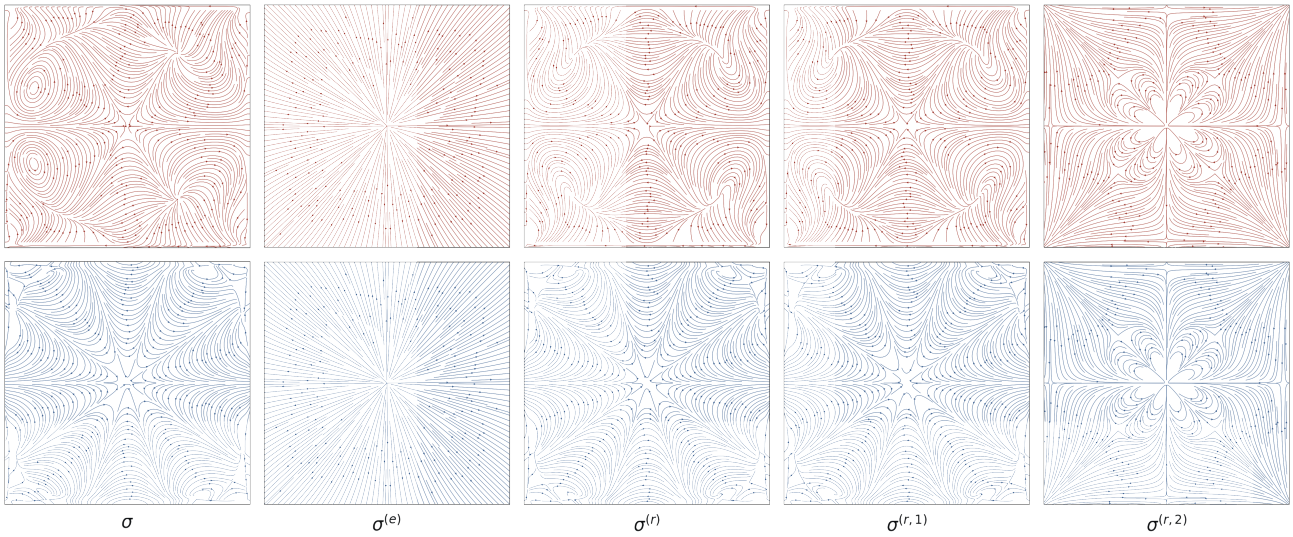

Figure 4.15: $p = 4$, $\eta = 100$, $\gamma = 1$.

Part III

Summary and conclusions

Chapter 5

The p-atic order parameter and dry p-atic universality

One of the defining characteristics of systems which exhibit collective order is the appearance of topological defects. In systems where the ordering is exhibited by the particles that make it up, topological defects manifest themselves as physical distortions, and they play a crucial role in determining such systems' material properties. The exact properties of the topological defects in a given system are, as the name suggests, intimately connected to the topology of the corresponding order parameter spaces.

In the case of p-atic liquid crystals, the structure of the order parameter space is directly determined by the polygonal structure of p-atic particles. The rotational symmetry of such particles gives the p-atic order parameter space a structure which is homeomorphic to a single space for all values of p, which allows one to treat all p-atic systems using a single comprehensive theoretical framework for the whole class of systems rather than having to consider them separately as has been the case historically.

In Chapter 3, we have seen how a complex scalar order parameter makes this fact manifest by virtue of it always taking its values on a circle[1] independently of the value of p. This is a major conceptual simplification to the other commonly used form of a p-atic order parameter, namely a rank-p tensor. Even for systems with a fairly low value of p - the two most commonly studied apart from $p = 2$ being triatics with $p = 3$ and a rank-3 order parameter tensor, and hexatics with $p = 6$ and a rank-6 order parameter tensor - the order parameter spaces are much harder to conceptualize and visualize. Consequently, the universal nature of p-atics is much less manifest in a tensorial formulation of the theory than it is in the complex scalar formulation.

Nevertheless, as the tensorial formulation of the physics of p-atics is well-established in the field, with some researchers and research groups formulating comprehensive theories of p-atics [13] in terms of the order parameter tensor, it is important to ensure that any reformulation of the theory of p-atics maintains a correspondence with the already established theory.

This is certainly true of the complex scalar p-atic order parameter which we constructed in order to reduce the conceptual and computational complexity inherent in the tensorial formulation. As we have seen in Chapter 3, the general definition of the p-atic order parameter tensor as a fully symmetric and fully traceless tensor fixes its structure such that it can always be reduced to only two independent components. Furthermore, the structure of the order parameter tensor doesn't only make it reducible to only two independent components, but it also gives these components the $2\pi/p$ rotational symmetry characteristic of the p-atic liquid crystals. Thus we were able to verify that the definition of the p-atic order parameter tensor as a fully symmetric and fully traceless rank-p tensor is indeed a reasonable definition for describing p-atics.

Furthermore, the fact that the p-atic order parameter tensor always has only two independent components means that it is uniquely mappable to a complex scalar, which is a much simpler object that can still carry essential information about the p-atic system, and which can therefore be used to describe their physics. However, the fact that the complex scalar order parameter is a simple object also means that one loses information about the finer details of the geometry and structure of p-atic ordering which the p-atic order parameter tensor carries. Nevertheless, as a complex scalar order parameter carries sufficient information for a formulation of the dynamics of p-atics, we argue that the sacrifice of the information carried in the order parameter tensor is worth the gain in

[1] Specifically, the complex scalar order parameter takes its values on a circle only in the microscopic case, and on a disk in the macroscopic case. Regardless, the crucial point is that the order parameter space associated with the complex scalar order parameter is the same for any value of p.

simplification and transparency of the theory. In the event that such information should be necessary, then one can always re-construct the order parameter tensor from the one-to-one correspondence between it and the complex scalar order parameter, and thus carry out all the necessary analyses.

As an explicit demonstration of this argument, we have shown how a complex scalar order parameter doesn't only help us expose the universality of p-atics in the topology of their associated order parameter space, but also in the domain of their dynamics. In particular, the formulation of the dynamics of dry p-atics in terms of the complex scalar order parameter - which is embodied in the expression of the p-atic free energy in eq. (3.25) - clearly demonstrates that every dry p-atic will be governed by exactly the same evolution equation, regardless of the value of p. This is exemplified in Supplementary Figure C.5 for $p = 2, 3, 4$, where it can be seen that given the same initial conditions, the evolution of these p-atics is identical. This feature of the dry p-atics is not as transparent in the tensorial formulation due to the fact that the order parameter (apparently) changes its structure with varying values of p.

The dynamics of dry p-atic are formulated in the regime where dissipative forces are the dominant influence in the system. A consequence of this is that the only dynamical variable in this regime is the p-atic order parameter itself. Therefore, the only thing that governs the evolution and physical behaviour of dry p-atics is the interactions of p-atic topological defects with each other. As demonstrated in Figure C.1 by numerical solution of eq. (3.29), a dry p-atic cannot sustain defects of higher charge than ± 1, as these will quickly dissociate into defects with a charge of the lowest magnitude which then continue to propagate through the system and interact with each other. This is precisely what we see in Figures 3.7, C.2 and C.5. Even when a system is started off in a maximally disordered state, it quickly evolves to a mostly ordered state where only elementary defects remain, which continue to interact with each other until they all annihilate. The dynamics of the dry p-atics also demonstrate the importance of understanding their topological defects, as they are configurations of the system which carry significantly more energy than configurations with no defects. This can be seen directly from the free energy in Figure C.3 for the evolution of the order parameter in Figure 3.7. Whenever a pair of defects annihilates, there is a visible drop in the free energy whose evolution is otherwise minimal beyond the point when most of the defects have annihilated each other - in this case beyond $t/\tau \approx 100$.

Because the physical behaviour of dry p-atics is governed by the interactions of its defects, it follows that in order to have a complete understanding of the physics of dry p-atics, it would be necessary to have a formulation for the dynamics of p-atic defects in the dry limit to supplement the evolution equation for the order parameter. One way in which the dynamics of the defects can be obtained is to use the defect density as defined in Ref. [12]. This would be an important point for future work towards the formulation of a complete hydrodynamic theory of p-atics using the complex scalar order parameter.

Chapter 6

Defect induced flows in p-atics

For all their uniqueness as a continuous anisotropic medium, dry p-atics are only an approximate image of a class of systems which can exhibit far greater variety in their physical behaviour than can be captured by the dynamics of dry p-atics. For a more comprehensive understanding of the physics of ordered systems of particles with dihedral symmetry, it is necessary to expand the description of the dynamics to situations where dissipative forces are not the dominant influence in the system. This vastly expands the possibilities for the kinds of phenomena one can expect to observe in such systems, with which also follows a great increase in the mathematical and conceptual complexity of any theory which attempts to describe such dynamics. The underlying reason for this is that the order parameter will no longer the only dynamical variable in such a theory, and its evolution will no longer be independent of all other dynamical variables which arise in more general situations. Of the greatest importance for the evolution of the order parameter is the velocity field that describes the flow of matter throughout the system - a phenomenon which is not present in dry p-atics. The evolution of the order parameter will thus be coupled to that of the order parameter, meaning that the two will influence each other in very non-trivial ways. Crucially, the interactions of the order parameter with the flow velocity will fundamentally depend on the structure of the p-atic particles.

One consequence of allowing for the flow of matter in the system is that any gradients in the flow velocity will give rise to various forms of stress, which is a phenomenon we observe even for isotropic fluids. However, because of the structured nature of p-atic particles, some forms hydrodynamic stresses that appear in p-atic liquid crystals will have a strong dependence on the anisotropies that result from the microscopic geometry, which is reflected by the dependence of these forms of hydrodynamic stress on the p-atic order parameter.

In Chapter 4 we used the tensorial formulations of these stresses from earlier work [15] to compute the flow velocities induced by an isolated elementary defect of charge $\pm 1/p$ for $p = 2, 3, 4$. Like in Chapter 3, we used the complex scalar order parameter to formulate the stresses, and the usefulness of the scalar order parameter made itself evident again in that it makes transparent which terms in the stress tensor contribute trivially and non-trivially to the flow profiles with varying values of p. Comparing eq.'s (4.2) and (4.6) with respectively eq.'s (4.7) and (4.8), it immediately becomes transparent that the elastic stress and the second term in the reactive stress in eq. (4.3) do not contribute non-trivially to the defect induced flow, as can also be verified from the second and fifth columns in Figures 4.1-4.15.

The only stress term that contributes non-trivially to the defect induced flow profiles is therefore seen to be the first term in eq. (4.4), which agrees with the analyses in Ref. [15]. What is different in our results from those in Ref. [15], however, is the much bigger variety of flow profiles that appear in the regimes with varying contributions from the viscosity and friction terms in eq. (4.10). The greatest resemblance between the flow profiles we obtained and those from Ref. [15] can be seen to be in the profiles obtained in the regime with no viscosity, shown in Figures 4.4-4.6 where eq. (4.10). Even then, there is still disagreement for the flow induced by the $+1/2$ defect.

One potential source for these discrepancies could be, of course, in the numerics and that the solution of eq. (4.10) is simply not implemented correctly. A less trivial source of error could be that the reformulation of the order parameter tensor to a complex scalar is too costly in terms of the information that is lost by using a complex scalar order parameter, and that this affects the resulting expressions for the reactive stress in a way that gives the wrong flow profiles. This could be further supported by the fact that although the flow profiles we obtained exhibit some degree of variety, they also do show the same general features found in the profiles in Ref. [15], particularly in the fold symmetry of the profiles in the vicinity of the defects. The potential implication of this is that there might be some subtle aspect of the structure of the order parameter that the reactive stress is dependent on, and that subtle aspect might lie precisely in the information lost in going from a tensorial order parameter to a complex scalar one.

Understanding the effect of a single p-atic defect on its surrounding system is a crucial first step towards understanding how multiple defects interact with each other in such systems. Therefore, the discrepancies we observe in the flow profiles from those in Ref. [15] clearly constitute an important avenue for further exploration and investigation.

Another thing our results leave to be desired is a closed form expression for the reactive stress $\sigma^{(r,1)}$. The expressions we obtained for the cases of $p = 2, 3, 4$ seem to hint that there should be some combinatorial relation which can be formulated in terms of the components of the complex scalar order parameter and its derivatives. This is also evident from the expression for $\sigma^{(r,1)}$ in the tensorial formulation in eq. (4.5) with the contraction of the gradients with the the molecular tensor. The derivation of a closed form expression for $\sigma^{(r,1)}$ - if it exists - could also prove useful in addressing the issues of discrepancy in the flow profiles by revealing the exact way in which the reactive stress depends on the order parameter, and that eventuality warrants further exploration in this direction also.

Part IV

Appendices

Chapter A

Rescaling of dynamical variables

For the sake of analytical and numerical simplicity, we will rescale our dynamical variables to make them dimensionless. This appendix is the only part of this thesis where we will work with dimensional quantities and equations. The equations and variables used in all other discussions throughout the thesis assume the dimensionless forms to be derived here.

The most straightforward variables to rescale are the coordinate and time variables. Given some characteristic length L of our systems, and some characteristic time τ, we define the following dimensionless coordinate and time variables:

$$\tilde{x_i} \equiv \frac{x_i}{l}\,,\ \tilde{t} \equiv \frac{t}{\tau}\,.$$

With this, we can express our physical variables as

$$x_i = l\tilde{x}_i\,,\ t = \tau\tilde{t}\,,$$

with corresponding differentials

$$dx_i = ld\tilde{x}_i\,,\ dt = \tau d\tilde{t}\,.$$

The rescaled coordinate variables also give us the dimensionless gradient:

$$\nabla = \frac{1}{l}\tilde{\nabla} \ \leftrightarrow\ \partial_x = \frac{1}{l}\partial_{\tilde{x}}\,,$$

and likewise for the derivative with respect to time:

$$\frac{d}{dt} = \frac{1}{\tau}\frac{d}{d\tilde{t}} \ \leftrightarrow\ \partial_t = \frac{1}{\tau}\partial_{\tilde{t}}\,.$$

With these dimensionless variables we can proceed to rescale the other dynamical variables as well as the equations of motion, starting with the dry p-atics.

A.1 Dry p-atic equations of motion

As we discussed in Section 3.2, we postulate that the time derivative of the order parameter can be set proportional to its thermodynamically conjugate field h_p, and from the definition of h_p in eq. (3.26) it is clear that h_p must have units of energy density. Meanwhile, because Ψ_p is a scalar, it follows that the units of $\partial_t\Psi_p$ must be

$$[\partial_t\Psi_p] = \frac{1}{T}\,.$$

Therefore, in order for eq. (3.27) to be dimensionally consistent, we must have

$$[\Gamma_p] = \frac{L^2}{ET}\,.$$

This means that we can define a dimensionless rotational viscosity $\tilde{\Gamma}_p$ as

$$\tilde{\Gamma}_p \equiv \Gamma_p\frac{\epsilon\tau}{l^2}\,,$$

or, in other words

$$\Gamma_p = \tilde{\Gamma}_p\frac{l^2}{\epsilon\tau}\,.$$

As for the units of the remaining parameters in the equation of motion for the dry p-atics - namely K_p and g_p - they can be found from the expression for the free energy in eq. (3.25). Because F_p has units of energy, it follows that the integrand in the expression for F_p must have units of energy *density*. Therefore, it readily follows that g_p must also have units of energy density, since it is the only dimensional quantity in the term in which it appears. Meanwhile, because of the square of the gradient of Ψ_p in the first term in the integrand, it follows that K_p must have units of energy. Therefore, we define the dimensionless quantities

$$\tilde{K}_p \equiv \frac{K_p}{\epsilon} \text{ and } \tilde{g}_p \equiv \frac{g_p}{\epsilon/l^2} ,$$

which means that

$$K_p = \tilde{K}_p \epsilon \text{ and } g_p = \tilde{g}_p \frac{\epsilon}{l^2} .$$

Inserting into eq. (3.28), and using the rescaled time derivative and gradient, we now get

$$\begin{aligned}
\frac{1}{\tau}\partial_{\tilde{t}}\Psi_p &= -\tilde{\Gamma}_p \frac{l^2}{\epsilon\tau}\frac{\delta F_p}{\delta \Psi_p} \\
&= \tilde{\Gamma}_p \frac{l^2}{\epsilon\tau}\left(\frac{\tilde{K}_p\epsilon}{2}\frac{1}{l^2}\tilde{\nabla}^2\Psi_p + \frac{\tilde{g}_p\left(\epsilon/l^2\right)}{2}\left[1-|\Psi_p|^2\right]\Psi_p\right) \\
&= \frac{1}{\tau}\tilde{\Gamma}_p\left(\frac{\tilde{K}_p}{2}\tilde{\nabla}^2\Psi_p + \frac{\tilde{g}_p}{2}\left[1-|\Psi_p|^2\right]\Psi_p\right) ,
\end{aligned}$$

which finally gives us the dimensionless equation of motion

$$\partial_{\tilde{t}}\Psi_p = \tilde{\Gamma}_p\left(\frac{\tilde{K}_p}{2}\tilde{\nabla}^2\Psi_p + \frac{\tilde{g}_p}{2}\left[1-|\Psi_p|^2\right]\Psi_p\right) .$$

Chapter B

Calculations

B.1 Calculations for Chapter 3

B.1.1 The rotation of a fully symmetric, fully traceless tensor

We want to compute the transformed component $A_{2'1'\ldots1'}$ of a fully symmetric fully traceless tensor A in analogy to the computation of $A_{1'1'\ldots1'}$ in the main text. The calculation for $A_{2'1'\ldots1'}$, although slightly more complicated is in principle exactly analogous to the calculation for $A_{1'\ldots1'}$. We have

$$\begin{aligned}
A_{2'1'\ldots1'} &= R_{2'i_1}R_{1'i_2}\ldots R_{1'i_p}A_{i_1i_2\ldots i_p} \\
&= \sum_{\{\pi^0\}} R_{2'\pi_1^0}R_{1'\pi_2^0}\ldots R_{1'\pi_p^0}A_{\pi_1^0\pi_2^0\ldots\pi_p^0} \\
&+ \sum_{\{\pi^1\}} R_{2'\pi_1^1}R_{1'\pi_2^1}\ldots R_{1'\pi_p^1}A_{\pi_1^1\pi_2^1\ldots\pi_p^1} \\
&+ \ldots \\
&+ \sum_{\{\pi^{p-1}\}} R_{2'\pi_1^{p-1}}R_{1'\pi_2^{p-1}}\ldots R_{1'\pi_p^{p-1}}A_{\pi_1^{p-1}\pi_2^{p-1}\ldots\pi_p^{p-1}} \\
&+ \sum_{\{\pi^p\}} R_{2'\pi_1^p}R_{1'\pi_2^p}\ldots R_{1'\pi_p^p}A_{\pi_1^p\pi_2^p\ldots\pi_p^p}\,,
\end{aligned}$$

Now, because the first index in the first factor R in every term is 2, we will not only get factors of the type $R_{1'1}$ and $R_{1'2}$ for any permutation of the dummy indices like we did in the calculation of $A_{1'1'\ldots1'}$. This time we will always get any three of the four factors from the rotation matrix for any given permutation of the dummy indices, so we need to split the sums up accordingly in order to be able to make way.

We can begin by counting how many of the dummy index permutations will begin with a 2 for a fixed number k of 2's, since those terms will all contain a factor $R_{2'2}$. The number of different index configurations that all have k 2's is given by the binomial coefficient $\binom{p}{k}$, and the fraction of these that begin with a 2 will be

$$\frac{k}{p}\binom{p}{k} = \binom{p-1}{k-1}.$$

The remaining configurations will all begin with a 1, and of these there are

$$\frac{p-k}{p}\binom{p}{k} = \binom{p-1}{k}.$$

This means that for some generic set of permutations $\{\pi^k\}$ of the dummy indices (i.e. for some fixed value of

$k \geqslant 1$), we will have

$$\begin{aligned}
\sum_{\{\pi^k\}} R_{2'\pi_1^k} R_{1'\pi_2^k} ... R_{1'\pi_p^k} A_{\pi_1^k \pi_2^k ... \pi_p^k} &= \binom{p-1}{k-1} R_{2'2} (R_{1'2})^{k-1} (R_{1'1})^{p-k} A_{\{\pi_1^k \pi_2^k ... \pi_p^k\}} \\
&+ \binom{p-1}{k} R_{2'1} (R_{1'2})^{k} (R_{1'1})^{p-k-1} A_{\{\pi_1^k \pi_2 .. \pi_p^k\}} \\
&= \left(\binom{p-1}{k-1} R_{1'1} (R_{1'2})^{k-1} (R_{1'1})^{p-k} \right. \\
&- \left. \binom{p-1}{k} R_{1'2} (R_{1'2})^{k} (R_{1'1})^{p-k-1} \right) A_{\{\pi_1^k \pi_2^k ... \pi_p^k\}} \\
&= \left(\binom{p-1}{k-1} (R_{1'2})^{k-1} (R_{1'1})^{p-k+1} \right. \\
&- \left. R_{1'2} \binom{p-1}{k} (R_{1'2})^{k} (R_{1'1})^{p-k-1} \right) A_{\{\pi_1^k \pi_2^k ... \pi_p^k\}} \\
&= \left(R_{1'1} \binom{p-1}{k-1} (R_{1'2})^{k-1} (R_{1'1})^{p-1-(k-1)} \right. \\
&- \left. R_{1'2} \binom{p-1}{k} (R_{1'2})^{k} (R_{1'1})^{p-k-1} \right) A_{\{\pi_1^k \pi_2^k ... \pi_p^k\}} ,
\end{aligned}$$

where $\{\pi_1^k \pi_2^k ... \pi_p^k\}$ indicates a fixed, but arbitrary permutation of the dummy indices (it doesn't matter which, since the components of A will all be equal for all the permutations due to symmetry), and we also use that $R_{1'1} = R_{2'2}$ and $R_{2'1} = -R_{1'2}$. Inserting this into our equation for $A_{2'1'...1'}$ and using that $A_{11...1} = a$ and $A_{21...1} = b$, we get

$$\begin{aligned}
A_{2'1'...1'} &= -R_{1'2} (R_{1'1})^{p-1} a \\
&+ \left(R_{1'1} \binom{p-1}{0} (R_{1'2})^0 (R_{1'1})^{p-1} - R_{1'2} \binom{p-1}{1} (R_{1'2})^1 (R_{1'1})^{p-2} \right) b \\
&- \left(R_{1'1} \binom{p-1}{1} (R_{1'2})^1 (R_{1'1})^{p-2} - R_{1'2} \binom{p-1}{2} (R_{1'2})^2 (R_{1'1})^{p-3} \right) a \\
&- \left(R_{1'1} \binom{p-1}{2} (R_{1'2})^2 (R_{1'1})^{p-3} - R_{1'2} \binom{p-1}{3} (R_{1'2})^3 (R_{1'1})^{p-4} \right) b \\
&+ ... \\
&= -\left(R_{1'2} \binom{p-1}{0} (R_{1'2})^0 (R_{1'1})^{p-1} - R_{1'2} \binom{p-1}{2} (R_{1'2})^2 (R_{1'1})^{p-3} + ... \right) a \\
&- \left(R_{1'1} \binom{p-1}{1} (R_{1'2})^1 (R_{1'1})^{p-2} - ... \right) a \\
&+ \left(R_{1'1} \binom{p-1}{0} (R_{1'2})^0 (R_{1'1})^{p-1} - R_{1'1} \binom{p-1}{2} (R_{1'2})^2 (R_{1'1})^{p-3} + ... \right) b \\
&- \left(R_{1'2} \binom{p-1}{1} (R_{1'2})^1 (R_{1'1})^{p-2} - R_{1'2} \binom{p-1}{3} (R_{1'2})^3 (R_{1'1})^{p-4} + ... \right) b
\end{aligned}$$

$$
\begin{aligned}
&= \sin\alpha\left(\binom{p-1}{0}(\sin\alpha)^0(\cos\alpha)^{p-1} - \binom{p-1}{2}(\sin\alpha)^2(\cos\alpha)^{p-3} + ...\right) a \\
&+ \cos\alpha\left(\binom{p-1}{1}(\sin\alpha)^1(\cos\alpha)^{p-2} - ...\right) a \\
&+ \cos\alpha\left(\binom{p-1}{0}(\sin\alpha)^0(\cos\alpha)^{p-1} - \binom{p-1}{2}(\sin\alpha)^2(\cos\alpha)^{p-3} + ...\right) b \\
&- \sin\alpha\left(\binom{p-1}{1}(\sin\alpha)^1(\cos\alpha)^{p-2} - \sin\alpha\binom{p-1}{3}(\sin\alpha)^3(\cos\alpha)^{p-4} + ...\right) b \\
&= (\sin\alpha\cos((p-1)\alpha) + \cos\alpha\sin((p-1)\alpha))\, a \\
&+ (\cos\alpha\cos((p-1)\alpha) - \sin\alpha\sin((p-1)\alpha))\, b \\
&= \sin((p-1)\alpha+\alpha)\, a + \cos((p-1)\alpha+\alpha)\, b \\
&= \sin(p\alpha)a + \cos(p\alpha)b\,.
\end{aligned}
$$

B.1.2 Reformulation of the free energy

We want to derive the dynamic equation for the complex scalar order parameter Ψ_p starting from the free energy functional in eq. (3.22). We will begin by computing the contractions in each of the terms in the integrand. For the first term, we have

$$
\begin{aligned}
\left|\nabla Q^{(p)}\right|^2 &= \partial_i Q^{(p)}_{k_1\ldots k_p}\partial_i Q^{(p)}_{k_1\ldots k_p} \\
&= \sum_{\alpha=0}^{p}\sum_{\{\pi^\alpha\}} \partial_i Q^{(p)}_{\pi^\alpha_1\ldots\pi^\alpha_p}\partial_i Q^{(p)}_{\pi^\alpha_1\ldots\pi^\alpha_p} \\
&= \sum_{\{\pi^0\}} \partial_i Q^{(p)}_{\pi^0_1\ldots\pi^0_p}\partial_i Q^{(p)}_{\pi^0_1\ldots\pi^0_p} + \sum_{\{\pi^1\}} \partial_i Q^{(p)}_{\pi^1_1\ldots\pi^1_p}\partial_i Q^{(p)}_{\pi^1_1\ldots\pi^1_p} + ... + \sum_{\{\pi^p\}} \partial_i Q^{(p)}_{\pi^p_1\ldots\pi^p_p}\partial_i Q^{(p)}_{\pi^p_1\ldots\pi^p_p} \\
&= \binom{p}{0}\partial_i\left(\sqrt{2^{-p}}\Psi_R\right)\partial_i\left(\sqrt{2^{-p}}\Psi_R\right) + \binom{p}{1}\partial_i\left(\sqrt{2^{-p}}\Psi_I\right)\partial_i\left(\sqrt{2^{-p}}\Psi_I\right) \\
&+ \binom{p}{2}\partial_i\left(-\sqrt{2^{-p}}\Psi_R\right)\partial_i\left(-\sqrt{2^{-p}}\Psi_R\right) + \binom{p}{3}\partial_i\left(-\sqrt{2^{-p}}\Psi_I\right)\partial_i\left(-\sqrt{2^{-p}}\Psi_I\right) + ... \\
&= 2^{-p}\left(\binom{p}{0} + \binom{p}{2} + \binom{p}{4} + ...\right)\partial_i\Psi_R\partial_i\Psi_R + 2^{-p}\left(\binom{p}{1} + \binom{p}{3} + \binom{p}{5} + ...\right)\partial_i\Psi_I\partial_i\Psi_I \\
&= 2^{-p}\sum_{k=0}^{\lfloor\frac{p}{2}\rfloor}\binom{p}{2k}\partial_i\Psi_R\partial_i\Psi_R + \binom{p}{2k+1}\partial_i\Psi_I\partial_i\Psi_I \\
&= 2^{-p}\cdot 2^{p-1}\left(\partial_i\Psi_R\partial_i\Psi_R + \partial_i\Psi_I\partial_i\Psi_I\right) \;=\; \frac{1}{2}\left|\nabla\Psi_p\right|^2\,,
\end{aligned}
$$

while for the second term, we have

$$
\begin{aligned}
Q^{(p)}_{k_1\ldots k_p}Q^{(p)}_{k_1\ldots k_p} &= \sum_{\alpha=0}^{p}\sum_{\{\pi^\alpha\}} Q^{(p)}_{\pi^\alpha_1\ldots\pi^\alpha_p}Q^{(p)}_{\pi^\alpha_1\ldots\phi^\alpha_p} \;=\; \sum_{\{\pi^0\}} Q^{(p)}_{\pi^0_0\ldots\pi^0_p}Q^{(p)}_{\pi^0_1\ldots\pi^0_p} + ... + \sum_{\{\pi^p\}} Q^{(p)}_{\pi^p_1\ldots\pi^p_p}Q^{(p)}_{\pi^p_p} \\
&= \binom{p}{0}\left(\sqrt{2^{-p}}\Psi_R\right)\left(\sqrt{2^{-p}}\Psi_R\right) + \binom{p}{1}\left(\sqrt{2^{-p}}\Psi_I\right)\left(\sqrt{2^{-p}}\Psi_I\right) \\
&+ \binom{p}{3}\left(-\sqrt{2^{-p}}\Psi_R\right)\left(-\sqrt{2^{-p}}\Psi_R\right) + \binom{p}{4}\left(-\sqrt{2^{-p}}\Psi_I\right)\left(-\sqrt{2^{-p}}\Psi_I\right) + ...
\end{aligned}
$$

$$= 2^{-p}\left(\binom{p}{0}+\binom{p}{2}+\binom{p}{4}+...\right)\Psi_R^2+2^{-p}\left(\binom{p}{1}+\binom{p}{3}+\binom{p}{5}+...\right)\Psi_I^2$$

$$= 2^{-p}\sum_{k=0}^{\lfloor\frac{p}{2}\rfloor}\binom{p}{2k}\Psi_R^2+\binom{p}{2k+1}\Psi_I^2 = 2^{-p}\cdot 2^{p-1}\left(\Psi_R^2+\Psi_I^2\right) = \frac{1}{2}\left|\Psi_p\right|^2 .$$

From this it immediately follows that we must also have

$$\left|Q^{(p)}\right|^4 = \left(\left|Q^{(p)}\right|^2\right)^2 = \frac{1}{4}\left|\Psi_p\right|^4 .$$

Inserting these expressions back into the original expression for the free energy functional, we now get

$$F_p\left[Q^{(p)}\right]\to F_p\left[\Psi_p\right] = \int \frac{L_p}{2}\frac{1}{2}\left|\nabla\Psi_p\right|^2+\frac{A_p}{2}\frac{1}{2}\left|\Psi_p\right|^2+\frac{B_p}{4}\frac{1}{4}\left|\Psi_p\right|^4 d\mathbf{r} = \int \frac{L_p}{4}\left|\nabla\Psi_p\right|^2+\frac{A_p}{4}\left|\Psi_p\right|^2+\frac{B_p}{16}\left|\Psi_p\right|^4 d\mathbf{r} .$$

Using the remapping for the phenomenological parameters in eq. (3.24), we finally get

$$F_p\left[\Psi_p\right] = \int \frac{K_p}{2}\left|\nabla\Psi_p\right|^2-\frac{g_p}{2}\left(1-\frac{1}{2}\left|\Psi_p\right|^2\right)\left|\Psi_p\right|^2 d\mathbf{r} = \int \frac{K_p}{2}\left|\nabla\Psi_p\right|^2-\frac{g_p}{2}\left|\Psi_p\right|^2+\frac{g_p}{4}\left|\Psi_p\right|^4 d\mathbf{r} .$$

With this expression for the free energy functional, we can now proceed to compute the variational with respect to Ψ_p. Specifically, since Ψ_p is a complex scalar, by the standard rules of variational calculus, we want to compute the variation in F_p under

$$\Psi_p\to\Psi_p+\delta\Psi_p \text{ and } \Psi_p^*\to\Psi^*+\delta\Psi_p^* .$$

To keep the length of the expressions manageable, we will begin by first computing the variations for the individual terms in the integral. For the first term, we have

$$\begin{aligned}
\left|\nabla\Psi_p\right|^2\to\left(\nabla\left[\Psi_p+\delta\Psi_p\right]\right)\cdot\left(\nabla\left[\Psi_p+\delta\Psi_p\right]\right)^* &= \left(\nabla\Psi_p+\nabla\left(\delta\Psi_p\right)\right)\cdot\left(\nabla\Psi_p+\nabla\left(\delta\Psi_p\right)\right)^* \\
&= \nabla\Psi_p\cdot\nabla\Psi_p^*+\nabla\Psi_p\cdot\nabla\left(\delta\Psi_p^*\right)+\nabla\Psi_p^*\cdot\nabla\left(\delta\Psi_p\right)+\nabla\left(\delta\Psi_p\right)\cdot\nabla\left(\delta\Psi_p^*\right) \\
&= \left|\nabla\Psi_p\right|^2+\left|\nabla\left(\delta\Psi_p\right)\right|^2+\nabla\Psi_p\cdot\nabla\left(\delta\Psi_p^*\right)+\nabla\Psi_p^*\cdot\nabla\left(\delta\Psi_p\right) .
\end{aligned}$$

Likewise, for the second term we get

$$\left|\Psi_p\right|^2\to\left(\Psi_p+\delta\Psi_p\right)\left(\Psi_p^*+\delta\Psi_p^*\right) = \Psi_p\Psi_p^*+\Psi_p\delta\Psi_p^*+\Psi_p^*\delta\Psi_p+\delta\Psi_p\delta\Psi_p^* = \left|\Psi_p\right|^2+\left|\delta\Psi_p\right|^2+\Psi_p\delta\Psi_p^*+\Psi_p^*\delta\Psi_p ,$$

and from this it also follows that

$$\begin{aligned}
\left|\Psi_p\right|^4 &= \left(\left|\Psi_p\right|^2+\left|\delta\Psi_p\right|^2+\Psi_p\delta\Psi_p^*+\Psi_p^*\delta\Psi_p\right)^2 \\
&= \left(\left|\Psi_p\right|^2+\left|\delta\Psi_p\right|^2+\Psi_p\delta\Psi_p^*+\Psi_p^*\delta\Psi_p\right)\left(\left|\Psi_p\right|^2+\left|\delta\Psi_p\right|^2+\Psi_p\delta\Psi_p^*+\Psi_p^*\delta\Psi_p\right) \\
&= \left|\Psi_p\right|^4+\left|\Psi_p\right|^2\left|\delta\Psi_p\right|^2+\left|\Psi_p\right|^2\Psi_p\delta\Psi_p^*+\left|\Psi_p\right|^2\Psi_p^*\delta\Psi_p \\
&+ \left|\Psi_p\right|^2\left|\delta\Psi_p\right|^2+\left|\delta\Psi_p\right|^4+\Psi_p\left|\delta\Psi_p\right|^2\delta\Psi_p^*+\Psi_p^*\left|\delta\Psi_p\right|^2\delta\Psi_p \\
&+ \left|\Psi_p\right|^2\Psi_p\delta\Psi_p^*+\Psi_p\left|\delta\Psi_p\right|^2\delta\Psi_p^*+\left(\Psi_p\delta\Psi_p^*\right)^2+\left|\Psi_p\right|^2\left|\delta\Psi_p\right|^2 \\
&+ \left|\Psi_p\right|^2\Psi_p^*\delta\Psi_p+\Psi_p^*\left|\delta\Psi_p\right|^2\delta\Psi_p+\left|\Psi_p\right|^2\left|\delta\Psi_p\right|^2+\left(\Psi_p^*\delta\Psi_p\right)^2 \\
&= \left|\Psi_p\right|^4+2\left|\Psi_p\right|^2\Psi_p\delta\Psi_p^*+2\left|\Psi_p\right|^2\Psi_p^*\delta\Psi_p+4\left|\Psi_p\right|^2\left|\delta\Psi_p\right|^2 \\
&+ \left(\Psi_p\delta\Psi_p^*\right)^2+\left(\Psi_p^*\delta\Psi_p\right)^2+2\Psi_p\left|\delta\Psi_p\right|^2\delta\Psi_p^*+2\Psi_p^*\left|\delta\Psi_p\right|^2\delta\Psi_p+\left|\delta\Psi_p\right|^4 .
\end{aligned}$$

Keeping the lowest order terms in $\delta\Psi_p$ and $\delta\Psi_p^*$, we now get

$$\begin{aligned}
F_p \to \tilde{F}_p &= \int \frac{K_p}{2}\left(|\nabla\Psi_p|^2 + \nabla\Psi_p\cdot\nabla\left(\delta\Psi_p^*\right) + \nabla\Psi_p^*\cdot\nabla\left(\delta\Psi_p\right)\right) \\
&\quad -\frac{g_p}{2}\left(|\Psi_p|^2 + \Psi_p\delta\Psi_p^* + \Psi_p^*\delta\Psi_p\right) + \frac{g_p}{4}\left(|\Psi_p|^4 + 2\,|\Psi_p|^2\,\Psi_p\delta\Psi_p^* + 2\,|\Psi_p|^2\,\Psi_p^*\delta\Psi_p\right) d\mathbf{r} \\
&= \int \frac{K_p}{2}|\nabla\Psi_p|^2 - \frac{g_p}{2}|\Psi_p|^2 + \frac{g_p}{4}|\Psi_p|^4 + \frac{K_p}{2}\nabla\Psi_p\cdot\nabla\left(\delta\Psi_p^*\right) - \frac{g_p}{2}\Psi_p\delta\Psi_p^* + \frac{g_p}{2}|\Psi_p|^2\,\Psi_p\delta\Psi_p^* \\
&\quad +\frac{K_p}{2}\nabla\Psi_p^*\cdot\nabla\left(\delta\Psi_p\right) - \frac{g_p}{2}\Psi_p^*\delta\Psi_p + \frac{g_p}{2}|\Psi_p|^2\,\Psi_p^*\delta\Psi_p\, d\mathbf{r} \\
&= \int \frac{K_p}{2}|\nabla\Psi_p|^2 - \frac{g_p}{2}\left(1-\frac{1}{2}|\Psi_p|^2\right)|\Psi_p|^2\, d\mathbf{r} + \int \frac{K_p}{2}\nabla\Psi_p\cdot\nabla\left(\delta\Psi_p^*\right) - \frac{g_p}{2}\Psi_p\delta\Psi_p^* + \frac{g_p}{2}|\Psi_p|^2\,\Psi_p\delta\Psi_p^*\, d\mathbf{r} \\
&+ \int \frac{K_p}{2}\nabla\Psi_p^*\cdot\nabla\left(\delta\Psi_p\right) - \frac{g_p}{2}\Psi_p^*\delta\Psi_p + \frac{g_p}{2}|\Psi_p|^2\,\Psi_p^*\delta\Psi_p\, d\mathbf{r}\,.
\end{aligned}$$

Clearly, the first integral is simply the original free energy F_p. Meanwhile, the last two integrals cannot be simplified any further in their current form due to the gradients of $\delta\Psi_p$ and $\delta\Psi_p^*$ in the first terms in their respective integrands. We can get around this by performing partial integration on these terms. For the first one, we have

$$\int_\Omega \frac{K_p}{2}\nabla\Psi_p\cdot\nabla\left(\delta\Psi_p^*\right)\, d\mathbf{r} = \left[\frac{K_p}{2}\nabla\Psi_p\cdot\hat{\mathbf{n}}\,\delta\Psi_p^*\right]_{\partial\Omega} - \int_\Omega \frac{K_p}{2}\nabla\cdot\nabla\Psi_p\delta\Psi_p^*\, d\mathbf{r} \;=\; -\int_\Omega \frac{K_p}{2}\nabla^2\Psi_p\delta\Psi_p^*\, d\mathbf{r}\,,$$

and likewise for the second one:

$$\int_\Omega \frac{K_p}{2}\nabla\Psi_p^*\cdot\nabla\left(\delta\Psi_p\right)\, d\mathbf{r} = \left[\frac{K_p}{2}\nabla\Psi_p^*\cdot\hat{\mathbf{n}}\,\delta\Psi_p\right]_{\partial\Omega} - \int_\Omega \frac{K_p}{2}\nabla\cdot\nabla\Psi_p^*\delta\Psi_p\, d\mathbf{r} \;=\; -\int_\Omega \frac{K_p}{2}\nabla^2\Psi_p^*\delta\Psi_p\, d\mathbf{r}\,,$$

where Ω is the domain of our system and $\partial\Omega$ its boundary, and $\hat{\mathbf{n}}$ is the unit normal vector to the boundary. In the last transitions in each integration we discard the boundary term by the usual assumption that the variation of Ψ_p is zero there. Inserting back into the main calculation, we get

$$\begin{aligned}
\tilde{F}_p &= F_p + \int\left(-\frac{K_p}{2}\nabla^2\Psi_p - \frac{g_p}{2}\Psi_p + \frac{g_p}{2}|\Psi_p|^2\,\Psi_p\right)\delta\Psi_p^*\, d\mathbf{r} \int\left(-\frac{K_p}{2}\nabla^2\Psi_p^* - \frac{g_p}{2}\Psi_p^* + \frac{g_p}{2}|\Psi_p|^2\,\Psi_p^*\right)\delta\Psi_p\, d\mathbf{r} \\
&\equiv F_p + \int\frac{\delta F_p}{\delta\Psi_p^*}\delta\Psi_p^*\, d\mathbf{r} + \int\frac{\delta F_p}{\delta\Psi_p}\delta\Psi_p\, d\mathbf{r}\,.
\end{aligned}$$

With the definition in eq. (3.27), we see that we must have

$$\partial_t\Psi_p = \Gamma_p\left(\frac{K_p}{2}\nabla^2\Psi_p + \frac{g_p}{2}\left(1-|\Psi_p|^2\right)\Psi_p\right) \;\text{ and }\; \partial_t\Psi_p^* = \Gamma_p\left(\frac{K_p}{2}\nabla^2\Psi_p^* + \frac{g_p}{2}\left(1-|\Psi_p|^2\right)\Psi_p^*\right)\,.$$

Obviously, these two equations are simply complex conjugates of each other, and so we use the first one as the dynamical equation for the p-atic order parameter.

B.1.3 Reformulation of the tensorial dynamical equation

In this subsection we will take a look at the second approach to deriving the dynamical equations for the complex scalar order parameter, which is to first derive them for the order parameter tensor $Q^{(p)}$, starting from the free energy functional in eq. (3.22), and then reformulate the result in terms of Ψ_p.

The standard way of defining the dynamical equations for dry p-atics in the tensorial formulation is the tensorial analogue of what was done in Section 3.2. Namely, we define the time evolution of the order parameter tensor $Q^{(p)}$ as

$$\partial_t Q^{(p)} = \frac{\Gamma_p}{4}H^{(p)}\,,$$

where $H^{(p)}$ is the *molecular field tensor*[1], defined as

$$H^{(p)} \equiv -\frac{\delta F_p}{\delta Q^{(p)}}\,. \tag{B.1}$$

[1] Or sometimes just the *molecular tensor*.

Therefore, in analogy with the complex scalar case, we want to compute the variation of the free energy functional with respect to the order parameter tensor. In other words, we want to compute the variation of F_p under $Q^{(p)} \to Q^{(p)} + \delta Q^{(p)}$. To avoid our expressions becoming too unwieldy, we will do this in steps, by first computing the variation of the individual terms in the integrand of the free energy functional. For the first term, we have

$$\begin{aligned}
\left|\nabla Q^{(p)}_{k_1\ldots k_p}\right|^2 &\to \left(\partial_i\left[Q^{(p)}_{k_1\ldots k_p} + \delta Q^{(p)}_{k_1\ldots k_p}\right]\right)\left(\partial_i\left[Q^{(p)}_{k_1\ldots k_p} + \delta Q^{(p)}_{k_1\ldots k_p}\right]\right) \\
&= \left(\partial_i Q^{(p)}_{k_1\ldots k_p} + \partial_i\left(\delta Q^{(p)}_{k_1\ldots k_p}\right)\right)\left(\partial_i Q^{(p)}_{k_1\ldots k_p} + \partial_i\left(\delta Q^{(p)}_{k_1\ldots k_p}\right)\right) \\
&= \partial_i Q^{(p)}_{k_1\ldots k_p}\partial_i Q^{(p)}_{k_1\ldots k_p} + 2\partial_i Q^{(p)}_{k_1\ldots k_p}\partial_i\left(\delta Q^{(p)}_{k_1\ldots k_p}\right) + \partial_i\left(\delta Q^{(p)}_{k_1\ldots k_p}\right)\partial_i\left(\delta Q^{(p)}_{k_1\ldots k_p}\right).
\end{aligned}$$

For the second term, we have

$$\begin{aligned}
\left|Q^{(p)}\right|^2 &\to \left(Q^{(p)}_{k_1\ldots k_p} + \delta Q^{(p)}_{k_1\ldots k_p}\right)\left(Q^{(p)}_{k_1\ldots k_p} + \delta Q^{(p)}_{k_1\ldots k_p}\right) \\
&= Q^{(p)}_{k_1\ldots k_p}Q^{(p)}_{k_1\ldots k_p} + 2Q^{(p)}_{k_1\ldots k_p}\delta Q^{(p)}_{k_1\ldots k_p} + \delta Q^{(p)}_{k_1\ldots k_p}\delta Q^{(p)}_{k_1\ldots k_p},
\end{aligned}$$

which gives us for the last term

$$\begin{aligned}
\left|Q^{(p)}\right|^4 &\to \left(Q^{(p)}_{k_1\ldots k_p}Q^{(p)}_{k_1\ldots k_p} + 2Q^{(p)}_{k_1\ldots k_p}\delta Q^{(p)}_{k_1\ldots k_p} + \delta Q^{(p)}_{k_1\ldots k_p}\delta Q^{(p)}_{k_1\ldots k_p}\right)^2 \\
&= \left(Q^{(p)}_{k_1\ldots k_p}Q^{(p)}_{k_1\ldots k_p}\right)^2 + 2Q^{(p)}_{k_1\ldots k_p}Q^{(p)}_{k_1\ldots k_p}Q^{(p)}_{m_1\ldots m_p}\delta Q^{(p)}_{m_1\ldots m_p} + Q^{(p)}_{k_1\ldots k_p}Q^{(p)}_{k_1\ldots k_p}\delta Q^{(p)}_{m_1\ldots m_p}\delta Q^{(p)}_{m_1\ldots m_p} \\
&+ 2Q^{(p)}_{k_1\ldots k_p}Q^{(p)}_{k_1\ldots k_p}Q^{(p)}_{m_1\ldots m_p}\delta Q^{(p)}_{m_1\ldots m_p} + 4Q^{(p)}_{k_1\ldots k_p}Q^{(p)}_{m_1\ldots m_p}\delta Q^{(p)}_{k_1\ldots k_p}\delta Q^{(p)}_{m_1\ldots m_p} \\
&+ 2Q^{(p)}_{k_1\ldots k_p}\delta Q^{(p)}_{k_1\ldots k_p}\delta Q^{(p)}_{m_1\ldots m_p}\delta Q^{(p)}_{m_1\ldots m_p} + Q^{(p)}_{k_1\ldots k_p}Q^{(p)}_{k_1\ldots k_p}\delta Q^{(p)}_{m_1\ldots m_p}\delta Q^{(p)}_{m_1\ldots m_p} \\
&+ 2Q^{(p)}_{k_1\ldots k_p}\delta Q^{(p)}_{k_1\ldots k_p}\delta Q^{(p)}_{m_1\ldots m_p}\delta Q^{(p)}_{m_1\ldots m_p} + \left(\delta Q^{(p)}_{k_1\ldots k_p}\delta Q^{(p)}_{k_1\ldots k_p}\right)^2 \\
&= \left(Q^{(p)}_{k_1\ldots k_p}Q^{(p)}_{k_1\ldots k_p}\right)^2 + 4Q^{(p)}_{k_1\ldots k_p}Q^{(p)}_{k_1\ldots k_p}Q^{(p)}_{m_1\ldots m_p}\delta Q^{(p)}_{m_1\ldots m_p} + 2Q^{(p)}_{k_1\ldots k_p}Q^{(p)}_{k_1\ldots k_p}\delta Q^{(p)}_{m_1\ldots m_p}\delta Q^{(p)}_{m_1\ldots m_p} \\
&+ 4Q^{(p)}_{k_1\ldots k_p}Q^{(p)}_{m_1\ldots m_p}\delta Q^{(p)}_{k_1\ldots k_p}\delta Q^{(p)}_{m_1\ldots m_p} + 4Q^{(p)}_{k_1\ldots k_p}\delta Q^{(p)}_{k_1\ldots k_p}\delta Q^{(p)}_{m_1\ldots m_p}\delta Q^{(p)}_{m_1\ldots m_p} + \left(\delta Q^{(p)}_{k_1\ldots k_p}\delta Q^{(p)}_{k_1\ldots k_p}\right)^2,
\end{aligned}$$

To leading order in $\delta Q^{(p)}$, we now get

$$\begin{aligned}
F_p &\to \int \frac{L_p}{2}\left(\partial_i Q^{(p)}_{k_1\ldots k_p}\partial_i Q^{(p)}_{k_1\ldots k_p} + 2\partial_i Q^{(p)}_{k_1\ldots k_p}\partial_i\left(\delta Q^{(p)}_{k_1\ldots k_p}\right)\right) + \frac{A_p}{2}\left(Q^{(p)}_{k_1\ldots k_p}Q^{(p)}_{k_1\ldots k_p} + 2Q^{(p)}_{k_1\ldots k_p}\delta Q^{(p)}_{k_1\ldots k_p}\right) \\
&+ \frac{B_p}{4}\left(\left(Q^{(p)}_{k_1\ldots k_p}Q^{(p)}_{k_1\ldots k_p}\right)^2 + 4Q^{(p)}_{k_1\ldots k_p}Q^{(p)}_{k_1\ldots k_p}Q^{(p)}_{m_1\ldots m_p}\delta Q^{(p)}_{m_1\ldots m_p}\right) d^2r \\
&= \int \frac{L_p}{2}\partial_i Q^{(p)}_{k_1\ldots k_p}\partial_i Q^{(p)}_{k_1\ldots k_p} + L_p\partial_i Q^{(p)}_{k_1\ldots k_p}\partial_i\left(\delta Q^{(p)}_{k_1\ldots k_p}\right) + \frac{A_p}{2}Q^{(p)}_{k_1\ldots k_p}Q^{(p)}_{k_1\ldots k_p} + A_pQ^{(p)}_{k_1\ldots k_p}\delta Q^{(p)}_{k_1\ldots k_p} \\
&+ \frac{B_p}{2}\left(Q^{(p)}_{k_1\ldots k_p}Q^{(p)}_{k_1\ldots k_p}\right)^2 + B_pQ^{(p)}_{k_1\ldots k_p}Q^{(p)}_{k_1\ldots k_p}Q^{(p)}_{m_1\ldots m_p}\delta Q^{(p)}_{m_1\ldots m_p}\, d^2r \\
&= \int \frac{L_p}{2}\left|\nabla Q^{(p)}\right|^2 + \frac{A_p}{2}\left|Q^{(p)}\right|^2 + \frac{B_p}{4}\left|Q^{(p)}\right|^4 d^2r \\
&+ \int L_p\partial_i Q^{(p)}_{k_1\ldots k_p}\partial_i\left(\delta Q^{(p)}_{k_1\ldots k_p}\right) + A_pQ^{(p)}_{k_1\ldots k_p}\delta Q^{(p)}_{k_1\ldots k_p} + B_pQ^{(p)}_{k_1\ldots k_p}Q^{(p)}_{k_1\ldots k_p}Q^{(p)}_{m_1\ldots m_p}\delta Q^{(p)}_{m_1\ldots m_p}\, d^2r \\
&= F_p + \int L_p\partial_i Q^{(p)}_{k_1\ldots k_p}\partial_i\left(\delta Q^{(p)}_{k_1\ldots k_p}\right) + \left(A_p + B_pQ^{(p)}_{k_1\ldots k_p}Q^{(p)}_{k_1\ldots k_p}\right)Q^{(p)}_{m_1\ldots m_p}\delta Q^{(p)}_{m_1\ldots m_p}\, d^2r\,.
\end{aligned}$$

As in the complex scalar case, the integrand cannot be simplified any further due to the gradient of $\delta Q^{(p)}_{k_1\ldots k_p}$, but in this case also, partial integration comes to the rescue:

$$\int\limits_\Omega \partial_i Q^{(p)}_{k_1\ldots k_p}\partial_i\left(\delta Q^{(p)}_{k_1\ldots k_p}\right) d^2r = \left[\partial_i Q^{(p)}_{k_1\ldots k_p}\delta Q^{(p)}_{k_1\ldots k_p}n_i\right]_{\partial\Omega} - \int\limits_\Omega \partial_i\partial_i Q^{(p)}_{k_1\ldots k_p}\delta Q^{(p)}_{k_1\ldots k_p}\, d^2r\,,$$

where n_i are the components of the unit vector perpendicular to the boundary $\partial\Omega$ of our system's domain Ω. Disregarding the boundary term under the assumption that the variation of $Q^{(p)}$ is zero there, we see that we must have

$$\begin{aligned} F_p &\rightarrow F_p + \int -L_p \partial_i \partial_i Q^{(p)}_{m_1 \ldots m_p} \delta Q^{(p)}_{m_1 \ldots m_p} + \left(A_p + B_p Q^{(p)}_{k_1 \ldots k_p} Q^{(p)}_{k_1 \ldots k_p} \right) Q^{(p)}_{m_1 \ldots m_p} \delta Q^{(p)}_{m_1 \ldots m_p} \, d^2 r \\ &= F_p + \int \left(-L_p \partial_i \partial_i Q^{(p)}_{m_1 \ldots m_p} + \left[A_p + B_p Q^{(p)}_{k_1 \ldots k_p} Q^{(p)}_{k_1 \ldots k_p} \right] Q^{(p)}_{m_1 \ldots m_p} \right) \delta Q^{(p)}_{m_1 \ldots m_p} \, d^2 r \\ &\equiv F_p + \int \frac{\delta F}{\delta Q^{(p)}} \delta Q^{(p)} \, d^2 r \, . \end{aligned}$$

With this, we see that the molecular tensor is

$$H^{(p)} \equiv -\frac{\delta F_p}{\delta Q^{(p)}} = L_p \nabla^2 Q^{(p)} - \left(A_p + B_p \left| Q^{(p)} \right|^2 \right) Q^{(p)} \, , \tag{B.2}$$

which gives us

$$\partial_t Q^{(p)} = \frac{\Gamma_p}{4} \left(L_p \nabla^2 Q^{(p)} - \left(A_p + B_p \left| Q^{(p)} \right|^2 \right) Q^{(p)} \right) . \tag{B.3}$$

To re-express this equation in terms of the complex scalar order parameter, we can use the inverse of the map in eq. (3.12) to first express the components of $Q^{(p)}$ in terms of Ψ_p. From eq. (3.12) we see that we must have

$$Q^{(p)}_{11\ldots1} = \sqrt{2^{-p}} \Psi_R \text{ and } Q^{(p)}_{21\ldots1} = \sqrt{2^{-p}} \Psi_I \, .$$

Therefore, we can write eq. (B.3) for these two components as

$$\begin{aligned} \partial_t \left(\sqrt{2^{-p}} \Psi_R \right) &= \frac{\Gamma_p}{4} \left(L_p \nabla^2 \left(\sqrt{2^{-p}} \Psi_R \right) - \left(A_p + B_p \frac{1}{2} \left| \Psi_p \right|^2 \right) \sqrt{2^{-p}} \Psi_R \right) , \\ \partial_t \left(\sqrt{2^{-p}} \Psi_I \right) &= \frac{\Gamma_p}{4} \left(L_p \nabla^2 \left(\sqrt{2^{-p}} \Psi_I \right) - \left(A_p + B_p \frac{1}{2} \left| \Psi_p \right|^2 \right) \sqrt{2^{-p}} \Psi_I \right) , \end{aligned}$$

or, combining with eq. (3.24)

$$\begin{aligned} \partial_t \Psi_R &= \frac{\Gamma_p}{4} \left(2K_p \nabla^2 \Psi_R - \left(-2g_p + \frac{4g_p}{2} \left| \Psi_p \right|^2 \right) \Psi_R \right) = \Gamma_p \left(\frac{K_p}{2} \nabla^2 \Psi_R + \frac{g_p}{2} \left[1 - \left| \Psi_p \right|^2 \right] \Psi_R \right) , \\ \partial_t \Psi_I &= \frac{\Gamma_p}{4} \left(2K_p \nabla^2 \Psi_I - \left(-2g_p + \frac{4g_p}{2} \left| \Psi_p \right|^2 \right) \Psi_I \right) = \Gamma_p \left(\frac{K_p}{2} \nabla^2 \Psi_I + \frac{g_p}{2} \left[1 - \left| \Psi_p \right|^2 \right] \Psi_I \right) . \end{aligned}$$

Finally, combining these two equations into one, we get

$$\partial_t \Psi_p = \Gamma_p \left(\frac{K_p}{2} \nabla^2 \Psi_p + \frac{g_p}{2} \left[1 - \left| \Psi_p \right|^2 \right] \Psi_p \right) ,$$

which is, of course, just eq. (3.29).

B.2 Calculations for Chapter 4

B.2.1 Reformulation of the stresses in terms of the complex scalar order parameter

We want to express the various forms of stress from eq.'s (**??**) and (**??**) in terms of the complex scalar order parameter Ψ_p. The simplest one to begin with is the elastic stress in eq. (**??**).

The elastic stress

In terms of the order parameter tensor $Q^{(p)}$, the elastic stress is given as

$$\sigma^{(e)}_{ij} = -L_p \partial_i Q^{(p)}_{k_1 \ldots k_p} \partial_j Q^{(p)}_{k1 \ldots k_p} \, .$$

Expanding the contraction, we get

$$\begin{aligned}
\sigma_{ij}^{(e)} &= -L_p \sum_{k=0}^{p} \sum_{\{\pi^k\}} \partial_i Q^{(p)}_{\pi_1^k \dots \pi_p^k} \partial_j Q^{(p)}_{\pi_1^k \dots \pi_p^k} \\
&= -L_p \left(\sum_{\{\pi^0\}} \partial_i Q^{(p)}_{\pi_1^0 \dots \pi_p^0} \partial_j Q^{(p)}_{\pi_1^0 \dots \pi_p^0} + \sum_{\{\pi^1\}} \partial_i Q^{(p)}_{\pi_1^1 \dots \pi_p^1} \partial_j Q^{(p)}_{\pi_1^1 \dots \pi_p^1} \right. \\
&\qquad \left. + \sum_{\{\pi^2\}} \partial_i Q^{(p)}_{\pi_1^2 \dots \pi_p^2} \partial_j Q^{(p)}_{\pi_1^2 \dots \pi_p^2} + \sum_{\{\pi^3\}} \partial_i Q^{(p)}_{\pi_1^3 \dots \pi_p^3} \partial_j Q^{(p)}_{\pi_1^3 \dots \pi_p^3} + \dots \right) \\
&= -L_p \left(2^{-p} \binom{p}{0} \partial_i \Psi_R \partial_j \Psi_R + 2^{-p} \binom{p}{1} \partial_i \Psi_I \partial_j \Psi_I - 2^{-p} \binom{p}{2} \partial_i \Psi_R \partial_j \Psi_R - 2^{-p} \binom{p}{3} \partial_i \Psi_I \partial_j \Psi_I + \dots \right) \\
&= -2^{-p} L_p \left(\left[\binom{p}{0} + \binom{p}{2} + \dots \right] \partial_i \Psi_R \partial_j \Psi_R + \left[\binom{p}{1} + \binom{p}{3} + \dots \right] \partial_i \Psi_I \partial_j \Psi_I \right) \\
&= -2^{-p} L_p \sum_{k=0}^{\lfloor \frac{p}{2} \rfloor} \left\{ \binom{p}{2k} \partial_i \Psi_R \partial_j \Psi_R + \binom{p}{2k+1} \partial_i \Psi_I \partial_j \Psi_I \right\} \\
&= -2^{-p} L_p \cdot 2^{p-1} \left(\partial_i \Psi_R \partial_j \Psi_R + \partial_i \Psi_I \partial_j \Psi_I \right) \\
&= -\frac{L_p}{2} \left(\partial_i \Psi_R \partial_j \Psi_R + \partial_i \Psi_I \partial_j \Psi_I \right) .
\end{aligned}$$

The reactive stress

Like for the elastic stress, we want to express the reactive stress in eq. (4.4) in terms of Ψ_p also. However, instead of computing the whole expression at once, we will first split the reactive stress into its constituent terms by defining

$$\sigma^{(r,1)} \equiv (-1)^{p-1} \lambda_p \nabla^{\otimes(p-2)} H^{(p)} \text{ and } \sigma^{(r,2)} \equiv \frac{p}{2} \left(Q^{(p)} \cdot H^{(p)} - H^{(p)} \cdot Q^{(p)} \right) .$$

such that

$$\sigma^{(r)} = \sigma^{(r,1)} + \sigma^{(r,2)} .$$

Between these two terms, the simplest one to express in terms of Ψ_p is $\sigma^{(r,2)}$, so we will address it first. In component form $\sigma^{(r,2)}$ can be written as

$$\sigma_{ij}^{(r,2)} = \frac{p}{2} \left(Q^{(p)}_{k_1 \dots k_{p-1} i} H^{(p)}_{k_1 \dots k_{p-1} j} - H^{(p)}_{k_1 \dots k_{p-1} i} Q^{(p)}_{k_1 \dots k_{p-1} j} \right) .$$

Expanding the contractions, and using the expression for the molecular tensor from eq. (B.2), we get

$$\begin{aligned}
\sigma_{ij}^{(r,2)} &= \frac{p}{2} \left(Q^{(p)}_{k_1 \dots k_{p-1} i} H^{(p)}_{k_1 \dots k_{p-1} j} - H^{(p)}_{k_1 \dots k_{p-1} i} Q^{(p)}_{k_1 \dots k_{p-1} j} \right) \\
&= \frac{p}{2} \left(Q^{(p)}_{k_1 \dots k_{p-1} i} \left[L_p \nabla^2 Q^{(p)}_{k_1 \dots k_{p-1} j} - \left(A_p + B_p \left| Q^{(p)} \right|^2 \right) Q^{(p)}_{k_1 \dots k_{p-1} j} \right] \right. \\
&- \left. \left[L_p \nabla^2 Q^{(p)}_{k_1 \dots k_{p-1} i} - \left(A_p + B_p \left| Q^{(p)} \right|^2 \right) Q^{(p)}_{k_1 \dots k_{p-1} i} \right] Q^{(p)}_{k_1 \dots k_{p-1} j} \right) \\
&= \frac{p}{2} \left(L_p Q^{(p)}_{k_1 \dots k_{p-1} i} \nabla^2 Q^{(p)}_{k_1 \dots k_{p-1} j} - \left(A_p + B_p \left| Q^{(p)} \right|^2 \right) Q^{(p)}_{k_1 \dots k_{p-1} i} Q^{(p)}_{k_1 \dots k_{p-1} j} \right. \\
&- \left. L_p Q^{(p)}_{k_1 \dots k_{p-1} j} \nabla^2 Q^{(p)}_{k_1 \dots k_{p-1} i} + \left(A_p + B_p \left| Q^{(p)} \right|^2 \right) Q^{(p)}_{k_1 \dots k_{p-1} i} Q^{(p)}_{k_1 \dots k_{p-1} j} \right) \\
&= \frac{p L_p}{2} \left(Q^{(p)}_{k_1 \dots k_{p-1} i} \nabla^2 Q^{(p)}_{k_1 \dots k_{p-1} j} - Q^{(p)}_{k_1 \dots k_{p-1} j} \nabla^2 Q^{(p)}_{k_1 \dots k_{p-1} i} \right) .
\end{aligned}$$

From this expression, it is manifest that $\sigma^{(r,2)}$ is an antisymmetric tensor, which means that we can compute its entire structure from just one component, say $\sigma_{12}^{(r,2)}$. Continuing on, we have

$$\begin{aligned}
\sigma_{12}^{(r,2)} &= \frac{pL_p}{2}\sum_{k=0}^{p-1}\sum_{\{\pi^k\}} Q^{(p)}_{\pi_1^k\ldots\pi_{p-1}^k 1}\nabla^2 Q^{(p)}_{\pi_1^k\ldots\pi_{p-1}^k 2} - Q^{(p)}_{\pi_1^k\ldots\pi_{p-1}^k 2}\nabla^2 Q^{(p)}_{\pi_1^k\ldots\pi_{p-1}^k 1} \\
&= \frac{pL_p}{2}\Bigg(\sum_{\{\pi^0\}} Q^{(p)}_{\pi_1^0\ldots\pi_{p-1}^0 1}\nabla^2 Q^{(p)}_{\pi_1^0\ldots\pi_{p-1}^0 2} - Q^{(p)}_{\pi_1^0\ldots\pi_{p-1}^0 2}\nabla^2 Q^{(p)}_{\pi_1^0\ldots\pi_{p-1}^0 1} \\
&\quad + \sum_{\{\pi^1\}} Q^{(p)}_{\pi_1^1\ldots\pi_{p-1}^1 1}\nabla^2 Q^{(p)}_{\pi_1^1\ldots\pi_{p-1}^1 2} - Q^{(p)}_{\pi_1^1\ldots\pi_{p-1}^1 2}\nabla^2 Q^{(p)}_{\pi_1^1\ldots\pi_{p-1}^1 1} \\
&\quad + \sum_{\{\pi^2\}} Q^{(p)}_{\pi_1^2\ldots\pi_{p-1}^2 1}\nabla^2 Q^{(p)}_{\pi_1^2\ldots\pi_{p-1}^2 2} - Q^{(p)}_{\pi_1^2\ldots\pi_{p-1}^2 2}\nabla^2 Q^{(p)}_{\pi_1^2\ldots\pi_{p-1}^2 1} \\
&\quad + \sum_{\{\pi^3\}} Q^{(p)}_{\pi_1^3\ldots\pi_{p-1}^3 1}\nabla^2 Q^{(p)}_{\pi_1^3\ldots\pi_{p-1}^3 2} - Q^{(p)}_{\pi_1^3\ldots\pi_{p-1}^3 2}\nabla^2 Q^{(p)}_{\pi_1^3\ldots\pi_{p-1}^3 1} + \ldots\Bigg) \\
&= \frac{pL_p}{2}\Bigg(2^{-p}\sum_{\{\pi^0\}} \Psi_R\nabla^2\Psi_I - \Psi_I\nabla^2\Psi_R + 2^{-p}\sum_{\{\pi^1\}} -\Psi_I\nabla^2\Psi_R + \Psi_R\nabla^2\Psi_I \\
&\quad + 2^{-p}\sum_{\{\pi^2\}} \Psi_R\nabla^2\Psi_I - \Psi_I\nabla^2\Psi_R + 2^{-p}\sum_{\{\pi^3\}} -\Psi_I\nabla^2\Psi_R + \Psi_R\nabla^2\Psi_I + \ldots\Bigg) \\
&= \frac{2^{-p}pL_p}{2}\Bigg(\binom{p-1}{0}\Psi_R\nabla^2\Psi_I - \Psi_I\nabla^2\Psi_R + \binom{p-1}{1}\Psi_R\nabla^2\Psi_I - \Psi_I\nabla^2\Psi_R \\
&\quad + \binom{p-1}{2}\Psi_R\nabla^2\Psi_I - \Psi_I\nabla^2\Psi_R + \binom{p-1}{3}\Psi_R\nabla^2\Psi_I - \Psi_I\nabla^2\Psi_R + \ldots\Bigg) \\
&= 2^{-p-1}pL_p\sum_{k=0}^{p-1}\binom{p-1}{k}\left(\Psi_R\nabla^2\Psi_I - \Psi_I\nabla^2\Psi_R\right) \\
&= 2^{-p-1}pL_p\cdot 2^{p-1}\left(\Psi_R\nabla^2\Psi_I - \Psi_I\nabla^2\Psi_R\right) \\
&= \frac{pL_p}{4}\left(\Psi_R\nabla^2\Psi_I - \Psi_I\nabla^2\Psi_R\right)
\end{aligned}$$

Finally, we also want to re-express the term $\sigma^{(r,1)}$ in the reactive stress in terms of Ψ_p. Specifically, we want to compute the explicit form of $\sigma^{(r,1)}$ in terms of Ψ_p for $p = 2, 3, 4$. In component form $\sigma^{(r,1)}$ can be written as

$$\sigma_{ij}^{(r,1)} = (-1)^{p-1}\lambda_p\partial_{k_1}\ldots\partial_{k_{p-2}}H^{(p)}_{k_1\ldots k_{p-2}ij}\,,$$

with $H^{(p)}_{k_1\ldots k_{p-2}ij}$ being

$$H^{(p)}_{k_1\ldots k_{p-2}ij} = L_p\nabla^2 Q^{(p)}_{k_1\ldots k_{p-2}ij} - \left(A_p + B_p\left|Q^{(p)}\right|^2\right)Q^{(p)}_{k_1\ldots k_{p-2}ij}\,.$$

Because we want to consider the stresses and the resulting induced flows from a single defect throughout the whole system, we want to do our calculations in the far field where $A_p + B_p\left|Q^{(p)}\right|^2 \approx 0$. This means that the molecular tensor will simply be

$$H^{(p)}_{k_1\ldots k_{p-2}ij} \approx L_p\nabla^2 Q^{(p)}_{k_1\ldots k_{p-2}ij}\,,$$

which gives us for $\sigma^{(r,1)}$

$$\sigma_{ij}^{(r,1)} \approx (-1)^{p-1}L_p\lambda_p\partial_{k_1}\ldots\partial_{k_{p-2}}\nabla^2 Q^{(p)}_{k_1\ldots k_{p-2}ij}\,. \tag{B.4}$$

From the simple dependence of $\sigma^{(r,1)}$ on $Q^{(p)}$ it immediately follows that $\sigma^{(r,1)}$ must be symmetric and traceless, just as $Q^{(p)}$ is. This means that we can compute the whole of $\sigma^{(r,1)}$ from just two components, which we will now do for $p = 2, 3, 4$.

For $p = 2$ eq. (B.4) reduces to simply

$$\sigma_{ij}^{(r,1)} = (-1)\, L_2\lambda_2\nabla^2 Q_{ij}^{(2)}\,.$$

As we've seen in Appendix [previous], the two independent components of $Q^{(p)}$ can be related to the real and imaginary parts of Ψ_p as

$$Q_{11\ldots1}^{(p)} = \sqrt{2^{-p}}\Psi_R \text{ and } Q_{21\ldots1}^{(p)} = \sqrt{2^{-p}}\Psi_I\,.$$

Specifically, for $Q^{(2)}$ it follows that

$$Q_{11}^{(2)} = \frac{1}{2}\Psi_R \text{ and } Q_{21}^{(2)} = \frac{1}{2}\Psi_I\,.$$

This means that

$$\sigma_{11}^{(r,1)} = -\sigma_{22}^{(r,1)} = -\frac{L_2\lambda_2}{2}\nabla^2\Psi_R \text{ and } \sigma_{12}^{(r,1)} = \sigma_{21}^{(r,1)} = -\frac{L_2\lambda_2}{2}\nabla^2\Psi_I\,,$$

or

$$\sigma^{(r,1)} = -\frac{L_2\lambda_2}{2}\begin{pmatrix} \nabla^2\Psi_R & \nabla^2\Psi_I \\ \nabla^2\Psi_I & -\nabla^2\Psi_R \end{pmatrix}. \tag{B.5}$$

For $p = 3$, eq. (B.4) gives

$$\sigma_{ij}^{(r,1)} = (-1)^2\, L_3\lambda_3\partial_k\nabla^2 Q_{kij}^{(3)} = L_3\lambda_3\left(\partial_x Q_{1ij}^{(3)} + \partial_y Q_{2ij}^{(3)}\right).$$

With the independent components of $Q^{(3)}$ being

$$Q_{111}^{(3)} = \frac{1}{2\sqrt{2}}\Psi_R \text{ and } Q_{211}^{(3)} = \frac{1}{2\sqrt{2}}\Psi_I\,,$$

we now have

$$\sigma_{11}^{(r,1)} = -\sigma_{22}^{(r,1} = L_3\lambda_3\left(\partial_x Q_{111}^{(3)} + \partial_y Q_{211}^{(3)}\right) = \frac{L_3\lambda_3}{2\sqrt{2}}\left(\partial_x\nabla^2\Psi_R + \partial_y\nabla^2\Psi_I\right),$$

and

$$\sigma_{12}^{(r,1)} = \sigma_{21}^{(r,1} = L_3\lambda_3\left(\partial_x Q_{112}^{(3)} + \partial_y Q_{212}^{(3)}\right) = \frac{L_3\lambda_3}{2\sqrt{2}}\left(\partial_x\nabla^2\Psi_I - \partial_y\nabla^2\Psi_R\right),$$

which means that

$$\sigma^{(r,1)} = \frac{L_3\lambda_3}{2\sqrt{2}}\begin{pmatrix} \partial_x\nabla^2\Psi_R + \partial_y\nabla^2\Psi_I & \partial_x\nabla^2\Psi_I - \partial_y\nabla^2\Psi_R \\ \partial_x\nabla^2\Psi_I - \partial_y\nabla^2\Psi_R & -\partial_x\nabla^2\Psi_R - \partial_y\nabla^2\Psi_I \end{pmatrix}. \tag{B.6}$$

Finally, for $p = 4$, eq. (B.4) gives

$$\begin{aligned}
\sigma_{ij}^{(r,1)} &= (-1)^3\, L_4\lambda_4\partial_m\partial_n\nabla^2 Q_{mnij}^{(4)} \\
&= -L_4\lambda_4\partial_m\left(\partial_x\nabla^2 Q_{m1ij}^{(4)} + \partial_y\nabla^2 Q_{m2ij}^{(4)}\right) \\
&= -L_4\lambda_4\left(\partial_x\partial_x\nabla^2 Q_{11ij}^{(4)} + \partial_x\partial_y\nabla^2 Q_{12ij}^{(4)} + \partial_y\partial_x\nabla^2 Q_{21ij}^{(4)} + \partial_y\partial_y\nabla^2 Q_{22ij}^{(4)}\right) \\
&= -L_4\lambda_4\left(\partial_x^2\nabla^2 Q_{11ij}^{(4)} + \partial_y^2\nabla^2 Q_{22ij}^{(4)} + 2\partial_x\partial_y\nabla^2 Q_{12ij}^{(4)}\right).
\end{aligned}$$

The independent components of $Q^{(4)}$ are

$$Q_{1111}^{(4)} = \frac{1}{4}\Psi_R \text{ and } Q_{2111}^{(4)} = \frac{1}{4}\Psi_I\,,$$

which gives us

$$\sigma_{11}^{(r,1)} = -L_4\lambda_4\left(\partial_x^2\nabla^2 Q_{1111}^{(4)} + \partial_y^2\nabla^2 Q_{2211}^{(4)} + 2\partial_x\partial_y\nabla^2 Q_{1211}^{(4)}\right) = -\frac{L_4\lambda_4}{4}\left(\partial_x^2\nabla^2\Psi_R - \partial_y^2\nabla^2\Psi_R + 2\partial_x\partial_y\nabla^2\Psi_I\right),$$

and

$$\sigma_{12}^{(r,1)} = -L_4\lambda_4\left(\partial_x^2\nabla^2 Q_{1112}^{(4)} + \partial_y^2\nabla^2 Q_{2212}^{(4)} + 2\partial_x\partial_y\nabla^2 Q_{1212}^{(4)}\right) = -\frac{L_4\lambda_4}{4}\left(\partial_x^2\nabla^2\Psi_I - \partial_y^2\nabla^2\Psi_I - 2\partial_x\partial_y\nabla^2\Psi_R\right).$$

Thus, for $p = 4$ the reactive stress $\sigma^{(r,1)}$ is

$$\sigma^{(r,1)} = -\frac{L_4\lambda_4}{4}\begin{pmatrix} \partial_x^2\nabla^2\Psi_R - \partial_y^2\nabla^2\Psi_R + 2\partial_x\partial_y\nabla^2\Psi_I & \partial_x^2\nabla^2\Psi_I - \partial_y^2\nabla^2\Psi_I - 2\partial_x\partial_y\nabla^2\Psi_R \\ \partial_x^2\nabla^2\Psi_I - \partial_y^2\nabla^2\Psi_I - 2\partial_x\partial_y\nabla^2\Psi_R & -\partial_x^2\nabla^2\Psi_R + \partial_y^2\nabla^2\Psi_R - 2\partial_x\partial_y\nabla^2\Psi_I \end{pmatrix}. \tag{B.7}$$

Chapter C

Supplementary figures

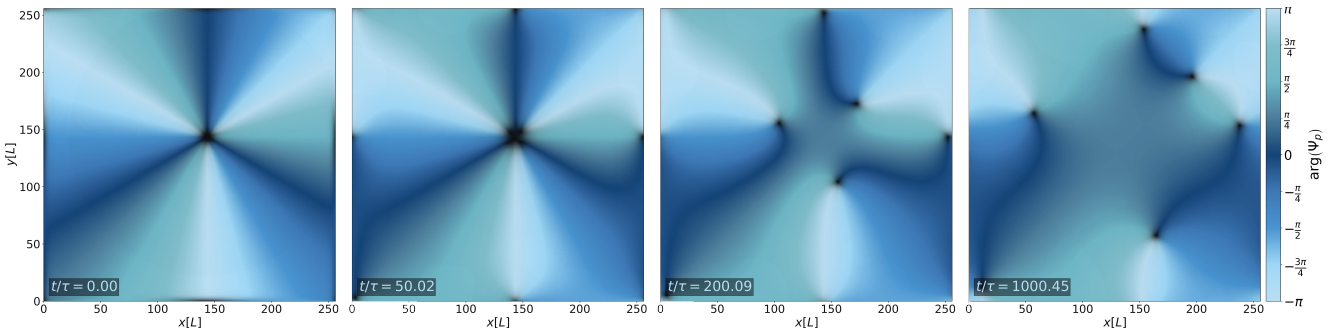

Figure C.1: Dissociation of a $m_p = 3$ defect in a dry p-atic into a group of three $+1$ defects.

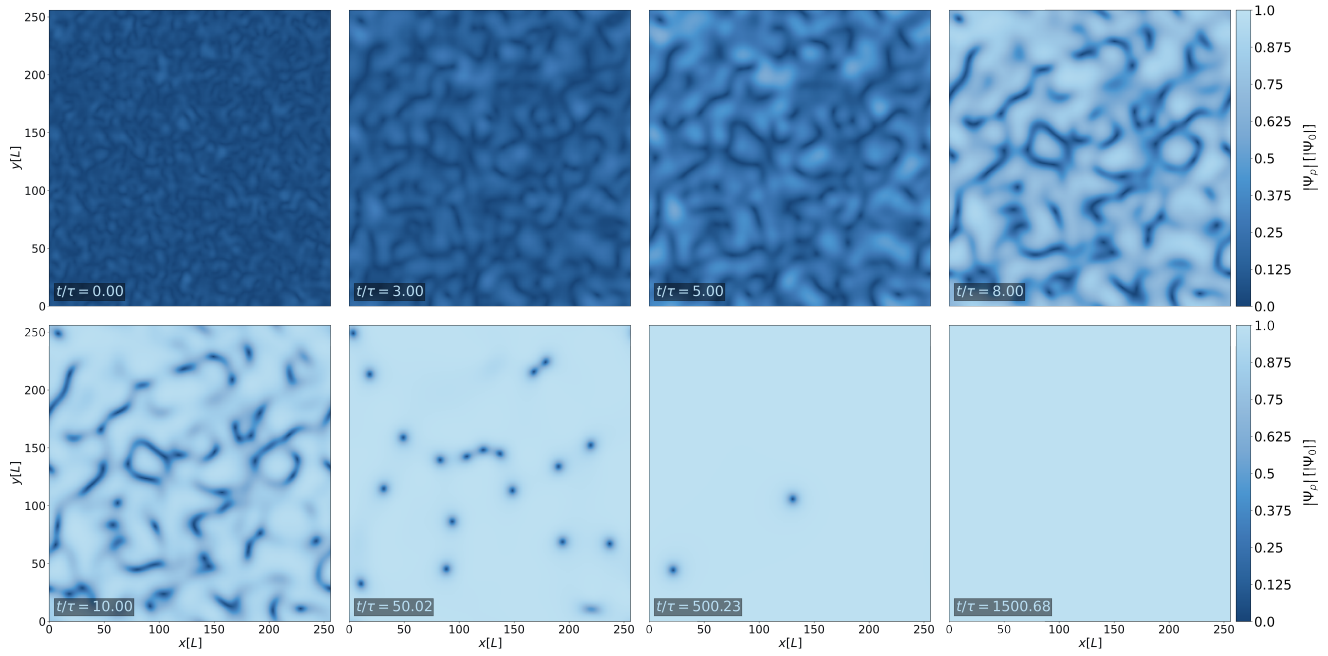

Figure C.2: Time series of the magnitude of the p-atic order parameter during the relaxation in Figure 3.7.

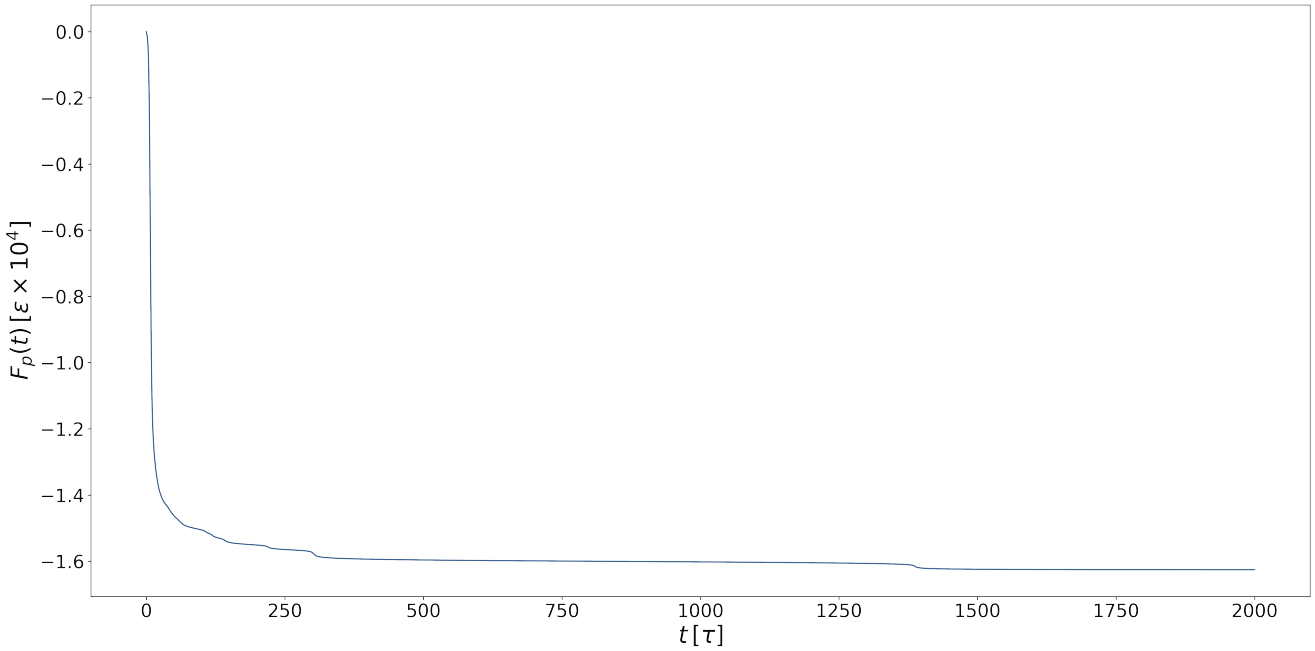

Figure C.3: The p-atic free energy as a function of time obtained from the numerical solution for the evolution of the order which is shown in Figure 3.7. The free energy is drastically minimized over a very short time early on in the relaxation of the order parameter, before the minimization slows down. When the number of defects in the system is reduced to a handful of defects, their annihilation shows as distinct drops in the free energy, as can be seen at $t/\tau \approx 1380$. This drop in the free energy results from the annihilation of the two defects which can be observed in Figure C.2 at $t\tau = 500$.

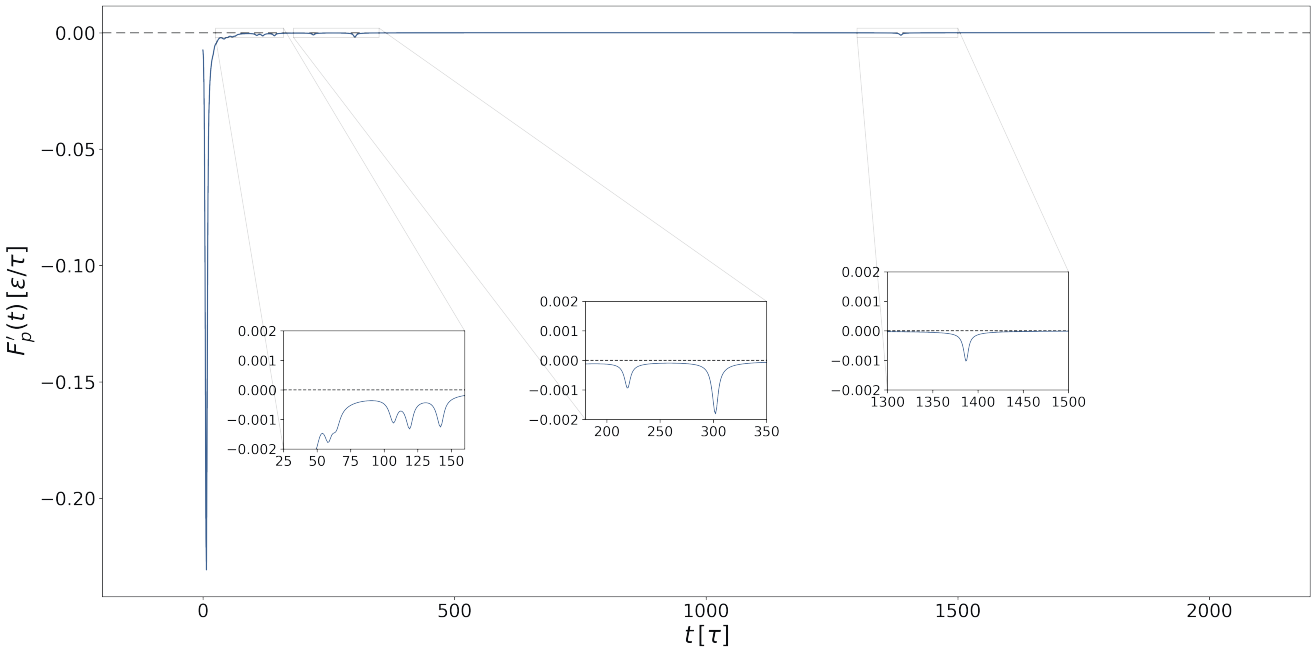

Figure C.4: The time derivative of the free energy in Figure C.3 obtained by numerical derivation. Staying below zero at all times, this numerical result verifies the result we obtained analytically in Chapter 3 that the dynamical equation for the order parameter of dry p-atics does indeed result in minimization of the free energy.

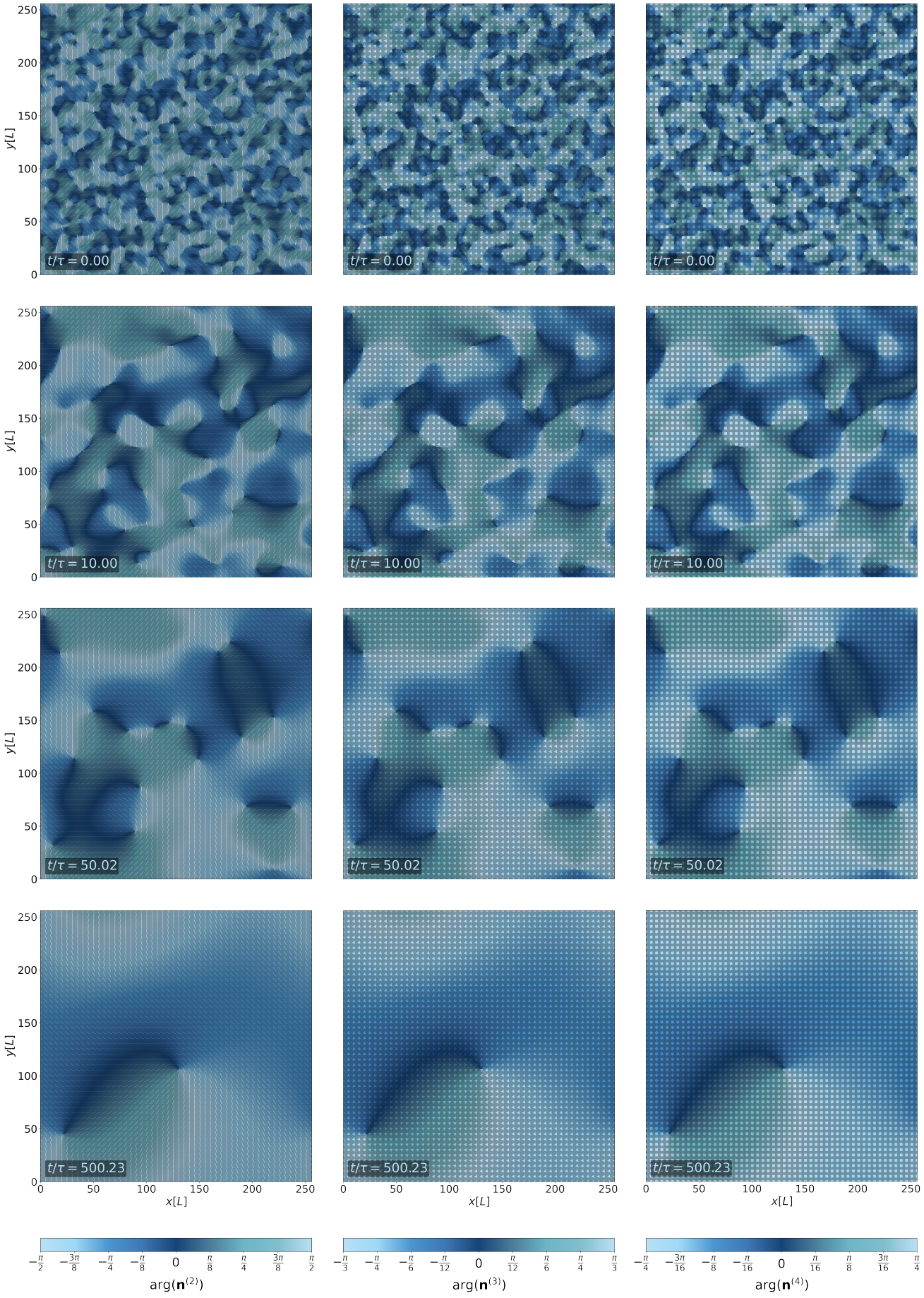

Figure C.5: Time evolution of the dry p-atic director $\mathbf{n}^{(p)}$ for $p = 2, 3, 4$ with the same initial conditions for each p. In addition to the phase plots, $\mathbf{n}^{(p)}$ is also represented by regular polygons (rods for $p = 2$) to emphasize that these are indeed different p-atics. Although the range of values of the director phase is different for each value of p, it is clear that the qualitative features of the evolution are identical, which demonstrates the universal nature of dry p-atics.

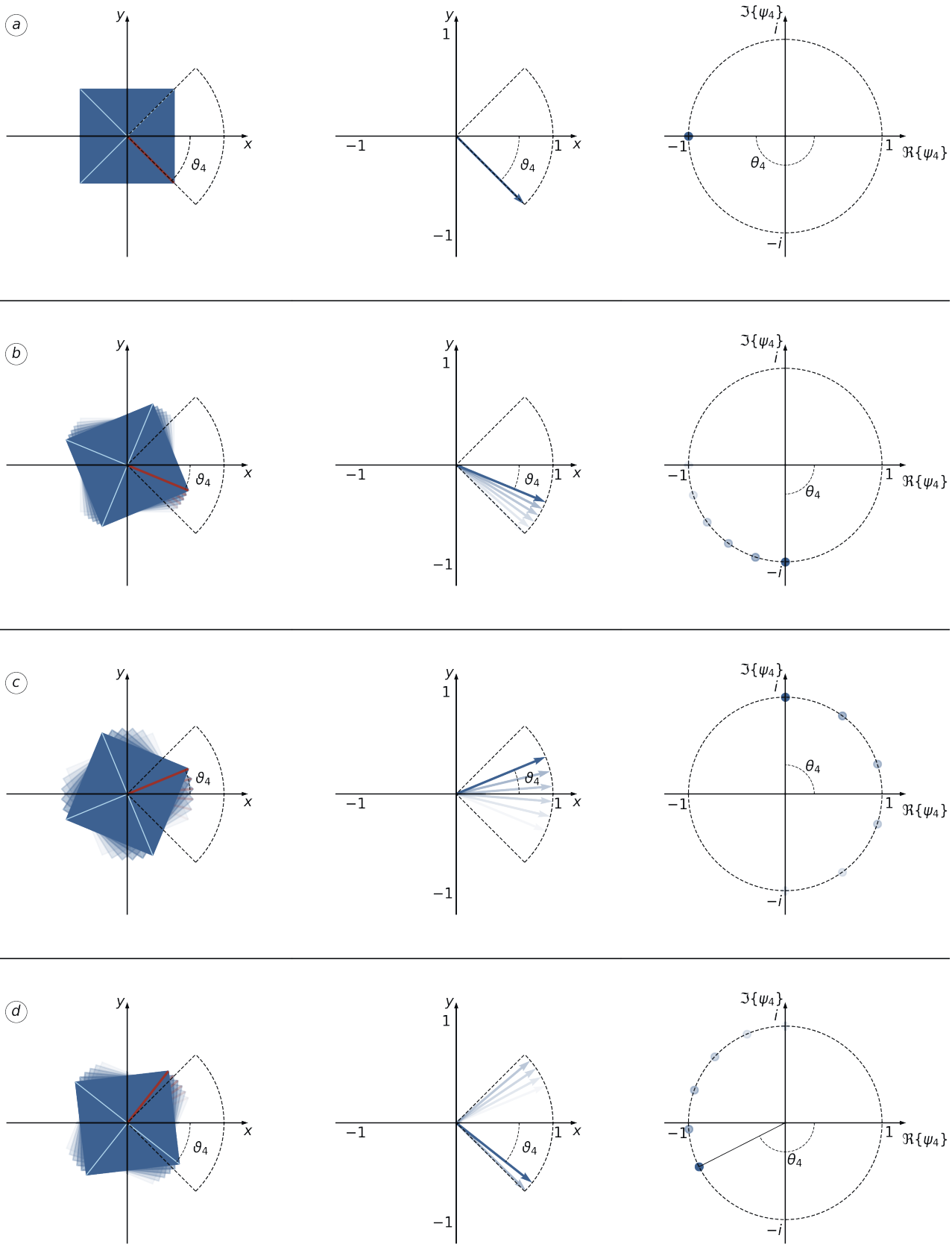

Figure C.6: Relationship between the orientation of a 4-atic particle, the corresponding director $\nu^{(4)}$ and order parameter ψ_4. See caption to Figure 3.5 for a full explanation.

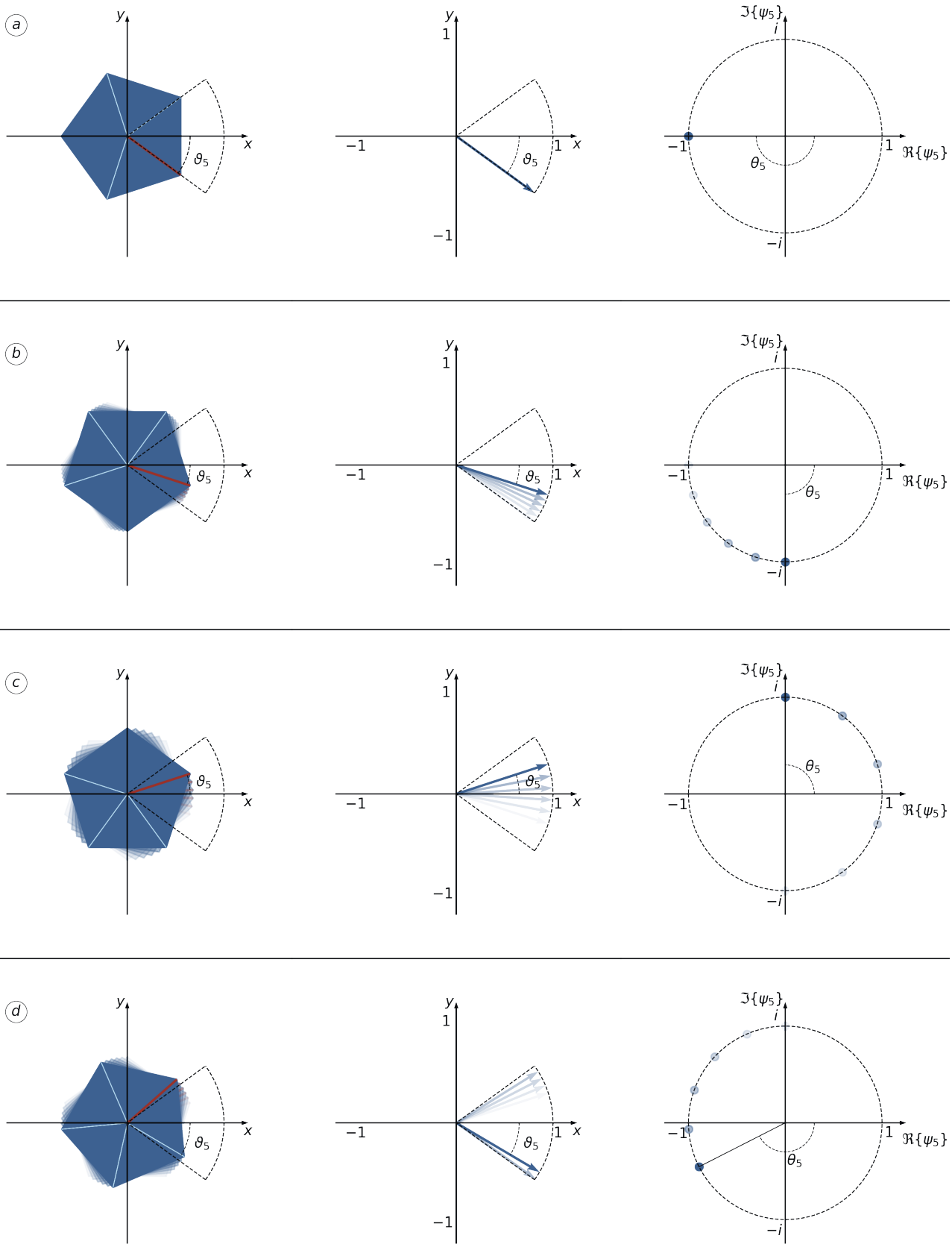

Figure C.7: Relationship between the orientation of the 5-atic particle, the corresponding director $\nu^{(5)}$ and order parameter ψ_5. See caption to Figure 3.5 for a full explanation.

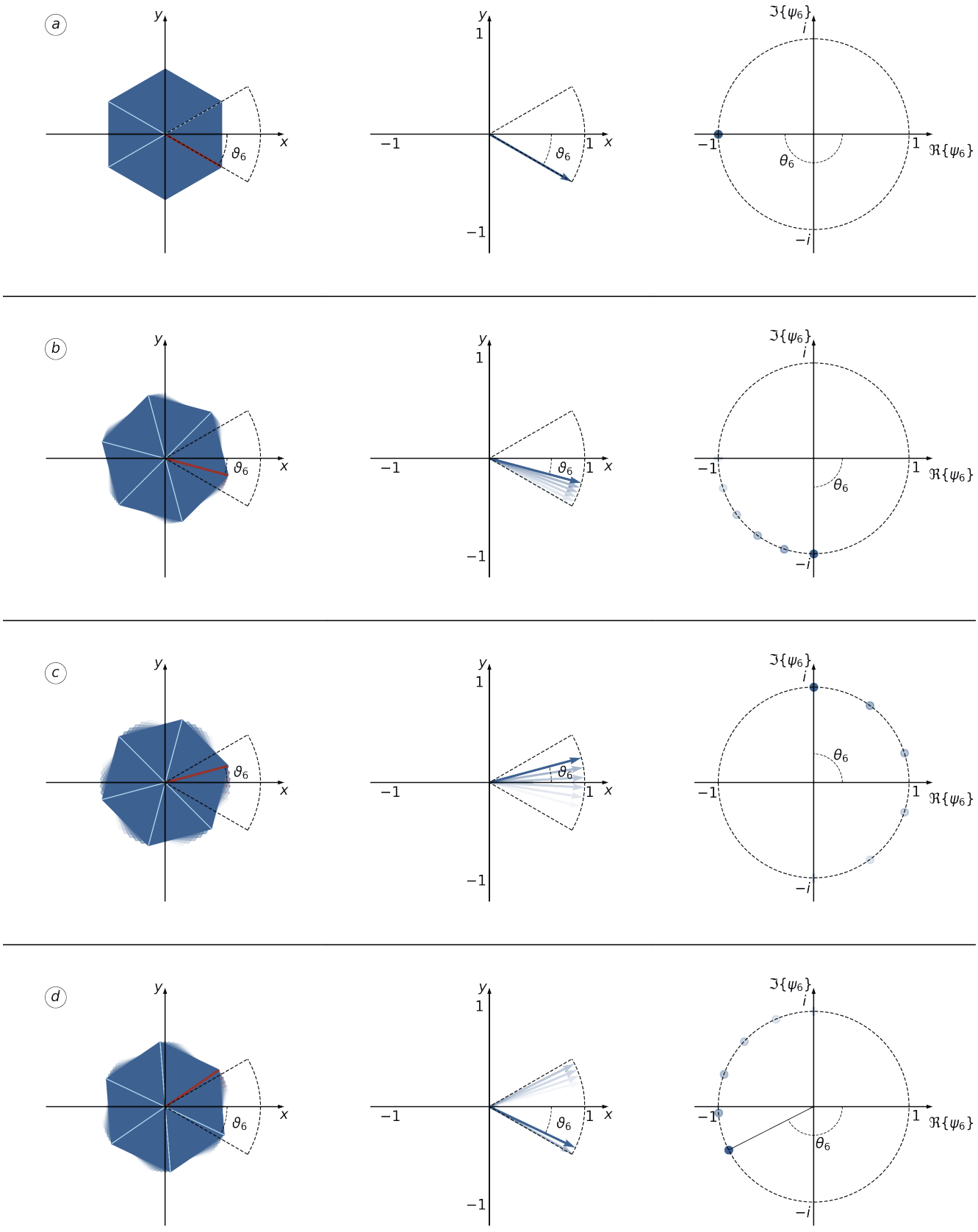

Figure C.8: Relationship between the orientation of the 6-atic particle, the corresponding director $\nu^{(6)}$ and order parameter ψ_6. See caption to Figure 3.5 for a full explanation.

Bibliography

1. Stebe, K. J., Lewandowski, E. & Ghosh, M. Oriented Assembly of Metamaterials. English. *Science* **325,** 159–160. ISSN: 0036-8075, 1095-9203. https://www.science.org/doi/10.1126/science.1174401 (2023) (July 2009).
2. Glotzer, S. C. & Solomon, M. J. Anisotropy of building blocks and their assembly into complex structures. English. *Nature Mater* **6,** 557–562. ISSN: 1476-1122, 1476-4660. https://www.nature.com/articles/nmat1949 (2023) (Aug. 2007).
3. Zhao, K., Bruinsma, R. & Mason, T. G. Local chiral symmetry breaking in triatic liquid crystals. English. *Nat Commun* **3,** 801. ISSN: 2041-1723. https://www.nature.com/articles/ncomms1803 (2023) (May 2012).
4. Bruinsma, R. & Nelson, D. R. Bond orientational order in smectic liquid crystals. English. *Phys. Rev. B* **23,** 402–410. ISSN: 0163-1829. https://link.aps.org/doi/10.1103/PhysRevB.23.402 (2023) (Jan. 1981).
5. Mazenko, G. F., Ramaswamy, S. & Toner, J. Breakdown of conventional hydrodynamics for smectic- A , hexatic- B , and cholesteric liquid crystals. English. *Phys. Rev. A* **28,** 1618–1636. ISSN: 0556-2791. https://link.aps.org/doi/10.1103/PhysRevA.28.1618 (2023) (Sept. 1983).
6. Link, D. R. *et al.* Spontaneous Formation of Macroscopic Chiral Domains in a Fluid Smectic Phase of Achiral Molecules. English. *Science* **278,** 1924–1927. ISSN: 0036-8075, 1095-9203. https://www.science.org/doi/10.1126/science.278.5345.1924 (2023) (Dec. 1997).
7. Brugués, A. *et al.* Forces driving epithelial wound healing. English. *Nature Phys* **10,** 683–690. ISSN: 1745-2473, 1745-2481. http://www.nature.com/articles/nphys3040 (2023) (Sept. 2014).
8. Zhang, Y. & Weinberg, R. A. Epithelial-to-mesenchymal transition in cancer: complexity and opportunities. en. *Front. Med.* **12,** 361–373. ISSN: 2095-0217, 2095-0225. http://link.springer.com/10.1007/s11684-018-0656-6 (2023) (Aug. 2018).
9. Wang, P.-Y. & Mason, T. G. A Brownian quasi-crystal of pre-assembled colloidal Penrose tiles. English. *Nature* **561,** 94–99. ISSN: 0028-0836, 1476-4687. http://www.nature.com/articles/s41586-018-0464-9 (2023) (Sept. 2018).
10. Mietke, A. & Dunkel, J. Anyonic Defect Braiding and Spontaneous Chiral Symmetry Breaking in Dihedral Liquid Crystals. English. *Phys. Rev. X* **12,** 011027. ISSN: 2160-3308. https://link.aps.org/doi/10.1103/PhysRevX.12.011027 (2023) (Feb. 2022).
11. Mermin, N. D. The topological theory of defects in ordered media. English. *Rev. Mod. Phys.* **51,** 591–648. ISSN: 0034-6861. https://link.aps.org/doi/10.1103/RevModPhys.51.591 (2023) (July 1979).
12. Skogvoll, V., Rønning, J., Salvalaglio, M. & Angheluta, L. *A unified field theory of topological defects and non-linear local excitations* English. arXiv:2302.03035 [cond-mat]. Feb. 2023. http://arxiv.org/abs/2302.03035 (2023).
13. Giomi, L., Toner, J. & Sarkar, N. Hydrodynamic theory of p-atic liquid crystals. English. *Phys. Rev. E* **106,** 024701. ISSN: 2470-0045, 2470-0053. https://link.aps.org/doi/10.1103/PhysRevE.106.024701 (2023) (Aug. 2022).
14. Hess, S. *Tensors for physics* ISBN: 978-3-319-12786-6 (Springer Berlin Heidelberg, New York, NY, 2015).
15. Krommydas, D., Carenza, L. N. & Giomi, L. Hydrodynamic Enhancement of p-atic Defect Dynamics. English. *Phys. Rev. Lett.* **130,** 098101. ISSN: 0031-9007, 1079-7114. https://link.aps.org/doi/10.1103/PhysRevLett.130.098101 (2023) (Mar. 2023).